ANALYSIS AND CHARACTERIZATION OF HYDROLOGICAL DROUGHT UNDER CLIMATE CHANGE IN HAMASSA WATERSHED, RIFT VALLEY BASIN, ETHIOPIA

MSc THESIS

REDIAT LEGESE SIME

HAWASSA UNIVERSITY, HAWASSA, ETHIOPIA

JUNE,2024

ANALYSIS AND CHARACTERIZATION OF HYDROLOGICAL DROUGHT UNDER CLIMATE CHANGE IN HAMASSA WATERSHED, RIFT VALLEY BASIN, ETHIOPIA

REDIAT LEGESE SIME

A THESIS SUBMITTED TO THE

DEPARTMENT OF HYDRAULIC AND WATER RESOURCE ENGINEERING,

INSTITUTE OF TECHNOLOGY, SCHOOL OF

GRADUATE STUDIES, HAWASSA UNIVERSITY,

HAWASSA, ETHIOPIA

IN PARTIAL FULFILLMENT OF THE REQUIREMENTS FOR

THE DEGREE OF

MASTER OF SCIENCE IN HYDRAULIC ENGINEERING

JUNE,2024

ADVISORS' APPROVAL SHEET

SCHOOL OF GRADUATE STUDIES

HAWASSA UNIVERSITY ADVISORS' APPROVAL SHEET

This is to certify that the thesis entitled "Analysis and characterization of hydrological drought under climate change in Hamassa watershed, Rift Valley Basin, Ethiopia" submitted in partial fulfillment of the requirements for the Degree of Master of Science with specialization in Hydraulic Engineering, Department of Hydraulic and Water Resources Engineering, has been carried out by **Rediat Legese ID.No. GpHydrR0011/14",** under our supervision. Therefore, we recommend that the student has fulfilled the requirements and hence hereby can submit the thesis to the department of Hydraulic and Water Resources Engineering.

Shemelis Asseffa (PhD)	_____	_____
Name of Major Advisor	Signature	Date
Lamiso Shura (MSc)	_____	_____
Name of Co-advisor	Signature	Date

EXAMINER'S APPROVAL SHEET

SCHOOL OF GRADUATE STUDIES

HAWASSA UNIVERSITY EXAMINERS' APPROVAL SHEET

We, the undersigned, members of the Board of Examiners of the final open defense by Rediat Legese Sime have read and evaluated her thesis entitled "Analysis and characterization of hydrological drought under climate change in Hamassa watershed, Rift Valley Basin, Ethiopia", and examined the candidate. This is therefore, to certify that the thesis has been accepted in partial fulfillment of the requirement for the degree masters of science.

Shimelis Assefa (PhD)	_____	_____
Name of Major Advisor	Signature	Date
Dr. Moltot Zewdie (PhD)	_____	_____
Name of Internal Examiner - I	Signature	Date
Mr. Petros Yohannes (MSc	_____	_____
Name of Internal Examiner - II	Signature	Date
Dr. Bahru Mekuria (PhD)	_____	01-June-2024
Name of External Examiner	Signature	Date
_____	_____	_____
SGS Approval	Signature	Date

DECLARATION

I hereby declare that this MSc thesis titled **"**Analysis and characterization of hydrological drought under climate change in Hamassa Watershed, Rift Valley Basin, Ethiopia**"** is my original work carried out under the supervision of Shimelis Asseffa (PhD) and Mr. Lamiso Shura (MSc). It has not been presented as a thesis in any other university and all sources of material used for this thesis have been duly acknowledged.

Rediat Legese	_____	_____
Name of Candidate	Signature	Date

ACKNOWLEDGEMENT

Above all, firstly I would like to express my deepest and special thanks of gratitude to Saint Mary and her son God the creator of all things, for giving me health, time, and strength to do this study. Secondly, I extend my profound gratitude to my advisors, Dr. Shimelis Asseffa and Mr. Lamiso Shura (MSc). Their unwavering support, encouragement, professional advice, and guidance have been instrumental in shaping this work. I am deeply grateful for their contributions and for always being there to steer me in the right direction.

I also want to acknowledge the love and support of my family and friends, which has been unwavering and invaluable. To my father, thank you for everything you have done in my life; your encouragement and support have been my anchor. Special thanks go to Mr. Manamno Beza for his significant contributions. Your assistance and support have been greatly appreciated.

TABLE OF CONTENTS

LIST OF FIGURES

LIST OF TABLES

LIST OF APPENDIXES

LIST OF ACRONYMS

CMhyd	Climate model data for hydrologic modeling
CORDEX	Coordinated regional climate downscaling experiment project
DEM	Digital elevation model
DrinC	Drought indices calculator
FAO	Food and agriculture organization
GCM	Global climate model
GIS	Geographical information science
GLUE	Generalized likelihood uncertainty estimation
HBV	Hydrologiska byråns vattenbalansavdelning
HRU	Hydrologic response unit
LULC	Land use land cover
MCMC	Markov chain Monte Carlo
MoWRE	Ministry of water resources and energy
MSRRI	Multivariate standardized reliability and resilience index
NDVI	Normalized difference vegetation index
NMI	National meteorological institute
PHDI	Palmer hydrological drought index
RCM	Regional climate models
RCP	Representative concentration pathway
SDI	Stream flow drought index
SUFI-2	Sequential uncertainty fitting version 2
SPI	Standardized precipitation index
SWAT	Soil and water assessment tool
SWAT-CUP	SWAT calibration and uncertainty program
SWSI	Surface water supply index
UTM	Universal transverse Mercator
VHI	Vegetation health index
WSRI	Water storage resilience indicator

ABSTRACT

Hydrological drought occurs when there is an extended period of significantly reduced water availability, leading to depleted water sources and severe impacts on ecosystem and communities. Water scarcity caused by prolonged periods of reduced rainfall due to climate change can lead to the natural disaster of drought. However, little has been done so far on hydrological drought under climate change in Hamassa watershed. This study aimed to analyze and characterize hydrological drought under climate change in the Hamassa watershed, Rift Valley Basin, Ethiopia. Hydrological data (1992-2015), meteorological data (1992-2022), future climate data 2030-2090), spatial data, DEM, land use land cover, and soil were collected. CMhyd software package was used for bias correction of the climate data. The hydrological model soil and water assessment tool (SWAT) was used for hydrological analysis. The simulation result was calibrated and validated using the SWAT calibration uncertainty procedure (SWAT-CUP). Standard precipitation index (SPI) and stream flow drought index (SDI) are used to decide drought conditions in a watershed and to identify drought-prone areas in the watershed. Temperature projections for both the near and long term indicate an increase compared to the current period under both RCP2.6 and RCP8.5 scenarios. Meanwhile, precipitation projections suggest a decrease for the periods 2040-2060 and 2061-2072 under both RCP2.6 and RCP8.5 scenarios. The standard precipitation index (SPI) and stream flow drought index (SDI) results showed that the watershed experiences mild (-0.5- -0.999), moderate (-1- -1.49), severe (-1.5- -1.99), and extreme (≤ - 2) drought events. Droughts are projected to occur in the periods 2040-2060 and 2061-2072 under both RCP2.6 and RCP8.5 scenarios. Sub-watersheds 7, 8, 9, 10, and 11 showed high vulnerability to severe and extreme drought. Drought-mitigating structures are needed to mitigate drought in the watershed.

Key Words: Climate Change, CMhyd, SDI, SPI, SWAT model, SWAT-CUP

1 INTRODUCTION

1.1 Background

Water scarcity caused by prolonged periods of reduced rainfall can lead to the natural disaster of drought (Najihah *et al.*, 2020). Drought, a complex phenomenon with no universal definition, has been interpreted differently by various authors Tallaksen and Van Lanen (2004); Wilhite and Knutson (2006); Mishra and Singh (2010), and Van Loon (2015). Hydrologists generally define drought as a water deficit compared to normal conditions. Changes in climate, environment, land use, and natural resource depletion have led to increased drought frequency and vulnerability (Lal, 2012).

Climate change is a major worldwide issue due to its uneven effects on socioeconomic and environmental factors. Climate change is currently affecting the hydrology of watersheds, which is leading to an imbalance in the natural water cycle and distribution (Chakilu *et al*., 2015). The distribution of water resources and hydrological cycles are impacted by climate change (Padron *et al*., 2020). Climate changes lead to hydrological extremes such as floods and droughts, regardless of their severity, duration, or frequency. Severe heat waves, atypical precipitation, and prolonged droughts are potential weather conditions. Increased evaporation from warmer temperatures reduces surface water and dries out vegetation and soils. Low streamflow results from this cause drought, which has an impact on agricultural systems, ecological stability, and water supply (Tenagashaw and Andualem, 2022a).

Drought is the most devastating of all-natural disasters and is considered one of the costliest disasters globally (Mishra and Singh, 2010). Insufficient rainfall causes meteorological droughts, leading to different drought types. Inadequate soil moisture can create soil moisture drought, while agricultural drought arises from a lack of moisture for crops. This water scarcity disrupts the hydrological cycle, reducing groundwater and river flow, causing hydrological droughts with low streamflow and depleted water levels in lakes, reservoirs, and groundwater (Tallaksen and Van Lanen, 2004; Van Loon, 2015).

Hydrological droughts reduce water levels in lakes, groundwater, and streamflow. Streamflow is crucial for evaluating water quantity, with reduced flow signaling a hydrological drought (Nalbantis and Tsakiris, 2009). Droughts are undoubtedly one of the most challenging and intricate natural disasters (Van Lanen *et al*., 2016; Wilhite *et al*., 2014). According to Gutiérrez *et al.* (2014), drought is a component of the climate that affects many countries globally, including Ethiopia, the Horn of Africa, and several other Sub-Saharan nations. Three developed countries that have faced drought in the past are Australia, Brazil, and the state of California in the United States. Droughts can have significant social and economic impacts, leading to various outcomes such as conflict, migration, gender inequalities, decreased hydropower generation, food insecurity, poverty, and adverse health effects (Pandey *et al*., 2008; Shadman *et al*., 2016). The gradual and elusive nature of drought makes it challenging to manage effectively, with traditional strategies often failing to provide timely solutions.

Globally, from 1900 to 2021, over 2.7 billion people have been affected by droughts, resulting in 11.7 million deaths and an economic impact exceeding 184 billion USD (Melesse and Kidanewold, 2022). Ethiopia has faced recurrent droughts over the past fifty years, particularly impacting the eastern, southeastern, and rift valley regions with seasonal rainfall levels typically 30% to 50% below average (Mera, 2018, 2020). The country experienced severe drought events in 1984, 2000, 2001, and 2009, with devastating consequences such as widespread crop failures and loss of life. These droughts have significantly affected Ethiopia's agricultural production, leading to famines and exacerbating water scarcity issues in the region (Mohammed *et al*., 2018; Viste *et al*., 2013; Gebre *et al*., 2015). The impact of climate change has intensified the frequency and severity of droughts, posing significant challenges to livelihoods and economies in Ethiopia (Liou and Mulualem, 2019; Melesse and Kidanewold, 2022; Viste *et al*., 2013b).

The study aims to analyze and characterize hydrological drought under climate change for the Hamassa watershed, Rift Valley Basin Ethiopia. The study used the Soil and water assessment tool (SWAT) model.

The SWAT model is one of the most recent models used to predict the impacts of land management practices on water, sediment, and agricultural chemical yields in watersheds with varying soils, land use, and management practices over extended periods (Neitsch *et al.*, 2002). Drought indices have been used to analyze and characterize droughts because they simplify complex meteorological functions and can quantify climatic anomalies in terms of severity, duration, and frequency (Svoboda and Fuchs, 2017).

1.2 Statement of problem

Hydrological droughts, characterized by reduced water availability in rivers, lakes, and groundwater, pose significant challenges to water resources management, agriculture, and socio-economic development (Van Loon, 2015a). Climate change extends these issues by changing precipitation patterns, increasing temperatures, and shifting hydrological cycles, leading to more repeated and severe drought events (Yuan *et al.,* 2016). In the Hamassa Watershed within the Rift Valley Basin of Ethiopia, these challenges are compounded by the region's reliance on rain-fed agriculture and the limited availability of other water sources.

Detailed analysis of drought events is crucial due to their varying time, space, and magnitude, for effective mitigation strategies. Analyzing hydrological droughts is essential for establishing effective long-term mitigation measures (Abera and Gebeyehu, 2022). Currently, the Hamassa Watershed lacks detailed analysis and characterization of hydrological droughts under projected climate change scenarios. This gap in knowledge hurdles the ability of local authorities, water resource managers, and policymakers to develop effective drought mitigation and adaptation strategies. Without a clear understanding of how future climate change will impact hydrological droughts, the region remains vulnerable to water shortages, agricultural losses, and economic instability.

Furthermore, the specific hydrological and climatic conditions of the Hamassa watershed are frequently unnoticed by hydrological models and drought assessment tools. To provide a reliable assessment of the risks of future drought, a customized strategy that combines local hydrological data with climate projections must be developed immediately.

Addressing this problem involves the development and application of SWAT hydrological models that can accurately simulate the impacts of climate change on water availability in the Hamassa watershed. This research aims to fill the critical knowledge gap by analyzing and characterizing hydrological droughts under future climate scenarios, thereby providing essential insights for sustainable water resource management and climate resilience planning in the region.

1.3 Objectives

1.3.1 General objective

The main objective of the study was to analyze and characterize hydrological drought under climate change for the Hamassa watershed, Rift Valley Basin, Ethiopia.

1.3.2 Specific objectives

1. To characterize the hydrological component of the watershed
2. To analyze the hydrological drought of the watershed at the existing condition
3. To analyze the hydrological drought of the watershed under climate change
4. To identify drought hotspot areas

1.4 Research questions

- ✓ What are the characteristics of hydrological components at existing conditions?
- ✓ What are the characteristics of hydrological components under climate change?
- ✓ What are the characteristics of hydrological drought in the watershed at existing conditions?
- ✓ What are the characteristics of hydrological drought in the watershed under climate change?
- ✓ Which part of the study area is more prone to drought?

1.5 Scope of the study

This research focuses on the analysis and characterization of hydrological drought under climate change in the Hamassa watershed, Rift Valley Basin. To achieve the study objectives, collect and prepared hydrological, meteorological, future climate, spatial data. CMhyd tool was used to correct bias in the simulated climate data. The SWAT model was then calibrated and validated using SWAT-CUP, with the standard precipitation and streamflow drought index used to assess drought conditions in the watershed.

1.6 Significance of the study

This study enhances the understanding of drought conditions in this region, the study serves as a crucial resource for planners, decision-makers, water managers, agricultural producers, and policymakers. It addresses existing and future knowledge gaps regarding drought conditions, thereby empowering these stakeholders to make informed decisions aimed at drought mitigation. Additionally, the results and recommendations generated by this research will provide essential information to the body of knowledge on hydrological drought, this study also offers valuable supplementary information that can benefit other researchers working within the same thematic area.

2 LITERATURE REVIEW

2.1 Global overview of drought

Drought is a global natural disaster that has detrimental effects on the economy, society, and environment (Shah *et al*., 2015). Severe hydrological events Today, flooding and drought are the two most concerning issues facing the world (Edossa *et al*., 2014). Drought is a prevalent natural calamity that negatively influences water resources and agricultural projects in numerous ways (Asadi and Vahdat, 2013). Flood studies garner more attention globally due to their rapid impact and short duration. Both droughts and floods hinder the economic advancement of many countries (Tareke and Awoke, 2022). Droughts particularly inflict substantial damage on water-related projects like irrigation, hydropower, and water supply. Hence, there is a growing interest in crafting effective drought mitigation strategies based on recent research on drought analysis and prediction (Jesus *et al*., 2020).

Drought is a complex phenomenon with no universally applicable definition, It can manifest in different forms: meteorological drought, characterized by insufficient precipitation (Schubert *et al.*, 2016); hydrological drought, marked by reduced streamflow and diminishing reservoir and lake levels (Van Loon, 2015); agricultural drought, resulting from low soil moisture content (Padhee, 2013); and socioeconomic drought, arising from supply-demand imbalances (Liu *et al.*, 2020). Meteorological and agricultural droughts primarily lead to crop failures, while hydrological droughts entail water scarcity, declining groundwater levels, reduced irrigation, and hydropower generation. Socioeconomic drought stems from the interplay of meteorological, agricultural, and hydrological droughts, exacerbating water supply-demand disparities. This disruption impacts the entire ecosystem of the region and can lead to fatalities (Dalezios *et al*., 2017). Employing scientific analysis to determine the likelihood of drought recurrence and persistence aids in formulating strategies for mobilizing and managing water resources effectively (Winkler, 2017). Rain-fed agriculture is a vital economic sector in African countries, but droughts can lead to food shortages, crop failures, and humanitarian crises (Tareke and Awoke, 2022b).

2.2 Drought in Ethiopia

Drought occurs severely in almost all parts of the world. However, its effects are more pronounced when it strikes developing countries, particularly in Africa. This is because a large percentage of the population relies on agriculture and is dependent on rainfall. Ethiopia is one of the African nations that has regularly faced extreme droughts and famines throughout its history (Gebrehiwot *et al*., 2011).

According to Mohammed *et al*. (2018), the northeast highlands of Ethiopia experienced the most severe drought years in 1984, 1987, 1988, 1992, 1993, 1999, 2003, 2004, 2007, and 2008. In Ethiopia the year 1984 was particularly notable for its severe drought impact, garnering global recognition (Tareke and Awoke, 2022b). The nationwide drought in 1984 significantly affected 8 million people and led to the loss of 1 million lives. Over the past ten to fifteen years, Ethiopia has observed an increase in drought frequency. While all regions experienced annual droughts, previous occurrences were more severe across most areas. Nationally, the year 2009 was ranked as the second driest year, following closely behind the significant drought of 1984. These drought years were assessed using meteorological drought indicators, particularly the standardized precipitation index and the Palmer drought severity index (Mera, 2020a).

A severe drought will affect Ethiopia in 2020–2022, impacting areas such as Oromia, Somalia, Afar, and the Southern Nations, Nationalities, and Peoples' Region. Lack of water and pasture due to the drought hurt livestock and agriculture. Almost one million cattle were lost in the Somali region, forcing families to relocate. Food security and humanitarian aid were also impacted by the drought, with 17 million people in need of help (Abera and Gebeyehu, 2022). Ethiopia has experienced numerous droughts throughout history, but current research is inadequate in addressing agricultural, hydrological, and socioeconomic droughts. Historical hydrological drought characteristics are crucial for effective water resource management and mitigation strategies, especially in critical sectors like irrigation, water supply, and hydropower (Tareke and Awoke, 2022a).

2.3 Hydrological drought

Hydrological drought is a critical aspect of water resource management, impacting surface and subsurface water supplies such as stream flow, reservoir levels, and groundwater. It is characterized by water losses over time, leading to decreased water levels that may not meet human and ecosystem needs (Awass,2009). Stream flow, a key water quantity variable, plays a crucial role in expressing surface water resources (Hasan *et al.,* 2019).

Van Loon, (2015) describes hydrological drought as a lack of water in the hydrological system, resulting in abnormally low stream flow and reduced levels in lakes, reservoirs, and groundwater. To assess hydrological drought severity, indices like the stream flow drought index and standardized streamflow index are used, particularly when surface water flow, storage, and diversions are critical for various purposes (Van Lanen *et al.,* 2016).

Hydrological drought assessment is vital for understanding the impact on water resources essential for human activities. Recovery from hydrological drought is often prolonged due to the time required for streams and lakes to recharge. Increased water consumption has amplified the magnitude of hydrological droughts by 10–50% and raised the global drought frequency by 30% (Van Lanen *et al*., 2016; Nalbantis, 2008). Hydrological droughts are noticeable through reduced surface water availability caused by decreased precipitation events or quantity (Hisdal and Tallaksen, 2003). They often lag behind meteorological droughts and manifest as low stream flow, drying of water bodies, and depletion of surface water resources. Effective water resource management is crucial to mitigate the impacts of hydrological droughts (Ali *et al.,* 2023).

Studies by Kwon and Kim (2010) in South Korea and Swetalina and Thomas (2016) in central India's Bundelkhand region have examined hydrological drought characteristics using various indices and thresholds. Similarly, Jahangir and Yarahmadi (2020) analyzed hydrological drought in Lorestan province, Iran, utilizing the stream flow drought index to assess severity and continuity over the years. These studies underscore the importance of

proactive water resource management to address the challenges posed by hydrological droughts and their significant socio-economic impacts on regions worldwide.

2.4 Climate change

Climate change is a significant environmental challenge in the 21st century, affecting human society and posing a wide-ranging impact on the world (Aragaw *et al*., 2023). Climate change alters extreme weather events, causing significant impacts on ecosystems, human development, and annual economic losses (Gebisa *et al*., 2023). Climate change is caused by natural processes like the sun's energy changes and the earth's orbit variations, as well as human activities like burning fossil fuels, heating buildings, and causing land degradation. These activities, along with deforestation, land degradation, soil erosion, urbanization, and population growth, significantly impact water resources planning and management (Dibaba *et al.*, 2020b). Management of water resources is particularly concerned about how river hydrology will be impacted by climate change. Assessing the impact of global climate change on watershed hydrology is crucial for predicting climate variables (Yersaw and Chane, 2024). Climate change significantly impacts human and ecological systems, particularly water balance components. Changes in precipitation and temperature can cause temporal/spatial variation in hydrological conditions and water resources. Changes in rainfall intensity and timing affect stream flows, leading to increased floods and droughts. Climate change is disrupting regional hydrology and water availability for agriculture. Greenhouse gas emissions are raising the earth's surface temperature, with the average global surface temperature potentially rising by up to 4.8°C by the end of the century (Aragaw *et al*., 2023).

2.4.1 Climate change on hydrological components

Climate change, a significant global issue influenced by socioeconomic and environmental factors, has led to unbalanced environmental effects, including unbalanced watershed hydrology (Blanco-Gómez *et al*., 2019). Climate change is accelerating the global hydrologic cycle, causing changes in precipitation patterns and increased evapotranspiration rates. Changes in streamflow are largely linked to precipitation variations, but small temperature

increases and evapotranspiration can cause larger variations in moisture-limited regions (Reshmidevi *et al*., 2017).

Hydrological cycles and the distribution of water resources are impacted by climate change, which is caused by an increase in greenhouse gas emissions. Evapotranspiration, runoff, and streamflow are impacted by variations in temperature and precipitation. Higher temperatures cause more evaporation, which diminishes soil and surface water and results in times of low streamflow. Low streamflow affects agricultural systems, ecological stability, and water supply because it is a result of hydrological abnormalities and human activity (Tenagashaw and Andualem, 2022b).

Blanco-Gómez *et al.* (2019), assessed the future impact of climate change on water balance components and droughts in El Salvador's Guajoyo River Basin using the soil and water assessment tool. The study predicts a decrease in precipitation and an increase in annual average temperatures by the end of the 20th century, indicating reduced water availability and severe droughts occur in the future.

Daniel and Abate, (2022b) assess the effect of climate change on streamflow in the Gelana watershed, Rift Valley basin, Ethiopia. The study predicts increased temperatures and potential evapotranspiration, leading to reduced rainfall and streamflow. This could result in a higher decline in surface runoff, groundwater, and water yield.

Balcha *et al*. (2023), evaluate how future climate change will affect the components of the water balance in Ethiopia's Central Rift Valley Lakes Basin. The study uses climate and hydrological models to investigate how climate change will affect water balance. It concludes that while future temperatures and rainfall will be statistically insignificant, they will result in a decrease in water yield. Annual water yields, however, will increase.

2.4.2 Climate change on hydrological drought

Climate change affects surface runoffs and water resources management, as it changes river hydrological regimes. Water demand is primarily from stream runoff, which can lead to

severe consequences like deteriorated water quality, crop failure, reduced electricity generation, disrupted habitats, and limited recreational activities. Accurate discharge prediction is crucial for planning and managing surface water resources. As climate change affects runoffs, future drought periods and severity will increase (Samavati *et al*., 2023).

Kamali *et al*. (2017), studied climate change's impact on drought in the Karkheh river basin using the SWAT model and drought hazard index to predict hydrological drought future projections showed a higher probability of severe and extreme drought intensities. Similarly, Salimi *et al*.(2021), investigated how hydrological droughts are affected by climate change. In the Navrood and Lighvan watersheds in northern Iran, they employed the standard precipitation index and the stream flow index and found a strong correlation between hydrological droughts. They also concluded that the most important factor influencing the likelihood of future droughts was climate change.

Kim *et al*. (2022), assess future hydrological drought under climate change in the Yeongsan River basin. This study proposes a framework to predict future hydrological droughts, considering agricultural water withdrawal for shared socioeconomic pathways. The relationship between agricultural water withdrawal and potential evapotranspiration is determined using a deep belief network model and projections of global climate models. The results show a higher occurrence of severe droughts shortly due to increased potential evapotranspiration due to rising temperatures.

Samavati *et al.* (2023), investigated the impact of climate change on potential hydrological drought in the Alvand mountain basin of Iran. They utilized the soil and water assessment tool model in combination with climate projections. The study findings indicated that all of the examined scenarios showed an increasing trend in drought intensity within the basin. The most significant reduction in annual runoff was observed during the summer season and on a monthly timescale.

2.4.3 Bias correction of climate data

Bias correction methods are often applied within climate impact assessment to correct the climate input data for systematic statistical deviations from observational data. Bias correction methods aim to adjust the mean, variance, and/or quintile of the model time series variable using a certain correction factor so that the corrected model time series matches closely with the observed variable. They generally adjust the long-term mean by adding the average difference between the simulated and observed data over the historical period to the simulated data, or by applying an associated multiplicative correction factor (Worku *et al*., 2020; Rathjens *et al*., 2016). In the studies of climate change, bias corrections for adjusting model data have become a standard practice (Soriano *et al*., 2019). To ensure accuracy in climate impact studies, it is essential to use bias-corrected climate data, such as precipitation and temperature records. This adjustment is crucial to minimize errors that typically arise from using raw climate models (Daniel, 2023). Bias correction techniques are designed to preserve the integrity of observed climate data. These methods generally involve developing a statistical relationship between historical model outputs and observed climate data. Bias correction methods can effectively reduce biases in RCM outputs their effectiveness is often dependent on the specific region's standard practice (Yersaw and Chane, 2024).

Numerous statistical bias correction techniques have been created to address biases in climate simulations and to generate simulated series with accurate statistical properties. These methods include linear scaling, gamma distribution adjustments, delta change, power transformation, variance scaling, and local intensity scaling (Tenagashaw and Andualem, 2022a). Research by Fang et al. (2015), revealed that power transformation and quantile mapping are superior methods for correcting precipitation biases when compared to linear scaling, gamma distribution adjustments, and local intensity scaling. Similarly, Teutschbein and Seibert, (2012) found that power transformation and distribution mapping outperformed linear scaling, delta change, and local intensity scaling for precipitation bias correction. Unlike precipitation, temperature cannot be corrected using a power law approach due to its approximate normal distribution. Instead, temperature biases are corrected through shifting

and scaling methods that adjust the mean and variance for each catchment (Tenagashaw and Andualem, 2022a). Yersaw and Chane (2024), identified variance scaling as the most effective method for temperature.

2.5 Hydrological model

Hydrological models have many of importance, they are used to estimate runoff from sequences of rainfall and the meteorological information needed to estimate potential evaporation, estimate river flows at ungauged sites, fill gaps in broken records or extend flow records for longer records of rainfall (WRA 2021). A general assessment of the water resources available in a region or a river basin is essential for finding sustainable solutions for water-related problems concerning both the quantity and quality of the water resources (Xu and Singh 2004).

Hydrologic models are simplified, conceptual representations of a part of the hydrologic cycle. It can be classified into three; lumped model, Semi-distributed, and distributed model. Parameters of lumped hydrologic models do not vary spatially within the basin and thus, basin response is evaluated only at the outlet, without explicitly accounting for the response of individual sub-basins. In a semi-distributed model, parameters partially vary with space by dividing the basins into smaller sub-basin units however in a distributed model changing with space is completely allowed but it needs a physical process in detail and large data (Wagner *et al*. 2011).

Some of the semi-distributed hydrological models for water assessment include Soil Conservation Service-Curve Number, WEAP, HEC- HMS, HBV, and SWAT. In this study, the SWAT model was selected due to; It is freely available software (commercial), unlike the other conventional conceptual simulation models it does not require much calibration. The model is physically based, computationally efficient, and capable of simulating a high level of spatial details by allowing the watershed to be divided into a large number of sub-watersheds and SWAT also has a weather simulation model that generates daily data for rainfall, solar radiation, relative humidity, wind speed and temperature from the average

monthly variables of these data. This provides a useful tool to fill in missing daily data in the observed records.

2.5.1 Over view of the soil and water assessment tool model

The soil and water assessment tool (SWAT) is a physically-based continuous-event hydrologic model developed to predict the impact of land management practices on water, sediment, and agricultural chemical yields in large, complex watersheds with varying soils, land use, and management conditions over long periods of time (Arnold *et al*. 2012). SWAT is a public domain hydrology model with the following components: weather, surface runoff, return flow, percolation, evapotranspiration, transmission losses, pond and reservoir storage, crop growth and irrigation, groundwater flow, reach routing, nutrient and pesticide loading, and water transfer (Neitsch *et al*. 2011).

It is especially designed modeling tool to deal with the complexities of large watershed using geospatial data-set. It works on daily time step but it can give output on daily, monthly, and yearly basis which can further focused into basin and reach wise. The model is divided into major eight components hydrology, weather, sedimentation, soil temperature, crop growth, nutrients, pesticides, and agricultural management. For calculating surface run-off, the curve number method has been used (Ikhar *et al*. 2018).

SWAT also has a weather simulation model that generates daily data for rainfall, solar radiation, relative humidity, wind speed and temperature from the average monthly variables of these data. This provides a useful tool to fill in missing daily data in the observed records. SWAT model is a data intensive model which requires meteorological data (precipitation, minimum and maximum temperature, relative humidity, solar radiation, and wind speed), soil, land use, topography and hydrological data (river flow and sediment)(Andualem *et al*. 2020). It uses hydrologic response units (HRUs) that consist of specific land use, soil and slope characteristics. The HRUs are used to describe spatial heterogeneity in terms of land cover, soil type and slope class within a watershed. The model estimates relevant hydrologic components such as evapotranspiration, surface runoff and peak rate of runoff, groundwater

flow and sediment yield for each HRUs unit. The hydrologic cycle simulated by SWAT is based on the water balance equation (Sisay *et al*. 2018).

2.5.2 Application of SWAT model in a watershed

There are many different reasons that need to model the rainfall-runoff process of hydrology. The main reason is however, a result of the limitations of hydrological measurement techniques. In fact, only a limited range of measurement techniques and a limited range of measurements in space and time. Therefore, there is a means of extrapolating from those available measurements in both space and time particularly to ungauged catchments. Hydrological modeling of ungauged basins is important and imperative for policymakers and stakeholders in water management. Thus the use of hydrologic models for un-gauged catchments becomes important issues in hydrological study to assess the potential of the water resource in the watershed. There are many different ways to determine the runoff in the ungauged watershed units. Some of which are mostly used in the past are unit hydrograph, empirical equation like rational method Area ratio method, SCS-CN(Hoeft *et al.* 2015*)* and use of the hydrological model such as HEC HMS*(Merwade 2012)*, WEAP*(*Mahamadou *et al.* 2011*)*, SWAT(ALLEN et al. 1997). But unit hydrography and rational method is limited with area distribution that is useful only less than a catchment area of 500km^2 and 50km^2 respectively. Therefore, use of hydrological model for assessing the water resource in a watershed is more reliable and accurate due to this a physically based SWAT hydrological model is selecting for water resource assessment.

In the past, many studies have been done to assess surface water resources by using SWAT tool ((Setegn et al. 2008);(G.Shimelis et al. 2010);(Melaku et al. 2018);(Tewodros Taffese 2013);(Addis et al. 2013);(Baker and Miller 2013);(Yifru et al. 2020)).

Setegn et al. (2008) Hydrological Modeling in the Lake Tana Basin using SWAT model. The main objective of this study was to test the performance and feasibility of the SWAT model for prediction of stream flow in the Lake Tana Basin. The model was calibrated and validated on four tributaries of Lake Tana; Gumera, GilgelAbay, Megech and Ribb rivers using SUFI-

2, GLUE and ParaSol algorithms. The result show that SUFI-2 and GLUE was give good result for the calibration and base flow (40% - 60%) is an important component of the total discharge within the study area that contributes more than the surface runoff.

G.Shimelis et al. (2010) Modeling of sediment yield from Anjeni watershed by using SWAT model. The objectives of this study were to evaluate the performance and applicability of SWAT model in predicting monthly sediment yield and assess the impacts of sub basin delineation and slope discretization on the prediction of sediment yield. The annual average simulated sediment yield was 27.8 and 29.5 tones/ha for calibration and validation periods, respectively. The study found that the observed values showed good agreement with the simulated sediment yield.

Melaku et al. (2018) Prediction of soil and water conservation structure impacts on runoff and erosion processes using SWAT model in the northern Ethiopian highlands. The model results indicated that SWC structures considerably reduced soil loss by as much as 25–38% in the treated watershed. The study demonstrated that SWAT performed well for both watersheds and can be a potential instrument for up scaling and assessing the impact of SWC structures on sediment loads in the highlands of Ethiopia.

Tewodros Taffese (2013) Hydrological modeling of a catchment using SWAT model in the upper Blue Nile basin of Ethiopia in case of Mizewa catchment. The results indicated that the model performance was in acceptable range and there are no many changes to predict the flow by the two versions of SWAT model. HRU analysis indicated that agricultural land were the most runoff generating areas. Soil evaporation compensation factor and curve number are the two most sensitive parameters indicating effective rainwater management interventions has a great impact in reducing soil erosion and land degradation.

2.6 Hydrological drought indicators

Drought indices are calculated to define drought and its related parameters, including intensity, duration, and severity (Mishra and Singh 2010). These indices are essential for

identifying drought, evaluating when it begins and ends, determining the severity of drought, analyzing drought occurrences, predicting future droughts, and projecting potential drought scenarios (Niemeyer, 2008; Tsakiris *et al*., 2007). Many different drought indices have been developed worldwide and are customized for particular regions. Hydrological drought assessment uses specific drought indicators, although many indicators are intended for meteorological and agricultural drought analysis. These include the standardized water level index, standardized precipitation index, surface water supply index, palmer hydrological drought index, and streamflow drought index (Svoboda and Fuchs, 2017).

Standardized indices for assessing hydrological drought utilize various hydrological parameters derived from observed or simulated data. Streamflow is typically the primary focus due to its widespread measurement, ease of simulation, and significance for water resource management. Additionally, hydrological drought indices may incorporate other variables such as groundwater levels and lake levels (Van Loon, 2015).

2.6.1 Standardized precipitation index

The standardized precipitation index, initially proposed by (Mckee *et al.*, 1993), serves as a valuable tool for monitoring meteorological drought. Widely recognized for its effectiveness in quantifying both meteorological and hydrological drought, this index utilizes long-term precipitation data fitted to a probability distribution, which is then normalized to a standard normal distribution for regional comparisons. It can be calculated over varying time scales and is particularly useful for approximating hydrological drought over extended periods (Szalai and Szinell, 2000; Zhai *et al.,* 2010). Following a recommendation from experts at a World Meteorological Organization workshop in 2009, the standardized precipitation index was advocated for use by national meteorological and hydrological services worldwide to characterize meteorological and hydrological drought (WMO, 2012).

In a study by Fendekova *et al.* (2018) focusing on Slovakia, the standardized precipitation index was utilized to analyze hydrological drought events across twelve river basins. The researchers assessed the occurrence and characteristics of hydrological drought in different

years, highlighting varying impacts across the basins. Moreover, Kamalanandhini *et al.* (2021) conducted an evaluation of hydrological drought severity in the Chengalpattu district of Tamil Nadu, India. Utilizing 30 years of rainfall data and the standardized precipitation index as an indicator, they forecasted rainfall trends for the next three decades. The results suggest that the region is currently experiencing a significant hydrological drought situation. Fendekova *et al.* (2018) and Kamalanandhini *et al.* (2021) used the standardized precipitation index to analyze hydrological drought events in Slovakia and Tamil Nadu, respectively, assessing drought severity and forecasting rainfall trends for the upcoming three decades.

2.6.2 Stream flow drought index

The stream flow drought index, created by (Nalbantis and Tsakiris, 2009), allows for the quantitative evaluation of drought conditions using indexes. It is employed to characterize stream flow drought conditions and relies on monthly stream flow data at different time scales. This method provides the benefit of effectively managing stream flow drought and water supply in the short, medium, and long term (Van Loon,2015). The stream flow drought index focuses on observed or simulated stream flow data (Vicente-Serrano *et al.* 2012). The values of this index are significantly influenced by the duration of the data record and the distribution chosen for fitting. Another difficulty with these indices is the requirement to determine a reference period, which can be problematic in the context of multi-decadal climate variations (Nunez *et al.*, 2014).

In a study by Tabari *et al.* (2013) in northwest Iran, the stream flow drought index was utilized across various durations at different hydrometric stations, revealing severe drought conditions at almost all stations. Sardou and Bahremand (2014) studied hydrological drought in Iran's Halilrud basin, assessing drought probability using the stream flow drought index, showing varying severity levels across different parts of the basin. Zamani *et al.* (2015) evaluated hydrological drought in the Karkheh basin, dividing the region into sub-regions for longer periods while maintaining consistency for the 3-month timescale. Simulation outcomes indicated reduced accuracy in quintile estimates with increasing return periods,

with a higher likelihood of severe droughts at the regional level compared to site-specific levels.

The studies by Tabari *et al.* (2013), Sardou and Bahremand (2014), and Zamani *et al.*(2015) all focused on assessing hydrological drought using the stream flow drought index in different regions of Iran. While Tabari *et al.* (2013) highlighted severe drought conditions at hydrometric stations over various durations, Sardou and Bahremand (2014) examined drought events in the Halilrud basin, showing varying severity levels. Zamani *et al.*(2015) evaluated hydrological drought in the Karkheh basin, emphasizing the reduction in quintile estimate accuracy with increased return periods and the higher likelihood of severe droughts at the regional level.

3 MATERIAL AND METHODS

3.1 Descriptions of the study area

3.1.1 Location

The Hamassa watershed is a part of the Rift Valley Basin situated between 6°36’ 00″ to 6°54’ 37″N latitude and 37°46’41″ to 37°54’21″E longitude (Figure 3.1). The elevation of the watershed ranges from 1,286 to 2,951m amsl. The watershed’s southern portion has the lowest height, while the northeastern tip has the higher elevation ranges. The Hamassa River is part of the Abaya Chamo sub-basin, ultimately flowing into Lake Abaya.

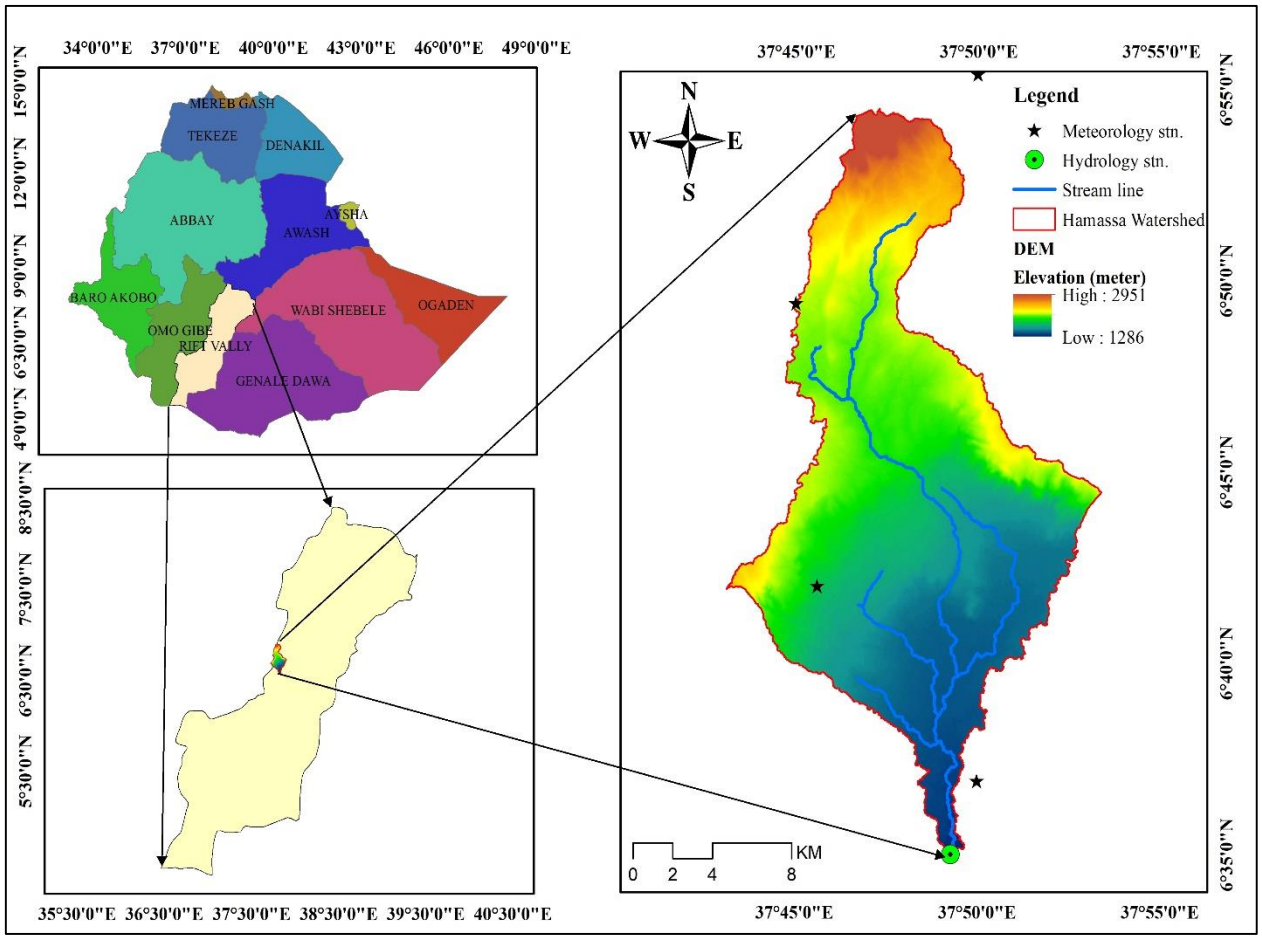

Figure 3.1 Location of the study area

3.1.2 Topography

The altitude varies from 1286 to 2951 meters above sea level. The topography ranges from lowland alluvial plains to rugged mountainous terrains, with steep slopes in the northeast and southwest, and gentler slopes in the central and southern parts, along with hilly terrains and steep river courses. The slope of the Hamassa watershed is determined using a digital elevation model (DEM). Areas that are flat or nearly flat have slopes ranging from 0 to 3%, while those with slopes between 3 to 8% are considered gently sloping. Terrain with slopes of 8 to 15% is classified as sloping, and areas with slopes between 15 to 30% are labeled as moderately steep. Regions with slopes greater than 30% are identified as steep, as indicated in a recent study by Wang *et al*. (2023). For this study, the slope classes in the Hamassa watershed are categorized as follows: flat or almost flat (0-3%), gently sloping (3-8%), sloping (8-15%), moderately steep (15-30%), and steep (>30%)(Figure3.2).

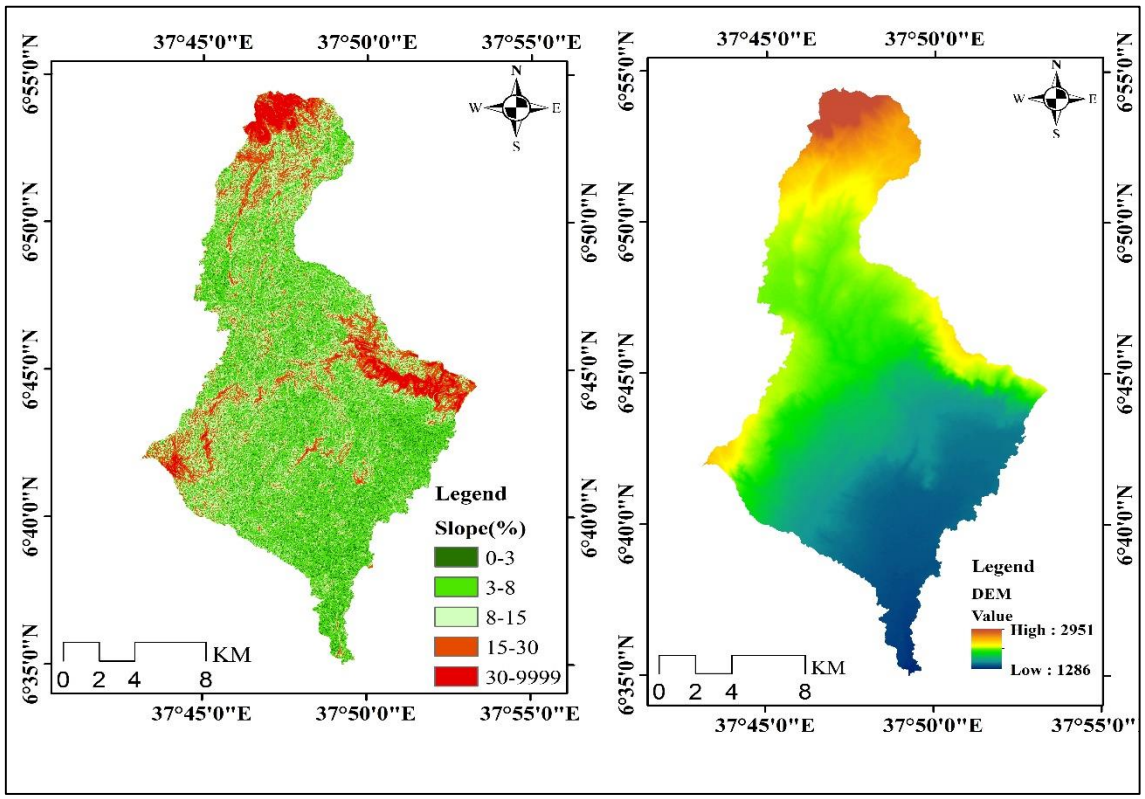

Figure 3.2 Slope class and topography of study area

3.1.3 Climate

The climate of the study area is characterized by three seasons depending on the position of the intertropical convergence zone, the amount of rainfall, and the timing. According to Gorfu and Ahmed (2012), the watershed is divided into three main agro-ecological zones based on Ethiopia's traditional agro-ecological zone classification methods: Kolla (hot lowlands) below 1500m amsl, Woina dega (midlands) ranging from 1500 to 2500m amsl, and Dega (highlands) covering areas from 2500 to 3000m amsl.

i. Rainfall

The annual rainfall in the watershed varies from 348.96 to 1851.2 mm, while the mean annual rainfall varies from 789.95 to 1332.52 mm and the mean monthly rainfall varies from 19.12 to 186.62 mm, as shown in Figures 3.3, and 3.4. The maximum mean monthly rainfall of the Hamassa watershed was recorded in April, May, July, and August. November to February dry period based on the metrological data of five stations Abayya, Billate, Bodity, Humbo, and Wolaita Sodo.

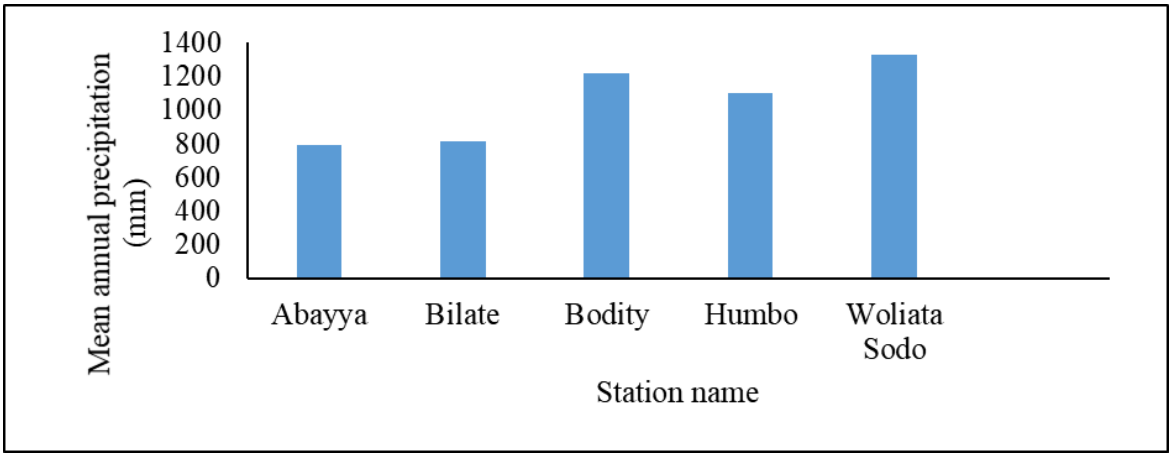

Figure 3.3 Mean annual precipitation of selected station in the Hamassa watershed

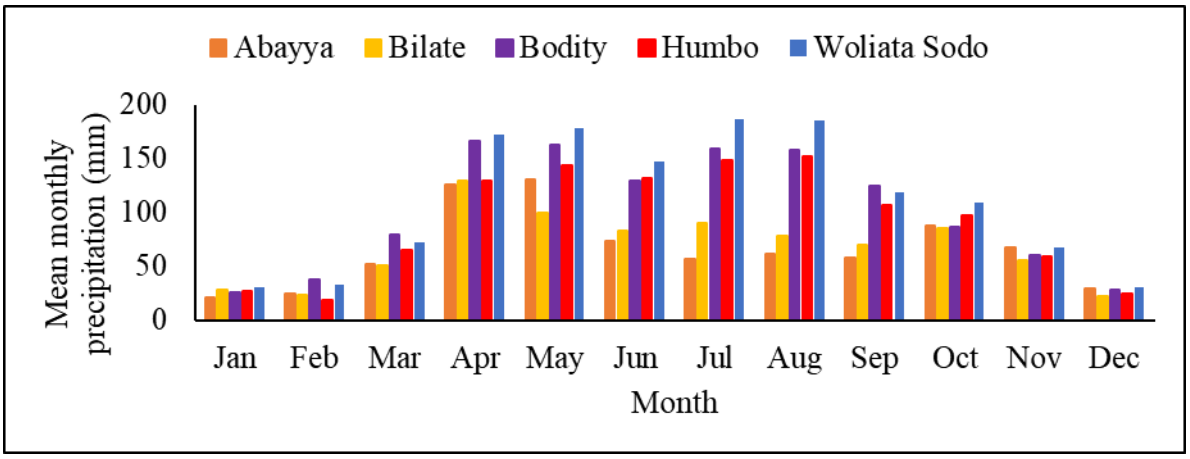

Figure 3.4 Mean monthly precipitation of selected station in the Hamassa watershed

ii. Temperature

As shown in Figure 3.5, the mean monthly minimum temperature in the Hamassa watershed's surrounding station ranged from 12.52℃ to 18.53℃, while the mean monthly maximum temperature varied from 21.29 ℃ to 33.1℃.

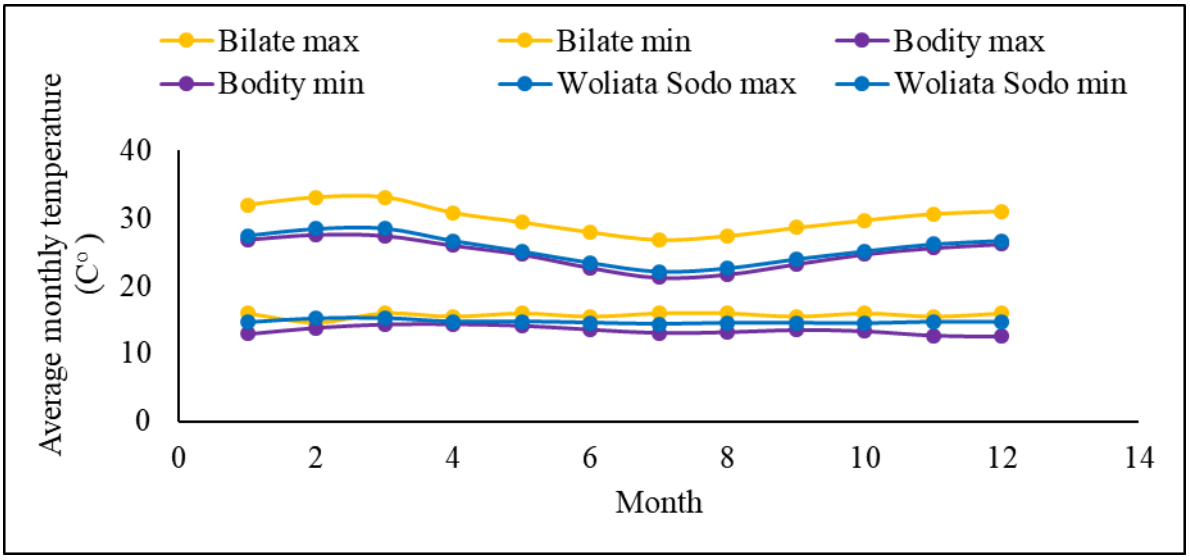

Figure 3.5 Average monthly temperature of the selected station in the Hamassa watershed

3.1.4 Soil and land use land cover

In the study area, the soil types include chromic luvisols, chromic vertisols, eutric nitosols, leptosols, pellic vertisols, and dystric nitisols. Among these soil types, chromic vertisols are the most common in the Hamassa watershed. The land use land cover in the Hamassa watershed are classified into five primary types, these primary land use land cover types in the Hamassa watershed consist of agricultural land, forested areas, grass area, shrub land and urban area.

3.2 Material used

i. ArcGIS

ArcGIS is a system for those who need accurate geographic information for decision-making. It allows collaboration, authoring of data, maps, and models, and sharing across desktops, browsers, or fields. It's a suite of GIS software by ESRI, useful in urban planning, resource management, and environmental science. It handles spatial data, analysis, and communication effectively. The goal is to provide a comprehensive platform for GIS mapping and analysis to aid in informed decision-making about the environment, resources, and infrastructure (Mittapalli and Gorthi, 2014). For this study, ArcGIS 10.3.1 was used for watershed delineation integrated with Arc SWAT, spatial data processing, and for identifying drought hotspot areas.

ii. Arc SWAT

Arc SWAT 2012, an extension of ArcGIS 10.3, provides a graphical user interface for the SWAT model. To create a SWAT dataset, it requires access to ArcGIS-compatible raster and vector datasets, along with database files containing watershed information. SWAT is a hydrologic model used to forecast the effects of land management practices on water, sediment, and agricultural yields in diverse watersheds over extended periods. It was used for stream flow modeling in this study. Arc SWAT serves as an interface for SWAT within ArcGIS, facilitating analysis (Winchell *et al*., 2013).

iii. Climate model data for hydrologic modeling

Climate model data for hydrologic modeling (CMhyd) tool, developed for bias correction of climate data from RCMs, uses a transformation algorithm to adjust climate model outputs, assuming that the correction parameters for current conditions will also apply to future conditions (Rathjens *et al*., 2016). The tool has been widely used for bias correction of precipitation and temperature for various applications (Mami *et al*., 2021; Worku *et al.*, 2020; Yeboah *et al*., 2022).

iv. Drought indices calculator

A drought indices calculator is used for the calculation of drought indices, suitable for drought characterization, drought monitoring, spatial analysis of drought, and investigation of climatic scenarios. Applicable for several types of droughts (meteorological, hydrological, agricultural) and different locations. It was also taken into account that drought studies are particularly essential in arid and semi-arid regions, where data availability is usually limited (Borg, 2009; Pashiardis and Michaelides, 2008; Tigkas *et al*., 2015). The drought indices calculator calculates the reconnaissance drought index, stream flow drought index, and standardized precipitation index. DrinC software includes three main stages data management and input parameters, selection of appropriate reference periods and time steps, and drought indices calculation (Tigkas *et al*., 2022). In this study, the Drinc software was used to calculate the standardized precipitation index (SPI) and the streamflow drought index (SDI) to characterize hydrological drought under both current conditions and projected climate change scenarios.

v. SWAT_CUP

An uncertainty analysis software tool called SWAT_CUP 5.1.6.2 is integrated with Arc SWAT. Its main duties include sensitivity analysis, validation, and calibration of the SWAT model. Stream flow data is frequently adjusted and verified using this software. Through the

application of SWAT_CUP 5.1.6.2, users can efficiently optimize the parameters of the SWAT model, verify its precision, and evaluate the model's responsiveness to diverse inputs, thereby augmenting the overall dependability of the model's forecasts (Truneh *et al*., 2022). It was used for sensitivity analysis, calibration, and validation of stream flows.

Table 3.1 Essential material, software, and tools

No	Software	Purpose
1	Arc GIS 10.3.1	Watershed delineation, spatial data processing, and running arc SWAT software
2	ArcSWAT2012_10.3.1	Hydrologic modeling purpose
3	CMhyd	To provide bias correction of climate data
4	DrinC	To calculate the SDI and SPI
5	Google Earth Pro 7.2.3	Investigation of the study area
6	SWAT-CUP 5.1.6.2	Model calibration and validation

3.3 Data collection

Studies of water resource development and management depend heavily on hydrological-meteorological data. Meteorological data such as rainfall, temperature, relative humidity, wind speed, and solar radiation, future climate data, spatial data like DEM, land use land cover, and soil data, and hydrological data including stream flow data. These data should be stationary, consistent, and homogeneous when used to simulate a hydrological system. Secondary data sources include the Alaska Satellite Facility (DEM), Coordinated Regional Climate Downscaling Experiment Project (CORDEX), the Ministry of Water Resources and Energy (MoWRE) for the land use land cover map, soil map, and hydrological data, and the National Meteorological Institute for weather data.

i. Digital elevation model (DEM)

One of the primary inputs of the SWAT model is the digital elevation model. The SWAT model uses DEM to delineate watersheds and, in combination with soil, and land use land cover data, defines hydrologic response units (HRUs). In Arc SWAT 2012 integrated with ArcGIS 10.3.1, the DEM helps delineate watersheds and analyze topography, elevation,

drainage patterns, and sub-basin parameters like slope gradient and stream characteristics. The DEM resolution is crucial, impacting sub-basin classification, stream networks, and overall model accuracy. Lower DEM resolution can reduce stream flow and watershed area, affecting watershed delineation and model projections (Gassman *et al*., 2007). The quality of DEM data significantly influences the hydrological model's output, emphasizing the importance of using the best available DEM data. For this study, the DEM of 12.5 m by 12.5 m resolution was downloaded from NASA's website: https://asf.alaska.edu.

The projected map was used in the watershed delineation in Arc SWAT which is the interface in the ArcMap to use it in the SWAT model. The minimum elevation is 1286m and the maximum elevation is 2951m above sea level.

ii. Land use land covers

One of the primary input datasets for the SWAT model is land use land cover, crucial for defining hydrological response units (HRUs) within the watershed (DeFries and Eshleman, 2004; Gebremichael *et al*., 2021). It is obtained from the Minister of Water Resources and Energy (MoWRE). Land use map reclassification was performed to categorize land use based on specific land cover types, with corresponding crop parameters selected from the SWAT database. A lookup table was created to map grid values to SWAT land cover classes using four-letter SWAT codes for different land cover types. The land use land cover within the Hamassa watershed are classified into five primary types, as illustrated in Figure 3.6. These primary land use land cover types in the Hamassa watershed consist of agricultural land (75.93%), forested areas (2.99%), Grass area (8.43%), shrub land (11.01%) and with the remaining (1.64%) of the watershed covered by urban area.

iii. Soil data

Soil data is important spatial input data for the SWAT model. SWAT model required different soil textures and physicochemical properties such as soil texture, available water

content, hydraulic conductivity, bulk density, and organic carbon content for different layers of each soil type.

Soil data of the study area is obtained from the Ministry of Water Resources and Energy (MoWRE). A lookup table was created to map grid values to SWAT soil type using four-letter SWAT codes. The soil type obtained from Ministry of Water Resources and Energy not include SWAT code in the SWAT database. Therefore, SWAT does not consider of soil data in the watershed. To fulfill this gap new soil data is downloaded from MWSWAT and their properties were added to the soil database by considering soil texture and soil group.

The watershed, include chromic luvisols, chromic vertisols, eutric nitosols, leptosols, pellic vertisols, and dystric nitisols soil type as indicated in Figure 3.6 and Table 3.2. Among these soil types, chromic vertisols are the most common in the Hamassa watershed, constituting 75.27% of the total soil composition. Following Chromic vertisols, chromic luvisols account for 9.71% of the soil types, while Dystric nitisols make up 7.6% of the soil distribution in the watershed. Clay soil texture predominates in nearly half of the Hamassa watershed region.

Table 3.2 Soil types, land use land cover, and their area coverage in the Hamassa watershed.

No	Soil type	SWAT soil code	Area (%)	Land use land cover	SWAT code	Area (%)
1	Chromic luvisols	Lc67-2b-730	9.7	Agricultural land	AGRL	75.93
2	Chromic vertisols	Vc1-2-3a-258	75.27	Forest	FRST	2.99
3	Dystric nitosols	Nd11-153	7.6	Grass land	RNGE	8.43
4	Eutric nitosols	Ne12-2c-155	1.21	Shrub land	RNGB	11.01
5	Leptosols	Lp12-1a-793	5.11	Urban area	URBN	1.64
6	Pellic vertisols	Vp1-3a-283	1.1			

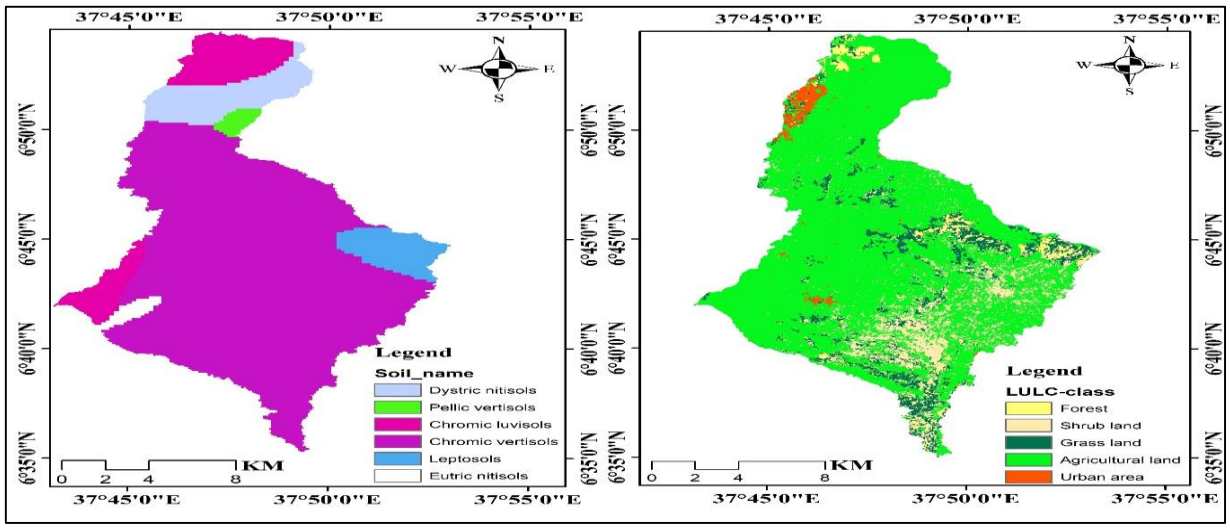

Figure 3.6 Soil type and land use land cover map of Hamassa watershed

iv. Meteorological data collection

The hydrological balance is influenced by weather factors such as relative humidity, wind speed, solar radiation, temperature, and precipitation. This data was provided by the National Meteorological Institute (NMI) and was collected from stations located in Abayya, Billate, Bodity, Humbo, and Wolaita sodo.

Table 3.3 Available climatic data of the selected stations

No	Station name	Precipitation	Temperature	Relative humidity	Wind speed	Sunshine hour	Observation period(daily)
1	Abayya	✓					1992-2022
2	Billate	✓	✓	✓	✓	✓	1992-2022
3	Bodity	✓					1992-2022
4	Humbo	✓					1992-2022
5	Wolaita	✓	✓	✓	✓	✓	1992-2022

v. Future climate data

Various Global and Regional Climate Models (GCMs and RCMs) are now available to simulate temperature and precipitation to a basin or local levels, helping to better understand and estimate acceptable future climate. (Gado *et al.*, 2022; Yeboah *et al*., 2022). The precipitation and maximum and minimum temperature data were derived from the future climate projections of the CORDEX project. The Coordinated Regional Climate Downscaling Experiment Project's climate model output has been used to gather historical and future meteorological data. Data source https://esgf-data.dkrz.de/search/cordex-dkrz/. The CORDEX Africa dataset is a CORDEX domain, developed specifically for climate impact study in the Africa zone.

Multiple RCMs were used in its design to provide rationalized, predictable variations in local climates and to assess any potential sources of projection uncertainty (Yeboah *et al*., 2022). Moreover, (Rathjens *et al*., 2016) state that it is a trustworthy source for regional climate models. Among the different data nodes in GCMS like Max Planck Institute for Meteorology Earth System Model version 1.2 (MPI-ESM1.2) (Mauritsen *et al*., 2019), the Centre National de Recherches Météorologiques (CNRM-CM5) (Voldoire *et al*., 2013), the Hadley Centre Global Environmental Model Earth System (HadGEM2-ES) (Collins *et al.*, 2011) and the GFDL NOAA's Earth System Models (ESMs) (Dunne *et al*., 2020).

This study has used only the Hadley Centre Global Environmental Model Earth System (HadGEM2-ES) model to develop climate scenarios under RCP2.6 and RCP8.5 concentration scenario. RCP2.6 and RCP 8.5 were selected because these concentration scenarios represent possible radiative forcing levels in the year 2100 relative to pre-industrialization. RCP8.5 represents high concentration scenarios with increasing radiative forcing pathway resulting in 8.5 W/m^2 by 2100, while RCP2.6 represents low concentration levels of 2.6W/m^2 that could be reached at stabilization after 2100.

vi. Hydrological data collection

The hydrological data is essential for conducting sensitivity analysis, calibration, and validation of the model. The observed flow data from the period 1992 to 2015, near the Wajjiffo gauge station was collected from the hydrology department of the Ministry of Water Resources and Energy (MoWRE).

Table 3.4 Secondary data type and source

Data category	Data type	Resolution	Source	Purpose
Meteorological data	Rainfall Temperature Relative humidity, Wind speed, and Sunshine hour	Daily	National meteorological institute	Input for SWAT Model
Future climate data	Precipitation Temperature	Daily	https://esgf-data.dkrz.de/search/cordex-dkrz/	Projection of climate variable
Hydrological data	Stream flow	Daily	Ministry of water resource and energy	SWAT Model calibration and validation
Spatial data	DEM	12.5m	https://asf.alaska.edu	Watershed delineation
	Soil data	250m	Ministry of water resource and energy	SWAT HRU definition input
	Land use land cover	30m	Ministry of water resource and energy	SWAT HRU definition Input

3.4 Data analysis

3.4.1 Fill missing data

All weather stations do not have to fulfill observation data because some weather stations may have instrumental errors or failures and others have a lack of record observers.

Therefore, it becomes essential to estimate or fill in these missing records. One method involves estimating missing precipitation data at a station by referencing observations from nearby stations, aiming for an even spatial distribution around the station with the missing data (Ajmi *et al*., 2019). As highlighted by Elshorbagy *et al*.(2000) and referenced by Merga, (2020), the issue of missing data is significant in hydrological analyses. To facilitate hydrological analysis and simulation, it is crucial to address and fill in missing data gaps effectively. In this study, two different methods were used to fill in missing rainfall data: the arithmetic mean method and the inverse distance method. The arithmetic mean method was used According to Chow *et al*. (1988), when less than 10% of the data was missing, while the inverse distance method was preferred when more than 10% of the data was missing, Inverse distance method is the most acceptable and is widely used for determining the missing precipitation for any scientific analysis.

Initially, missing data was filled using the normal ratio method to ensure the dataset was complete. After that, the consistency of the imputed values was checked. However, the inverse distance method was given higher priority for meteorological stations due to its superior consistency in filling in missing data. According to Richard H. (1998), the two formulas described in equation 3.1 and 3.2.

Arithmetic mean method

$$P_X = \frac{P_1+P_2+P_3\ldots\ldots\ldots\ldots\ldots P_n}{N} \qquad (3.1)$$

Where: N = number of index stations.,P_X= the precipitation from the station with the missed record and $P_1, P_2\ , P_3 \ldots\ldots\ldots\ldots P_n$ is the corresponding index station.

Inverse distance weighing method

$$P_X = \frac{\sum_{i=1}^{n} P_i * W_i}{\sum_{i=1}^{n} W_i} \qquad (3.2)$$

Where: P_X is unknown /missing precipitation, P_i value of known points, $W_i=\frac{1}{D^2}$, and $D^2=(\Delta x^2+\Delta y^2)$ is the distance of the station in x and y coordinates, taking in the missing precipitation station at (0,0) position.

Also, the missing stream flow data records were filled by a simple linear regression method developing a correlation between the station with missing data and any of the adjacent stations with the same hydrological features of the stream flow station. The correlation equations used for the near Wajjifo gauging station in terms of the Humbo olfino gauging station. The two stream flow gages near Wajjiffo (let Y) and Humbo olfino (let X) have the records of daily stream flow, i.e. Y1, Y2, ..., YN and X1, X2 ..., X N. The stream flow Y_t is missing. The filling of missed data is taken based on a simple linear regression method (Equation 3.3).

$$Yt = a + bXt \tag{3.3}$$

In which the parameters a and b can be estimated by:

$$\hat{a} = \bar{Y} - \hat{b}\bar{X} \text{ and } \hat{b} = rxy\frac{Sy*}{Sx*} \tag{3.4}$$

Where *Y and X* are the sample means, *S *Y* and *S *X* are the sample unbiased standard deviations of *Y* and *X*, respectively, and *rXY* is the cross-correlation coefficient between *X* and *Y*. The latter term can be estimated as:

$$rxy = \frac{\frac{1}{N}\sum[(Xt-\bar{X})(Yt-\overline{Yt})}{SxSy} \tag{3.5}$$

Where *Sy* and *Sx* are the sample-biased standard deviations rxy indicates the relationship between the two variables. The higher the square value of rxy indicates the best fit of the regression equation.

3.4.2 Consistency of meteorological data

The consistency of rainfall records at a specific station can be influenced by various factors. To evaluate the homogeneity and consistency of time-series observational data, it is essential to ensure that periodic data are proportionate to an appropriate simultaneous period. This proportionality can be examined through a double mass analysis, as outlined by Terakawa,

(2003), involving the plotting of accumulated rainfall and hydrological data against the average value of all neighboring stations (Figure3.7). This method helps in assessing the reliability and uniformity of rainfall data for further applications. The equation was described below to check the consistency of rainfall data (Equation 3.6).

$$P_{CX} = P_X * \frac{M_C}{M_a} \quad (3.6)$$

Where: P_{CX}= Corrected precipitation at any period t at station X; P_X = Originally recorded precipitation at period t at station X; M_C=Corrected slope of double mass curve; M_a=Original slope of the double mass curve.

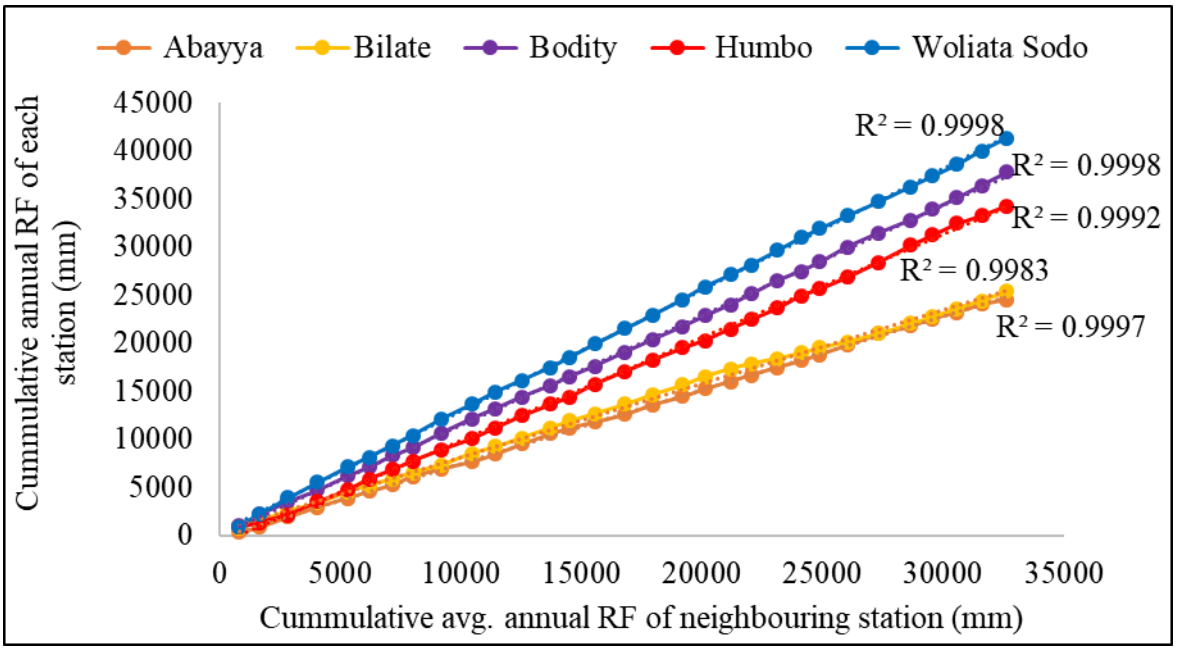

Figure 3.7 Double mass curve plot of each station

3.4.3 Homogeneity test

In research, it is crucial to have reliable data without any artificial patterns or unexpected changes. To ensure data reliability, the homogeneity test is employed to detect any deviations in statistical properties within a time series, which can stem from natural or human-induced

factors like land use modifications or observation station relocations. When selecting a meteorological station for annual rainfall estimation, assessing the homogeneity of a group of stations is crucial (Bickici Arikan and Kahya, 2019). The homogeneity test was an arithmetical procedure used to determine whether a data series was derived from homogeneous sources and to identify data changeability. The homogeneity test for this study was conducted using the Rainbow software (Raes *et al.,* 2006) all stations were checked at a 5% significance level and satisfied the test for homogeneity (Appendix) and non-dimensional method (Figure 3.8).

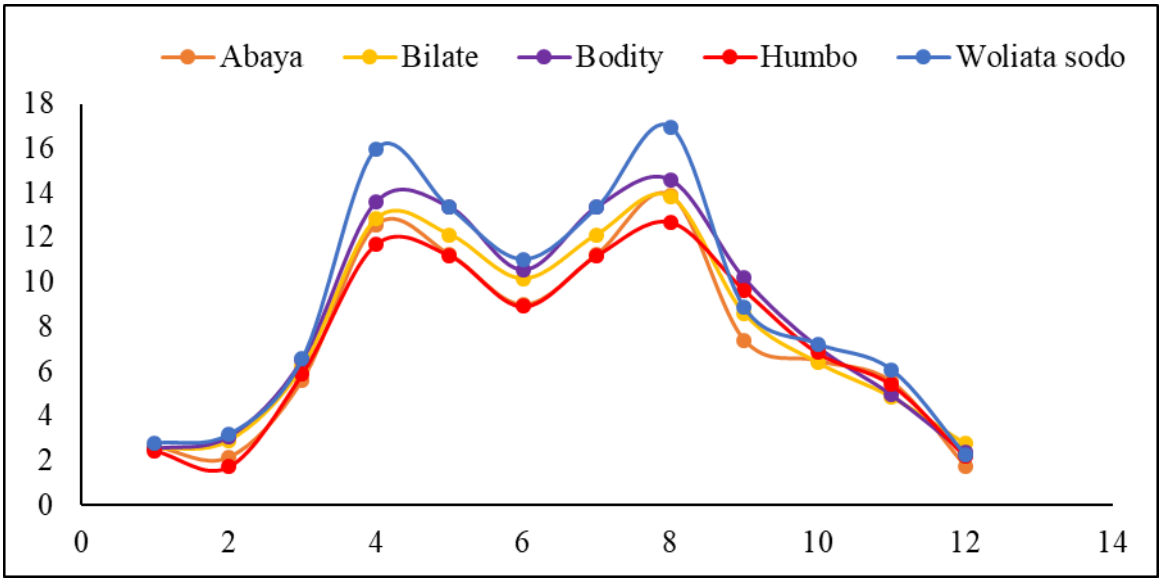

Figure 3.8 Homogeneity test of each station

3.4.4 Outlier test

According to Cunderlik (1992), the first step in the stream flow data screening process is a fast visual scan of the data time series to identify gross errors like incorrect peak flow, missing recordings, and flow of constant filling missing data. Outliers' tests were made in this research to check the quality of flow data. The flow data which was prepared as per the model requirement, was then used for model calibration and validation. The daily observed streamflow data changed to monthly streamflow data by using Excel.

A data point that deviates considerably from the trend of the remaining data and falls outside of threshold bounds is called an outlier. The magnitude of the statistical parameters calculated from the data, particularly the small sample size, is strongly impacted by the retention and deletion of these outliers. Tests for high outliers are prioritized if the station skew is greater than (+0.4); tests for low outliers are prioritized if the station skew is less than (-0.4). Before removing any outliers from the data set, tests for both high and low outliers should be conducted when the station skew is between (±0.4). Tests for both high and low outliers should be applied before detecting any outliers from the data set (Blagojevic *et al*., 2014).

The following frequency equation can be used to detect high outliers:

$$XH = Xav + KnS \quad (3.7)$$

Where XH = Logarithmic high-outlier test threshold, S standard deviation, Kn is frequency factor representing the statistic that depends on significance level a and sample size n. For 10% significance- -level and sample size n from the normal distribution

$$Kn = -0.9043 + 3.345\sqrt{LogN} - 0.4046LogNKnS \quad (3.8)$$

If the logarithms of values in a sample are greater than XH in the above equations, then they are considered high outliers. A similar equation can be used to detect low outliers:

$$XL = Xav - KnS \quad (3.9)$$

XL: - logarithmic low- outlier test threshold

The outlier test result shows that the largest recorded value does not exceed the high outlier test threshold value and the smallest recorded value is not below the low outlier test threshold value. Consequently, no high or low outliers were found (Appendix 7.8).

3.4.5 Bias correction

Climate variables such as rainfall and temperature obtained from coarse-resolution climate models are highly affected by different factors such as mountains and clouds which may not probably be taken into consideration in the global climate models development process because of their coarse resolution (Rathjens *et al.,* 2016). Thus, to reduce the deviation of climate model output from the real observed data of meteorological stations, the bias correction process was needed. For this study, the power transformation method for precipitation and variance scaling for temperature bias correction was selected.

Power transformation of precipitation: The precipitation is usually varied spatially, temporal, and highly nonlinear. Power transformation is a nonlinear method that corrects both the mean and variance of precipitation(Teutschbein and Seibert, 2012). In this nonlinear correction in an exponential form, $a.P^b$ can be used to adjust the variance statistics of a precipitation time series. The parameters a and b are determined for each month. The correction method is applied by comparing the daily observed precipitation at each station with the nearest grid point of the RCM considering the grid points as a single station on the watershed. The power transformation method is explained in (Equation 3.10)

$$P^* = a \times P^b \tag{3.10}$$

Where, $P^*$is corrected precipitation, and P is simulated precipitation. Parameters a and b are estimated by equalizing the coefficient of variation (CV) of the corrected simulations and the CV of the observed values. The remaining parameters and procedures for estimating the corrected precipitation are expressed in (Teutschbein & Seibert, 2012).

Variance scaling of temperature: The power transformation method is an effective method to correct both the mean and variance of precipitation, but it cannot be used to correct temperature time series, as the temperature is known to be approximately normally distributed (Bhatti *et al*., 2016).

This method was developed to correct both the mean and variance of normally distributed variables like temperature (Teutschbein and Seibert, 2012) using (Equation 3.11).

$$T_{corr} = \mu_{obs} + \frac{\sigma_{obs}}{\sigma_{rcm}}(T_{rcm} - \mu_{rcm}) \quad (3.11)$$

Where, T_{corr} is the corrected daily temperature, T_{rcm} is the uncorrected daily temperature obtained from the RCM model, T_{obs} is observed daily temperature while $\mu_{obs}\ and\ \mu_{rcm}$ is the mean of the observed and simulated daily temperature and σ_{obs} and σ_{rcm} is the standard deviation of the observed and simulated daily temperature.

The observed data of 1992–2004 was used for bias correction of the historical RCM data of the corresponding grids. The power transformation for precipitation and variance scale methods for the temperature was used to correct the future climate data for both RCP2.6 and RCP8.5 scenarios. The observed and the corrected RCP precipitation under both scenarios (Figure 3.9) (Figure 3.12). Similarly, the minimum and maximum temperatures observed and corrected RCP data under both scenarios (Figure 3.10, Figure 3.11, Figure 3.13, and Figure 3.14).

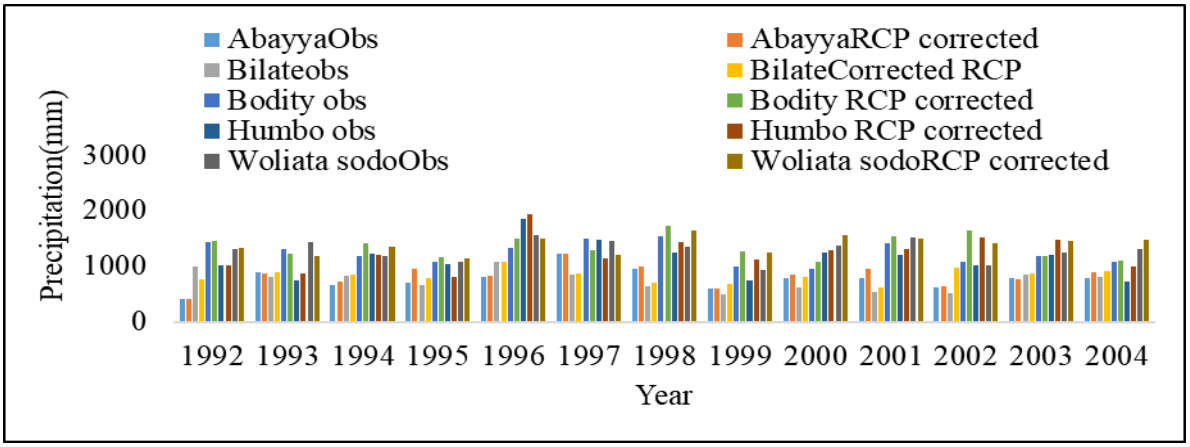

Figure 3.9 Observed and corrected precipitation under RCP2.6

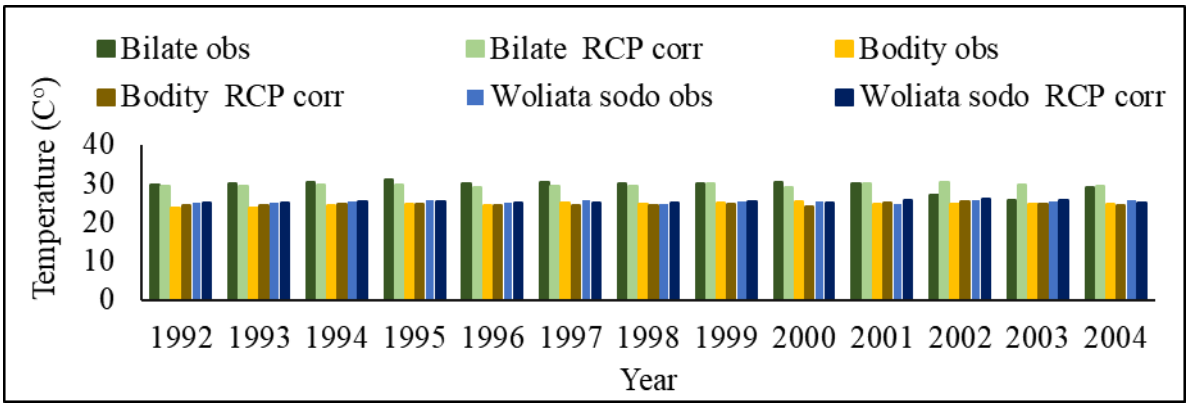

Figure 3.10 Observed and corrected maximum temperature under RCP2.6

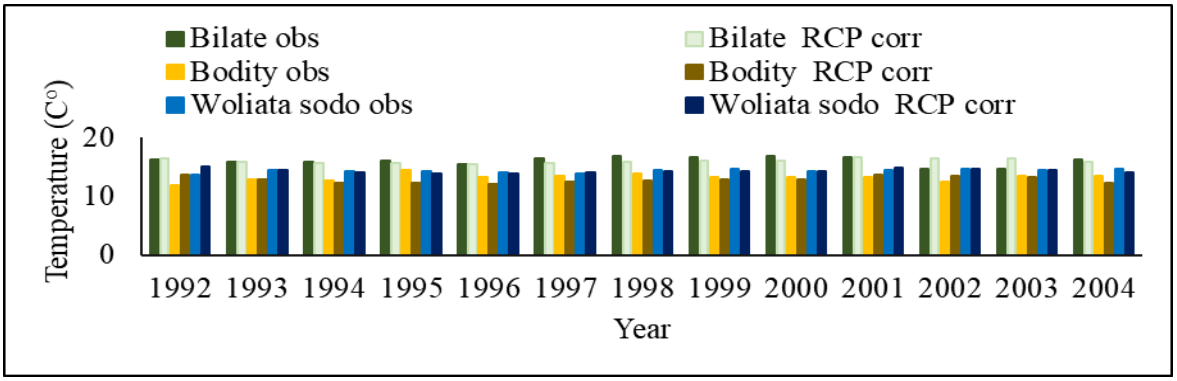

Figure 3.11 Observed and corrected minimum temperature under RCP2.6

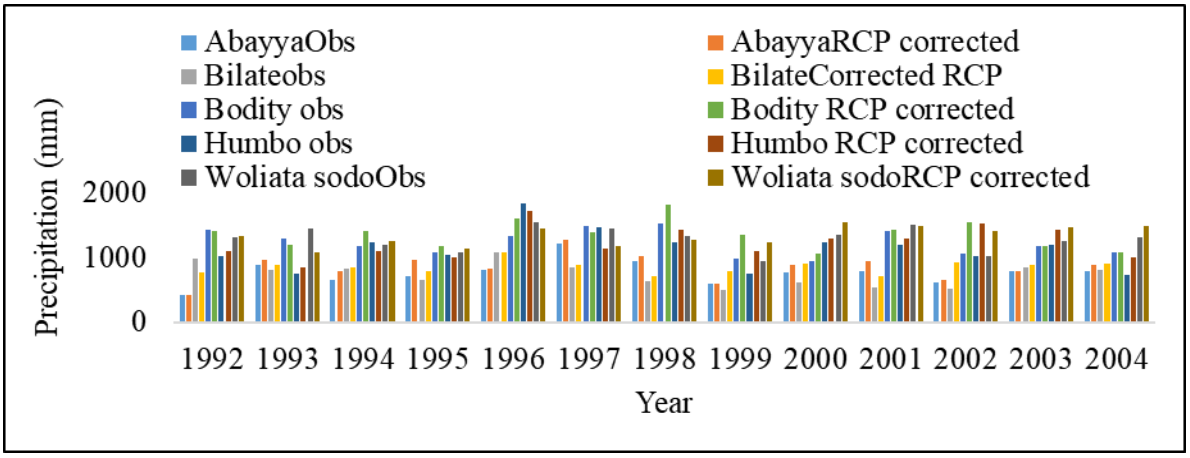

Figure 3.12 Observed and corrected precipitation underRCP8.5

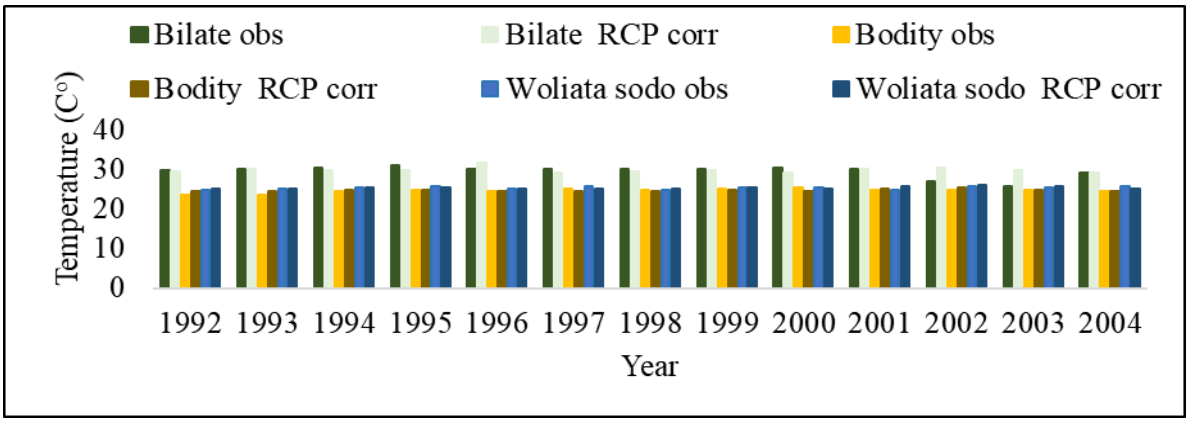

Figure 3.13 Observed and corrected maximum temperature under RCP8.5

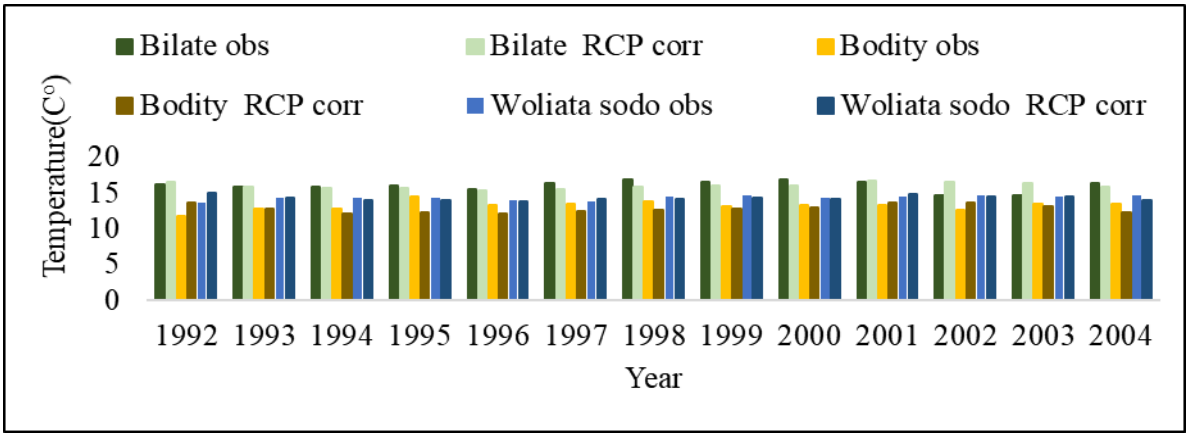

Figure 3.14 Observed and corrected minimum temperature under RCP8.5

3.5 SWAT Model setup

The soil and water assessment tool (SWAT) is a widely recognized hydrological modeling tool utilized for a range of hydrologic and environmental simulations (Guug *et al*., 2020; Tan *et al*., 2020). Mainly, SWAT is employed to assess water resources and stream flow, understand the impact of a watershed, analyze the influence of land use management on agriculture and water quality, and evaluate the effects of climate change on watershed hydrology (Arnold *et al*., 2012).

The model calculates important hydrologic elements such as evapotranspiration, surface runoff, peak runoff rate, groundwater flow, and sediment yield for each hydrologic response

unit (HRU). The water balance equation within the SWAT model is utilized to replicate the hydrologic cycle (Equation 3.12).

$$SW_t = SW_t + \sum_{i=1}^{n} R_{day} - Q_{surf} - E_a - W_{sep} - Q_{gw}) \quad (3.12)$$

Where:- SW_t is the final water content (mm), SW_o is the initial soil water content on the day I (mm), t is the time in a day, Rday is the precipitation amount on specific days(mm), Q_{surf} is the runoff amount on a specific day i (mm),$E_a$is evapotranspiration amount on day i (mm H2O), W_{seep} is the amount of water percolated into the vadose zones on a day i (mm), day i (mm H2O), Q_{gw} is the return amount of flow on a day i (mm).

The SWAT model comprises various key elements, one of which is the estimation of surface runoff using different approaches. Among these, the modified SCS-CN2 method (Mishra and Singh, 2013) with a daily time step, or the Green-Ampt Mein–Larson infiltration equation (Beza *et al*., 2023) with hourly or sub-daily time steps, are the most commonly utilized methods for estimating surface runoff in SWAT models.

The SCS curve number method requires less data compared to the Green-Ampt method. Therefore, the SCS curve number method (Equation 3.13) was used to estimate the surface runoff volume in this study.

$$Q_{surf} = \frac{(R_{day} - I_a)\hat{}2}{(R_{day} - I_a + S)} \quad (3.13)$$

Where:- Q_{surf} is the depth of runoff in (mm), R_{day} is effective precipitation in (mm), $I_a$is the initial abstraction which includes surface storage, interception, and infiltration before runoff (mm), and S is the retention parameter (mm).

The retention parameter changes spatially due to changes in soil, land use, management, and slope and temporally due to changes in soil water content. The retention parameter is defined as land use, management, and slope and temporally due to changes in soil water content. the retention parameter is defined as

$$S = 25.4\left(\frac{100}{CN} - 100\right) \quad (3.14)$$

Where: -CN is the curve number for the day as a function of soil permeability, land use, and antecedent moisture content. The initial abstraction, Ia, is commonly approximated as 0.2S, and equation 3.13 becomes.

$$Q_{surf} = \frac{(R_{day} - 0.2S)\text{^}2}{(R_{day} + 0.8S)} \quad (3.15)$$

3.5.1 Watershed delineation

In this study, automated watershed delineation embedded in the Arc SWAT interface was used to delineate the watershed. The delineation process was based on DEM data as the primary input. The DEM data for the study area was first projected into the UTM zone 37N coordinate system of Ethiopia using ArcGIS software. This DEM data was then incorporated into the Arc SWAT model. The SWAT watershed delineation process involves five key steps: DEM setup, stream definition, outlet and inlet definition, watershed outlet selection, and the calculation of sub-basin parameters. For the stream definition, a threshold-based approach was employed to define the minimum size of the sub-watersheds. This helped minimize the uncertainty associated with the model outputs. Additionally, the flow direction and accumulation tools in Arc SWAT were utilized to compute the DEM cells and identify the outlet of the watershed, which was determined to be the lowest point where water flows out of the area. The outcome of the delineation process was the determination of the Hamassa watershed area as 28640.5 hectares, and the formation of 11 sub-watersheds within the overall watershed, as shown in Figure 3.15.

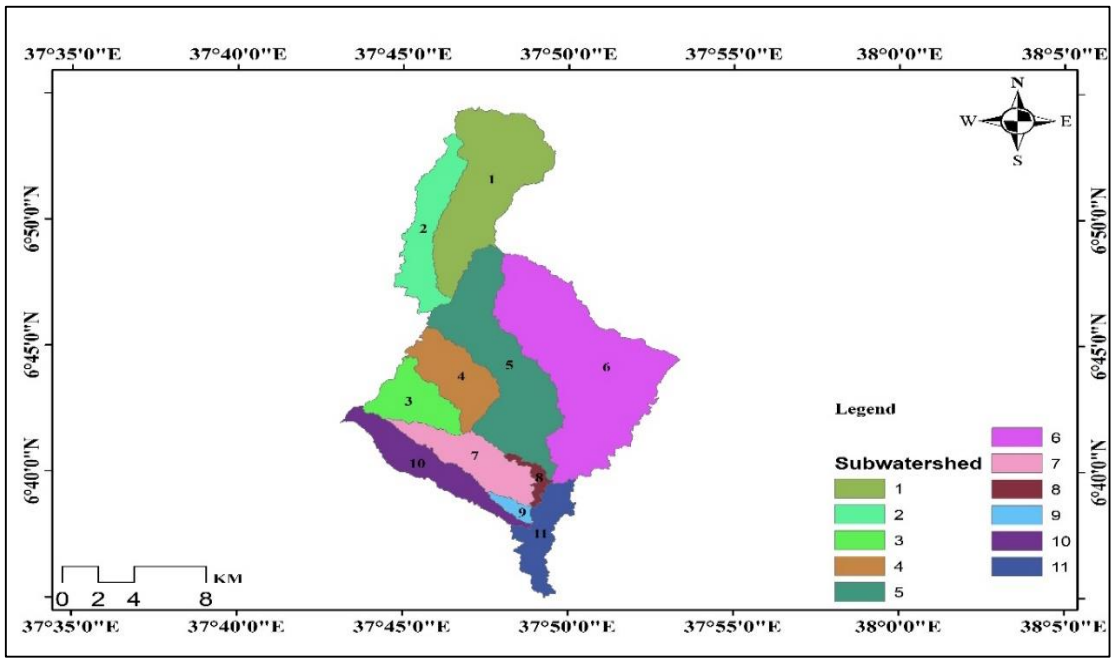

Figure 3.15 Number of sub-watersheds in Hamassa watershed

3.5.2 Hydrological response units

The sub-watersheds were divided into HRUs by assigning the threshold values of land use and land cover, soil, and slope percentage. The HRU analysis section takes land use, soil, and slope data, and divides each sub-basin into hydrologic response units, with specific combinations of the three layers 'respective characterizations. The land use land cover and the soil map were loaded into the SWAT interface separately to the delineated watershed and overlapped almost 100%. The soil map was linked to SWAT soil database information by loading a soil look-up table prepared according to SWAT input format, the parameters corresponding to each soil type loaded to the SWAT database. The multiple slope option which considers different slope classes for HRU definition was preferred over the single slope and the slope was classified According to Husen and Abate (2020) into five classes the bottom slope (0-3%), (3-8%), (8-15), (15-30) and greater than 30%. The definition of the watershed was given 10% for soil, 5% for LULC, and 15% for slope (Appendix 7.9). This classification depended on the objective of the study and was obtained from the literature (Setegn *et al*., 2008).

3.5.3 Weather generator

The long-period climatic data for full and realistic periods are scarce in developing countries. To solve this problem, the weather generator generates data using the observed one (Danuso, 2002). The SWAT Model contains a weather generator model called WXGEN (Williams, 1990). The Model requires the daily values of all climatic variables from measured data or generated from values using monthly average data for years. SWAT weather generator model (WGEN) was used to fill in missing values in weather data of precipitation, maximum and minimum temperature, relative humidity, wind speed, and solar radiation. This study uses a weather generator developed for Billate (Appendix 7.10) and Wolaita sodo (Appendix 7.11) meteorological station using the SWAT generator database.

3.5.4 Writing input tables and running the SWAT model

After all, reprocessing is done on DEM, land use, and slope data to create sub-basins and HRUs, the next step is to build database files that include information needed to generate other input for the SWAT model including weather data. Daily time series of weather data, which include precipitation, maximum and minimum air temperature data, relative humidity, solar radiation, and wind speed are required for the SWAT modeling. The periods of the measured weather data, obtained from the National Meteorology Institute of Ethiopia (NMI), differed from station to station. The SWAT database is updated to generate other weather variables using other stations that have full records of weather variables. Then, input database files using land use, soil, DEM, and weather data of the study were created as input data, and all commands were written to create the initial values of the model.

3.6 Model performance evaluations

3.6.1 Sensitivity analysis

The SWAT model has a large number of flow parameters, so it's crucial to identify the most sensitive parameters to improve the calibration of the hydrological model. The goal of sensitivity analysis is to determine the parameters that have the greatest impact on the flow

process. The parameter ranking is derived from the last iterations of SUFI-2, based on the t-stat and p-value. The t-stat represents the sensitivity of the parameter, with a higher absolute value indicating a more sensitive parameter. The p-value, on the other hand, represents the statistical significance of the parameter, with a lower p-value suggesting a more influential parameter.

By identifying the most sensitive parameters, the modeler can focus on calibrating those parameters more precisely, leading to a more accurate and reliable hydrological model (Daniel and Abate, 2022; Dibaba *et al*., 2020). Sensitivity analysis is a crucial method for determining the relationship between changes in model inputs (parameters) and the corresponding changes in model outputs. It serves two primary purposes: identifying the key parameters that significantly influence the simulated process, and determining the level of parameter precision required for effective model calibration (Arnold *et al*., 2012). Furthermore, sensitivity analysis provides a measure of the effect that changing one parameter has on another. Identifying the most sensitive parameters, allows the modeler to minimize the number of parameters that need to be calibrated, thereby reducing the time and effort required for the calibration and validation process. This approach also increases the accuracy of the calibration by reducing the overall uncertainty in the model (Gassman *et al*., 2014).

The SWAT-CUP (SWAT Calibration and Uncertainty Procedures) was run monthly from January 1, 1992, to December 31, 2015. The first 2 years, from January 1, 1992, to December 31, 1993, were used for model warm-up. The initial 21 parameters were selected based on studies conducted in the Rift Valley basin watersheds located near the Hamassa watershed (Daniel, 2024; Moshe *et al*., 2024). Additionally, they were chosen by considering the scenario (default) results from the Txt-In-Out folder after the SWAT model simulation. The streamflow simulation took into account several hydrological input parameters, including groundwater (.gw), management (. mgt), soil (.sol), hydrologic response units (. hru), routing (. rte), and sub-basin (. bsn) categories, as shown in Table 3.5.

Table 3.5 SWAT model parameters selected for sensitivity analysis source (Daniel, 2024)

NO	Parameter	Description	Range	Category
1	ALPHA_BF	Base flow alpha factor (days)	0–1	.gw
2	BIOMIX	Biological mixing efficiency	0–1	.mgt
3	CANMX	Maximum canopy storage	0–100	.hru
4	CH_K2	Effective hydraulic conductivity in main channel alluvium (mm/hr)	-0.01-500	.rte
5	CH_N2	Manning's 'n' value for the main channel	-0.01 -0.3	.rte
6	CN2	SCS runoff curve number (Initial SCS CN II value)	35–98	.mgt
7	EPCO	Plant uptake compensation factor	0–1	.hru
8	ESCO	Soil evaporation compensation factor	0–1	.hru
9	GW_DELAY	Groundwater delay (days)	0–500	.gw
10	GW_REVAP	Groundwater 'revap' coefficient	0.02–0.2	.gw
11	GWQMN	The threshold depth of water in the shallow aquifer required for return flow to occur (mm)	0–5000	.gw
12	HRU_SLP	Average slope steepness (m/m)	0–1	.hru
13	OV_N	Manning's 'n' value for overland flow	0.01–1	.hru
14	REVAPMN	Threshold depth of water in the shallow aquifer for 'revap' to occur (mm)	0–500	.gw
15	RCHRG_DP	Deep aquifer percolation fraction	0–1	.gw
16	SOL_AWC	Available water capacity of the soil layer	0–1	.sol
17	SOL_BD	Moisture bulk density	0.9-2.5	.sol
18	SOL_K	Saturated hydraulic conductivity	0–2,000	.sol
19	SOL_Z	Depth from the soil surface to the bottom of the layer	0–3,500	.sol
20	SURLAG	Surface runoff lag time	0.05–24	.bsn
21	SLSUBBSN	Average slope length (m)	10–150	.hru

The results of the global sensitivity procedure indicate that thirteen parameters (Table 3.6) were found to be sensitive, ranging from high to low sensitivity. These parameters include Curve number (R_CN2), Moist bulk density (R__SOL_BD(..).sol), Groundwater "revap"

coefficient (R__GW_REVAP.gw), Available water capacity of the soil layer (R__SOL_AWC(..).sol), Saturated hydraulic conductivity (R__SOL_K(..).sol), and base-flow alpha factor (V__ALPHA_BF.gw), which emerged as the top sensitive parameters. This finding can be further supported by a previous study conducted by Moshe *et al*. (2024), which performed a sensitivity analysis on a watershed model using the SUFI-2 algorithm in the Kalte watershed, Rift Valley River Basin, employing the absolute value of p-value and t-stat to indicate parameter sensitivity.

The study revealed parameters such as CN2.mgt, and GW_REVAP.gw, SOL_AWC.sol, SOL_K.sol, ALPHA_BF.gw, GW_DELAY.gw, SOL_BD.sol, GWQMN.gw, ESCO.hru, and SURLAG.bsn were identified as the most sensitive, a finding that closely aligns with the results of this study. This similarity may be attributed to the resemblance in land use land cover, and groundwater characteristics in the watersheds, indicating similarities in watershed management and ground model parameters also Hamassa watershed is in the Rift Valley Basin.

Table 3.6 List of parameters and their sensitivity rank

NO	Parameter	T-stat	P-value	Fitted value	Sensitivity rank
1	R__CN2.mgt	4.823	0.000003480	-0.212344	1
2	R__SOL_BD(..).sol	4.653	0.000007332	0.293661	2
3	V__GW_REVAP.gw	3.869	0.000164382	0.147248	3
4	R__SOL_AWC(..).sol	3.797	0.000215068	0.029488	4
5	R__SOL_K(..).sol	2.917	0.004100640	0.118184	5
6	V__ALPHA_BF.gw	2.704	0.007669953	0.715153	6
7	V__SURLAG.bsn	2.363	0.019464233	16.981316	7
8	V__ESCO.hru	2.308	0.022409765	0.864377	8
9	V__REVAPMN.gw	2.142	0.033843125	318.414612	9
10	V__CH_K2.rte	1.925	0.056244444	0.396108	10
11	V__GWQMN.gw	1.693	0.092531686	4148.507324	11
12	V__BIOMIX.mgt	1.2027	0.231030188	0.728107	12
13	V__GW_DELAY.gw	1.515	0.131723515	487.811127	13

r-existing parameter value is multiplied by (1± given value), v-existing parameter value is to be replaced by a given value, and a-a given value is added to the existing parameter value.

3.6.2 Model calibration and validation

Calibration serves as a fundamental aspect of minimizing prediction uncertainty within a model. It involves adjusting model parameters to align the model output with observed data and watershed characteristics. There are various types of SWAT calibration options auto-calibration, manual calibration, and a combination of two. The adjustment parameter can be used for manual or auto-calibration. In this study, the calibration process was done over 14 years observing stream flow data using automatic calibration from the period January 1, 1994-December 31, 2008 auto-calibration facilitated calibrate at least until the minimum recommended values were embraced by the model that is R^2, > 0.6, NSE > 0.5, and PBIAS < ±15 (Arnold *et al*., 2012) (Figure 3.16).

Validation is the process of comparing or examining the model's output data without making any changes in light of the goal. Validation's goal is to verify accuracy concerning the ground truth. The validation procedure involved running the model with the parameters determined during the calibration process and comparing the prediction with the observed data period (Refsgaard, 1997). Checking the R^2, NSE, and PBIAS values. In this study, the validation process was done using measured 7 years' stream flow data from the period January 1, 2009, to December 31, 2015, which is one-third of the measured stream flow data without further adjustment of the parameters (Figure 3.16).

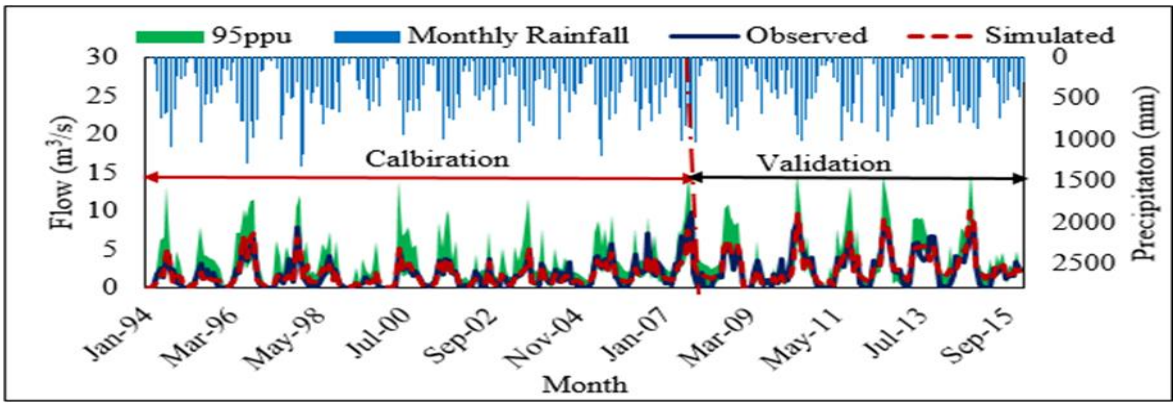

Figure 3.16 Model calibration and validation

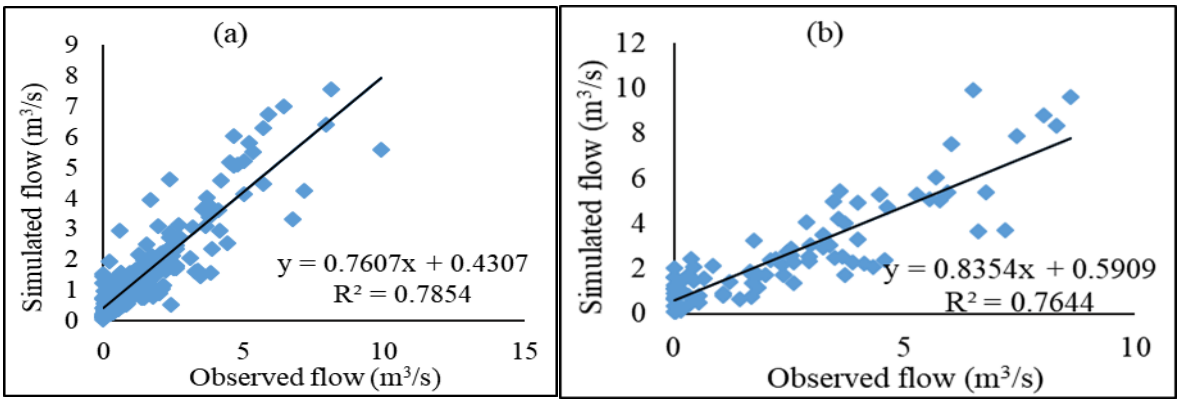

Figure 3.17 Scatter plot of model calibration (a) and validation (b)

In this study, the goodness-of-fit between the simulated and measured variables during both calibration and validation periods were evaluated using the graphical and statistical parameters such as Nash Sutcliff Efficiency (NSE), Coefficient of determination (R^2), and Percent bias (PBIAS). The model's performance was assessed through a time series plot of observed and simulated values, along with statistical measures such as R^2, NSE, and PBIAS. The analysis indicated very good agreement between observed and simulated monthly flow, as demonstrated in Table 3.8 and Figure 3.17 (a), the R^2, NSE, and PBIAS values (0.79, 0.78, and -1.0% respectively) aligning with the specified ranges for monthly model calibration.

Similarly, as shown in Table 3.8 and Figure 3.17 (b), the R^2, NSE, and PBIAS values for the monthly model validation (0.76, 0.75, and -6.1% respectively). Both calibration and validation results fulfilled the requirements suggested by (Arnold *et al*., 2012) for R^2, > 0.6, NSE > 0.5, and PBIAS < ±15% respectively as shown in (Table 3.7).

Table 3.7 Model performance rating Source (Arnold *et al*., 2012)

Performance Rating	NSE	%PBIAS	R^2
Very good	0.75<NSE<=1	PBIAS <= ±10	0.75 to 1
Good	0.65<NSE<=0.75	±10<= PBIAS <±15	0.65 to 0.75
Satisfactory	0.5< NSE = 0.65	±15 < = PBIAS < ± 25	0.5 to 0.65
Unsatisfactory	NSE<=0.5	PBIAS > = ± 25	<0.5

Table 3.8 Model performance

Objective function	Calibration	Validation
NSE	0.78	0.75
R^2	0.79	0.76
PBIAS (%)	-1.0	-6.1

The general framework that shows input data, process and out puts to achieve the objective of the study was prepared Figure (3.15).

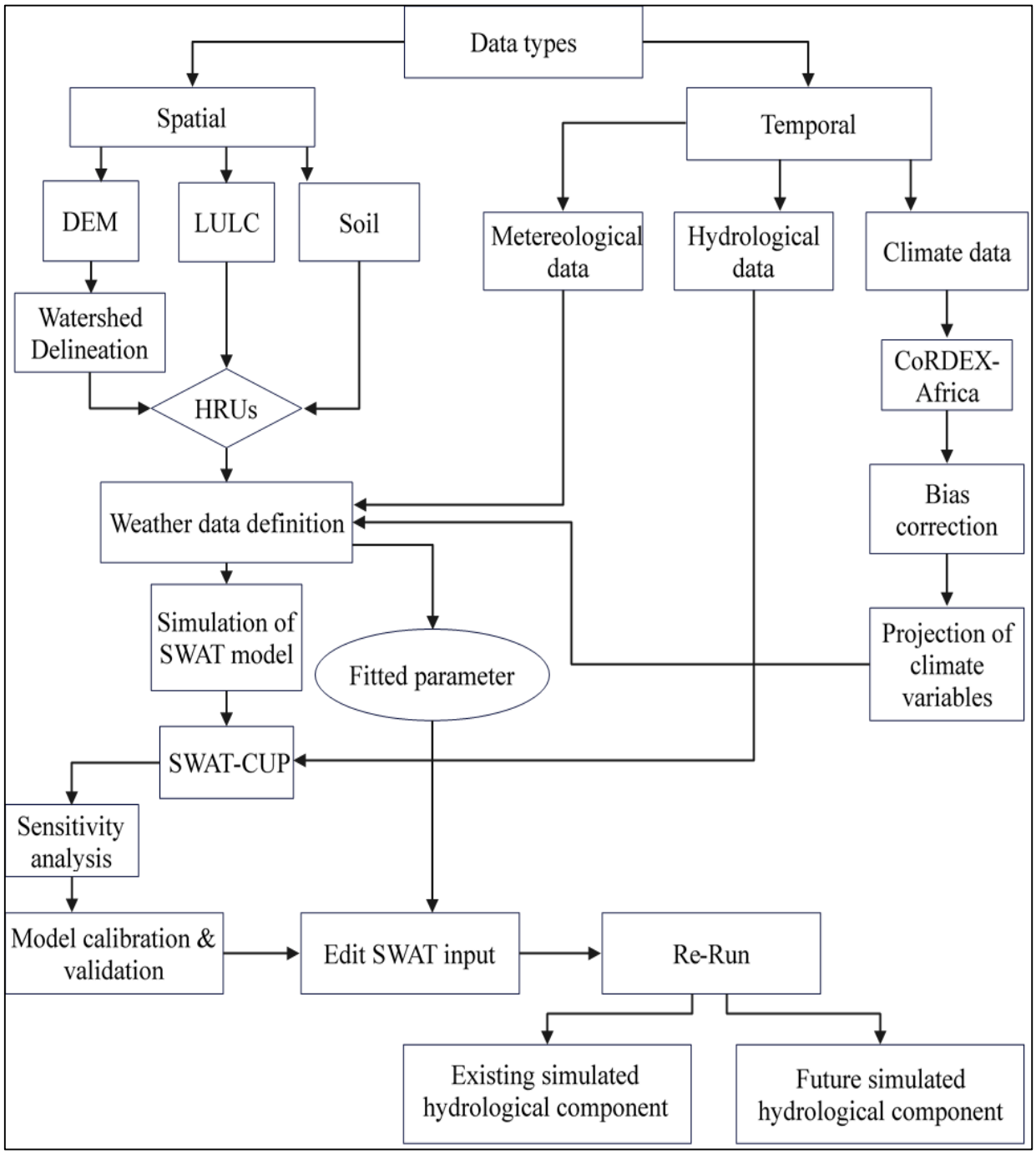

Figure 3.18 General frame work of the study

3.7 Hydrological drought analysis

To analyze hydrological drought in the Hamassa watershed, uses DrinC software to calculate the standardized precipitation index (SPI) and the streamflow drought index (SDI). Hydrological drought analysis using the standardized precipitation index (SPI) was conducted using monthly precipitation data. The SPI was calculated based on data from five stations (Abayya, Billate, Bodity, Humbo, and Wolaita Sodo) over 31 years to identify drought conditions under current conditions. Additionally, precipitation data from Regional Climate Models (RCM) was used to assess drought under climate change scenarios. This data was input into the DrinC software, which generated SPI values to analyze the annual drought severity in the study area. The SPI values range from -2 to +2, with extremely dry and wet conditions indicated by values below -2 and above +2, respectively as indicated in (Table 3.9) (Shah *et al*.,2015).

Hydrological drought conditions can be characterized using the streamflow drought index (SDI), which is effective for analyzing drought over various time scales. In this study, monthly simulated streamflow data was used to calculate the SDI. The data was organized as input into the DrinC software, which then generated the SDI values. These values were subsequently analyzed to determine the annual severity of drought in the study area. The SDI values range from -2 to +2, with values below -2 indicating extremely dry conditions and values above +2 indicating extremely wet conditions as indicated in (Table 3.9) (Nalbantis and Tsakiris, 2009). This range allows for a clear distinction between different levels of wetness and dryness, facilitating effective drought analysis and management.

3.8 Spatial variability analysis to identify drought hotspot area

Identifying the spatial extent of drought across a watershed is a crucial aspect of drought analysis and monitoring (Yisehak *et al*., 2021). This study employed spatial variability analysis using the streamflow drought index (SDI) to identify drought-prone areas within the watershed.

The analysis was conducted using ArcGIS software, and the SDI values for selected drought years were used as input to create a spatial distribution map of the watershed. The spatial variability analysis and visualization of the SDI in ArcGIS provided a comprehensive understanding of the drought dynamics within the watershed. This information is crucial for water resource managers and decision-makers to prioritize drought mitigation and adaptation strategies, targeting the identified drought hotspot areas and enhancing the overall drought resilience of the region.

Table 3.9 Drought classification according to SDI source (Nalbantis and Tsakiris, 2009) and SPI source (Shah *et al*.,2015).

No	SDI range	Category	SPI range	Category
1	≥2	Extremely wet	+2 and more	Extremely wet
2	1.5-1.99	Severely wet	1.5 to 1.9	Very wet
3	1-1.49	Moderately wet	1to1.49	Moderate wet
4	-0.49-+0.499	Normal	-0.99 to 0.99	Normal
5	-0.5- -0.999	Mild drought	-1 to -1.49	Moderately drought
6	-1- -1.49	Moderately drought	-1.5 to -1.9	Severely drought
7	-1.5- -1.99	Severely drought	-2 less	Extremely drought
8	≤ - 2	Extremely drought		

4 RESULTS AND DISCUSSIONS

4.1 Climate projection

The corrected future climate data are grouped into two near-term projections (2030 – 2060) and long-term projections (2061 – 2090). To assess climate change, the raw and corrected historical period (1992 – 2004), were compared to the corresponding raw and bias-corrected future precipitations and temperature based on the two scenarios RCP2.6 and RCP8.5, for near-term (2030 – 2060), and long-term (2061 – 2090).

4.1.1 The near-term projection (2030 – 2060)

The existing values of average minimum and maximum temperature of the watershed are 14.62C^{o} and 26.82 C^{o} respectively. The average annual minimum temperature for RCP2.6 and RCP8.5 were 15.95C^{o} and 17.8C^{o}, respectively which shows an increase of 1.33C^{o} in the case of RCP2.6 and 3.18C^{o} in the case of RCP8.5 from the existing period Figure 4.1 (a). The average annual maximum temperature for RCP2.6 and RCP8.5 were 28.2C^{o} and 29.2C^{o}, respectively which shows an increase of 1.38C^{o} in the case of RCP2.6 and 2.38C^{o} in the case of RCP8.5 from the existing period. Annually, the highest temperature occurs 28.8C^{o} in 2049 for RCP2.6 and 30.5C^{o} in 2053for RCP8.5, respectively Figure 4.1 (b).

Annually, the minimum precipitation was 776.85 mm in RCP2.6 and 511.1mm in RCP8.5, which occurs in 2049 and 2053 respectively and maximum precipitation was 2650.3 mm in RCP2.6 and 2688.2 mm in RCP8.5, which occurs in 2030 (Figure 4.2). The maximum precipitation occurs in July which has a value of 419.92 mm and 375.2 mm for RCP2.6 and RCP8.5 scenarios, respectively. Seasonally, the rainfall of the Hamassa watershed is high during the summer (Kiremt) season, under both scenarios RCP 2.6 and RCP 8.5. In contrast, the rainfall is low during the winter (Bega) season.

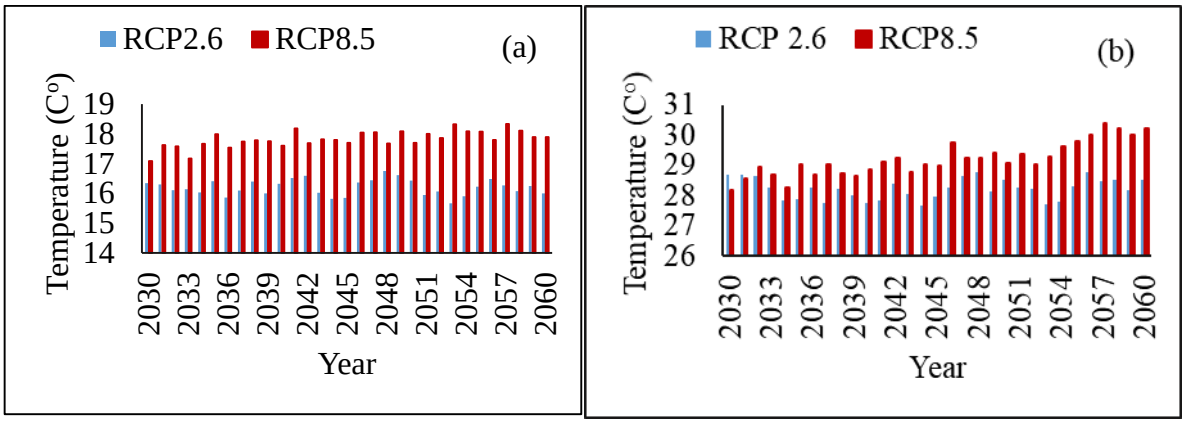

Figure 4.1 Near-term annual minimum and maximum temperature for both scenarios

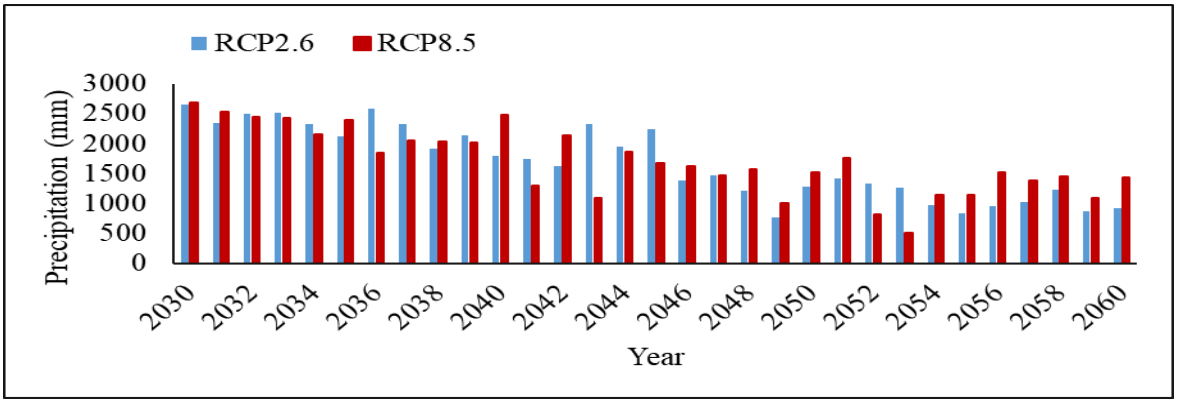

Figure 4.2 Near-term annual precipitation for both scenarios

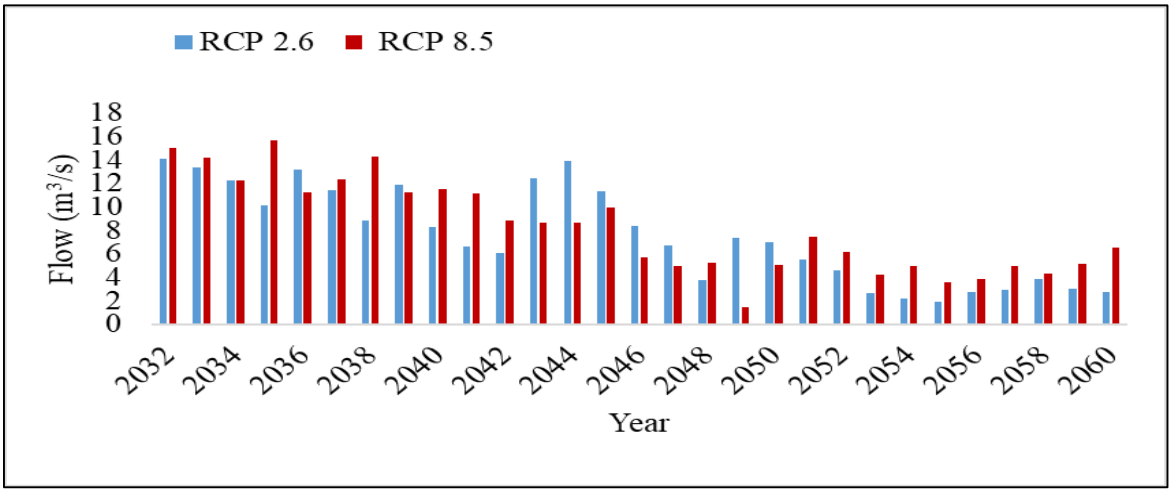

Figure 4.3 Near-term average flow for both scenarios

4.1.2 The long-term projection (2061 – 2090)

The average annual minimum temperature for RCP2.6 and RCP8.5 were 16.0C^{o} and 18.22C^{o}, respectively which shows an increase of 1.38C^{o} in the case of RCP2.6 and 3.5C^{o} in the case of RCP8.5 from the existing period Figure 4.4 (a). The average annual maximum temperature for RCP2.6 and RCP8.5 were 28.35C^{o} and 30.88C^{o}, respectively which shows an increase of 1.53C^{o} in the case of RCP2.6 and 3.9C^{o} in the case of RCP8.5 from the existing period. Annually, the highest temperature occurs 29.2C^{o} for RCP2.6 and 31.87C^{o} for RCP8.5, respectively which occurs in 2062 Figure 4.4 (b).

Annually, the minimum precipitation 818.33 mm in RCP2.6 and 712.75 mm in RCP8.5, will occurs in 2062 and the maximum precipitation will occur in 2089 and 2084 under RCP2.6, RCP8.5 respectively (Figure 4.5). The maximum precipitation occurs in July which has a value of 588.68 mm and 572.09 mm for RCP2.6 and RCP8.5 scenarios, respectively. Similar to the near-term projection, the rainfall in the Hamassa watershed is expected to be high during the summer (Kiremt) season and low during the winter (Bega) season.

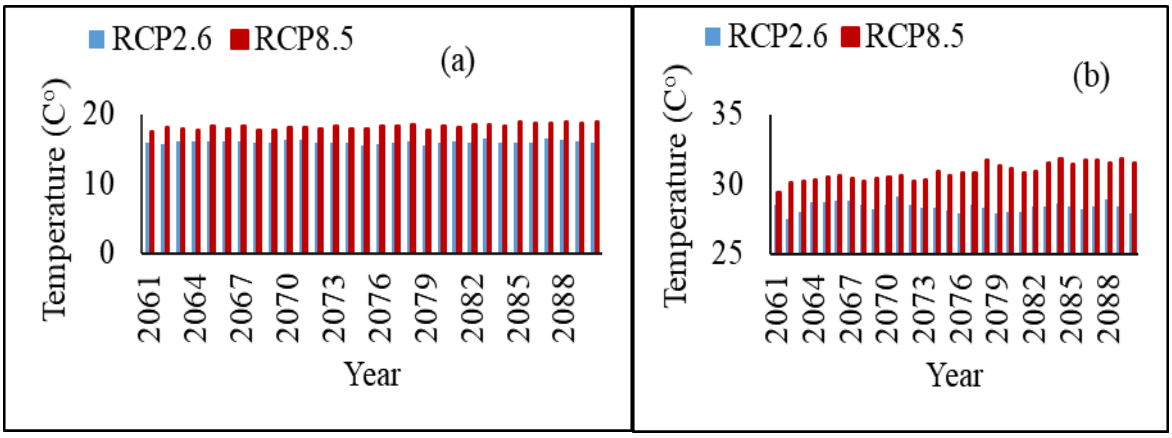

Figure 4.4 Long-term annual minimum and maximum temperature for both scenarios

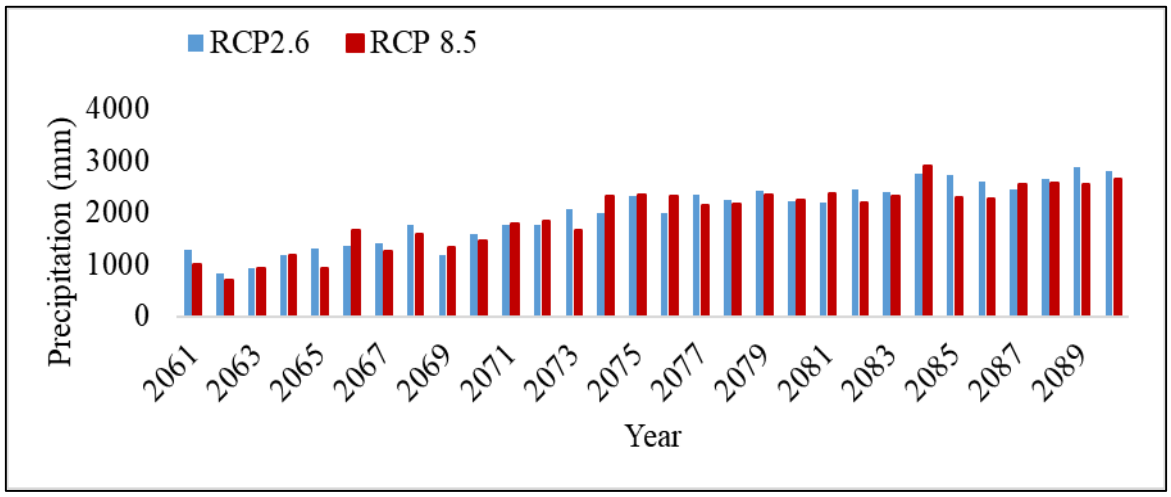

Figure 4.5 Long-term annual precipitation for both scenarios

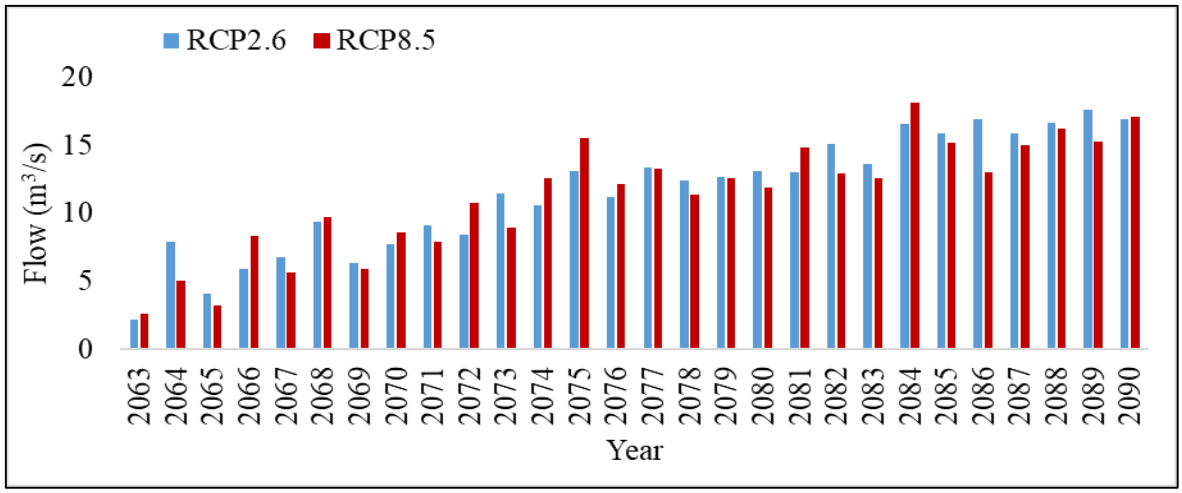

Figure 4.6 Long-term average flow for both scenarios

The temperature projections for both the near and long term indicate an increase compared to the current period under both RCP2.6 and RCP8.5 scenarios, temperature projection values (2061-2090) are higher than the near-term projections (2030-2060) for both RCP2.6 and RCP8.5 scenarios. A previous study conducted by Daniel and Abate (2022b) effect of climate change on streamflow in the Gelana watershed, Rift Valley Basin, Ethiopia predicts that the maximum and minimum temperatures will increase in the future supporting this finding.

In the Hamassa watershed, minimum precipitation is projected for 2049 under the RCP2.6 scenarios and 2053 under the RCP8.5 scenarios for the short term (2030-2060). Conversely, maximum precipitation is expected to occur in 2030 under both the RCP2.6 and RCP8.5 scenarios. For the long term (2061-2090), minimum precipitation is expected in 2062 under both RCP2.6 and RCP8.5, while maximum precipitation is projected for 2089 under RCP2.6 and 2084 under RCP8.5. These findings are supported by a study conducted by Tenagashaw and Andualem (2022a), which indicates that climate change in Ethiopia leads to hydrological extremes, such as floods and droughts. The frequency of both maximum precipitation (flood) and minimum precipitation (droughts) is expected to increase in the future, with floods becoming more frequent in the summer and autumn, and droughts more common in the winter and spring.

4.2 Hydrological characteristics of the watershed at the existing condition

The SWAT model simulation for the Hamassa watershed highlights significant relationships and seasonal patterns in its water balance. Key hydrological components such as rainfall, surface runoff, stream flow, and total water yield show direct correlations. In contrast, these components are inversely related to temperature and potential evapotranspiration, indicating that higher temperatures and potential evapotranspiration typically reduce water availability.

The Hamassa watershed exhibits distinct seasonal variations in its hydrology. During the summer (Kiremt) season, the watershed receives high rainfall amounting to 499.74 mm on average. This significant precipitation results in substantial surface runoff of 217.67 mm, translating to a runoff volume of 62 million cubic meters. Additionally, potential evapotranspiration is relatively high during the Kiremt season at 234.82 mm, allowing more water to contribute to runoff and streamflow. In contrast, the winter (Bega) season is characterized by much lower water balance. Rainfall drops to 92.37 mm, leading to a surface runoff depth of only 20.38 mm and a corresponding runoff volume of 5.83 MCM. Potential evapotranspiration during the Bega season is 303.72 mm, further reducing the amount of water available for runoff and streamflow.

Overall, the total annual surface water runoff for the watershed is 472.3 mm, with a total annual rainfall of 1236.8 mm. This generates an annual runoff volume of 135.26 million cubic meters from the 286.41 km² watershed area.

4.3 Hydrological characteristics of watershed under climate change

4.3.1 The near-term projection

The Hamassa watershed experiences different seasonal variations in its water balance, between the summer (Kiremt) and winter (Bega) seasons. During the Kiremt season, the watershed receives extensive rainfall, resulting in a high water balance. Under the RCP2.6 scenarios, total rainfall amounts to 878.68 mm, generating a stream flow of 64.73 m³/s and a surface runoff depth of 569.43 mm, which corresponds to a runoff volume of 163 million cubic meters and potential evapotranspiration 212.29 mm. In contrast, the Bega season sees a much lower water balance, total rainfall is only 72.99 mm, with a stream flow of 2.3 m³/s and a surface runoff depth of 6.2 mm, resulting in a small runoff volume of 1.78 MCM. Potential evapotranspiration during this season is 338.54 mm. Under the RCP8.5 scenarios, total rainfall amounts to 805.16 mm, generating a stream flow of 56.84 m³/s and a surface runoff depth of 518.2mm, which corresponds to a runoff volume of 148.4million cubic meters with potential evapotranspiration 221.89 mm and the water balance is low during the winter (Bega) season.

The minimum annual precipitation recorded is 776.85 mm under RCP2.6 in 2049 and 511.118 mm under RCP8.5 in 2053. Low stream flow occurred in 2049 under RCP2.6 and in 2053 under RCP8.5. The watershed produces a total surface water runoff of 729.63 mm under RCP2.6 and 722.01 mm under RCP8.5, respectively, generating annual runoff volumes of 209 MCM and 206.7 MCM.

4.3.2 The long-term projection

The watershed water balance is high during the summer (Kiremt) season, with a total rainfall of 1452.08 mm, stream flow of 114 m^3/s, surface runoff of 1054.82mm, resulting in a volume

of 302 MCM and potential evapotranspiration 214.61mm under RCP2.6. In contrast, the water balance is low during the winter (Bega) season, with a total rainfall of 12.65mm, stream flow of 1.4 m^3/s, a surface runoff depth of 0.01mm leading to a volume of 2864 cubic meter and potential evapotranspiration 332.01mm under RCP 2.6. Under RCP 8.5, during summer season increase in rainfall 1420.5 mm, stream flow 111.4 m^3/s, surface runoff 1022.64mm, volume 292.88 MCM, decrease in potential evapotranspiration 230.29 mm and the water balance is low during the winter (Bega) season. Annually, the minimum precipitation was 818.33 mm in RCP2.6 and 712.75 mm in RCP8.5, which occurs in 2062. Low flow is occurred in 2063 in RCP2.6 and 2065 in RCP8.5. The watershed produces a total surface water runoff of 1233.8 mm under RCP 2.6 and 1230 mm under RCP 8.5, respectively, generating annual runoff volumes of 353 MCM and 352 MCM.

The projected watershed characteristics shows, increase in rainfall, stream flow, surface runoff, water yield and decrease in potential evapotranspiration occurring in the summer (Kiremt) season, while decrease in rainfall, stream flow, surface runoff, water yield and increase in potential evapotranspiration occurring in the winter (Bega) season under both RCP2.6 and RCP8.5 scenarios. For 2030 to 2060 (short term), the maximum precipitation occurs in 2030 under both scenarios and the minimum in the 2049 under RCP2.6 and 2053 under RCP8.5; for 2061 to 2090 (long term), the highest annual precipitation is in 2089 under RCP2.6 and in 2084 under RCP8.5 and the lowest in 2062. Rainfall, surface runoff and stream flow are directly related, while they are inversely related to temperature, and potential evapotranspiration.

An increase in temperature results in decreased precipitation, stream flow and surface runoff, alongside increased potential evapotranspiration, this reduction of precipitation, stream flow leading to hydrological drought in the future. These findings align with a study by Balcha *et al*, (2023) on the Katar and Meki watersheds in Ethiopia's Central Rift Valley Lakes Basin, which projected during temperature increases and corresponding decreases in precipitation, stream flow, surface runoff, and water yield, alongside increased potential evapotranspiration under future climate scenarios.

4.4 Hydrological drought at existing conditions using drought indices

The hydrological drought analysis using the standardized precipitation index (SPI) over the past 31 years revealed varying levels of drought severity at different stations. Humbo station experienced significant impacts with 4 extreme, 2 severe, and 4 moderate drought years, while Abayya station had 2 extreme, 2 severe, and 2 moderate drought years. In contrast, Billate station faced 4 severe and 6 moderate drought years, Bodity station encountered 2 severe and 8 moderate drought years, and Wolaita Sodo, the wettest station, only had moderate drought years.

Overall, the analysis showed 12 years of moderate drought, 8 years of severe drought, and 4 years of extreme drought across all stations. Specific periods of severe drought included Billate in 1998-1999 and 2001-2002, and Bodity in 2007-2008, while Humbo experienced extreme drought in 2020-2021 and 2021-2022. Abayya face extreme drought in 2021-2022 and severe drought in 2007-2008. Moderate drought years were frequent across the stations, particularly in 1996-1997, 1998-1999, and 2021-2022 (Table 4.1).

Table 4.1 Existing hydrological drought condition using SPI drought index

No	Station	Drought condition		
		Extreme	Severe	Moderate
1	Billate		1998-1999, 2001-2002	1996-1997,1999-2000 2000-2001
2	Bodity		2007-2008	1998-1999,1999-2000 2016-2017,2021-2022
3	Humbo	2020-2021 2021-2022	2003-2004	1998-1999,2014-2015
4	Abayya	2021-2022	2007-2008	1996-1997
5	Wolaita sodo			1996-1997,1998-1999 2008-2009,2016-2017 2021-2022

The analysis of the stream flow drought index (SDI) for the eleven sub-watersheds, based on simulated stream flow data, exposed varying levels of drought intensity across different periods. Sub-watershed 1 experienced severe drought in 1998-1999, moderate drought in 1994-1995, 2001-2002, 2008-2009, and 2016-2017, and mild drought in several other periods. Similarly, sub-watershed 2 faced severe drought in 1998-1999, moderate drought in various periods including 1994-1995, 2001-2002, 2008-2009, 2016-2017, and mild drought in 2002-2003, 2003-2014. Sub-watersheds 3 and 4 showed severe drought in 2020-2021, with moderate and mild drought in multiple years. Sub-watersheds 5 and 6 were significantly impacted, with severe droughts in 1996-1997, 1998-1999, and extreme droughts in 2020-2021, respectively. Additionally, sub-watersheds 7 through 11 demonstrated significant drought levels, with sub-watersheds 8, 9, and 11 particularly exposed to extreme droughts. Overall, the watershed was most affected by drought in 2020-2021, with varying levels of vulnerability across the sub-watersheds: 11 sub-watersheds experienced mild to moderate drought, 8 faced severe impacts, and 7 were extremely affected. Sub-watersheds, 8, 10, and 11 exhibited high susceptibilities to extreme and severe droughts, while sub-watersheds 1, 2, and 5 showed a lower frequency of extreme drought occurrences (Table 4.2).

Table 4.2 Existing hydrological drought condition using SDI drought index

No	Sub watershed	Drought condition			
		Mild	Moderate	Severe	Extreme
1	1	2003, 2004, 2010, 2011, 2020, 2021	1994, 1995,2001, 2002, 2016, 2017	1998,1999	
2	2	2003, 2004, 2010, 2011, 2020, 2021	1994, 1995, 2001, 2002, 2008, 2009, 2016, 2017	1998, 1999	
3	3	1994, 1995, 1996, 1997, 2001, 2002, 2014, 2015	1998, 1999, 2003, 2004		2020, 2021,
4	4	1994, 1995, 1996, 1997, 2001, 2002	1998, 1999, 2003, 2004, 2014, 2015		2020, 2021

5	5	1994, 1995, 2020, 2021	2001, 2002, 2003, 2004, 2008, 2009, 2014, 2015	1996, 1997, 1998, 1999	
6	6	1994, 1995, 1996, 1997, 2001, 2002	1998, 1999, 2003, 2004, 2014, 2015		2020, 2021
7	7	1994, 1995, 1996, 1997, 2001, 2002	1998, 1999, 2003, 2004, 2014, 2015		2020, 2021
8	8	1994, 1995, 2014, 2015, 2016, 2017	1996, 1997, 2001, 2002, 2008, 2009	1998, 1999, 2003, 2004, 2020, 2021	2021, 2022
9	9	1994, 1995, 2014, 2015, 2016, 2017	1998, 1999, 2014, 2015	1998, 1999, 2003, 2004	2020, 2021, 2022
10	10	1994, 1995, 1996, 1997, 2001, 2002	1998, 1999, 2003, 2004, 2014, 2015	2021, 2022	2020, 2021
11	11	1994, 1995, 2014, 2015, 2016, 2017	1996, 1997, 2001, 2002, 2008, 2009	1998, 1999, 2003, 2004	2020, 2021, 2022

The analysis of hydrological drought using the SPI and SDI revealed varying levels of drought severity across stations and sub-watersheds over the past 31 years. According to the analysis drought in the watershed area has increased over time from mild to moderate, and moderate to severe, and drought has affected watershed severely and extremely in the last three years. Stations like Humbo and Abayya experienced extreme drought, while Billate and Bodity faced severe drought periods. Sub-watersheds, 8, 9, and 11 were highly susceptible to extreme and severe droughts. Even though there is a limitation of hydrological drought at the watershed level these finding is supported by a previous study studied by Tareke and Awoke, (2022), in all of Ethiopia, the study also concluded that Rift Valley Basins were frequently affected by severe hydrological drought.

4.5 Hydrological drought under climate change

4.5.1 Hydrological drought under climate change near-term projection

The hydrological drought analysis, using the standardized precipitation index (SPI), forecasts varying levels of drought severity across different stations over the next 30 years (2030-2060) under two scenarios: RCP2.6 and RCP8.5. Under the RCP2.6 scenarios, the Humbo station is expected to experience extreme, severe, and moderate droughts. Similarly, the Abayya station will face extreme, severe, and moderate droughts. The Bilate station is projected to experience extreme, severe, and moderate droughts, while the Bodity station is expected to see extreme, severe, and moderate droughts. The Wolaita Sodo station is likely to have extreme, severe, and moderate droughts. Generally, under the RCP2.6 scenarios, all stations will experience moderate, severe, and extreme droughts, as shown Table 4.3.

Under the RCP8.5 scenarios, the projections for the Humbo station include extreme, severe, and moderate drought. The Abayya station is expected to meet extreme, severe, and moderate droughts, while the Bilate station is forecasted to face extreme, severe, and moderate droughts. The Bodity station is anticipated to experience extreme, severe, and moderate drought years, and the Wolaita Sodo station is predicted to have extreme, severe, and moderate drought years. Overall, under the RCP8.5 scenarios, all stations will face an increased frequency and severity of droughts compared to current conditions, as shown in Table 4.4. The analysis shown that all stations will experience a significantly increase in drought frequency and severity in the future under both RCP2.6 and RCP8.5 scenarios.

Table 4.3 Hydrological drought under climate change using SPI near-term projection RCP2.6

No	Station	Drought condition		
		Moderate	Severe	Extreme
1	Abayya	2045-2046, 2046-2047, 2047-2048, 2051-2052, 2052-2053	2049-2050, 2050-2051, 2056-2057, 2058-2059, 2059-2060	2048-2049, 2053-2054, 2054-2055, 2055-2056
2	Bilate	2045-2046, 2046-2047, 2047-2048,	2049-2050, 2050-2051, 2053-2054,	2048-2049, 2054-2055

			2051-2052, 2057-2058, 2059-2060	2055-2056, 2056-2057, 2058-2059	
3		Bodity	2045-2046, 2046-2047, 2047-2048, 2049-2050, 2050-2051, 2051-2052, 2057-2058	2053-2054, 2055-2056, 2056-2057, 2058-2059	2048-2049, 2054-2055
4		Humbo	2045-2046, 2046-2047, 2052-2053, 2057-2058	2047-2048, 2049-2050, 2050-2051, 2051-2052, 2053-2054, 2056-2057, 2059-2060	2048-2049, 2054-2055, 2055-2056, 2058-2059
5		Wolaita sodo	2045-2046, 2046-2047, 2047-2048, 2049-2050, 2050-2051, 2051-2052, 2057-2058, 2059-2060	2053-2054, 2055-2056, 2056-2057, 2058-2059	2048-2049, 2054-2055

Table 4.4 Hydrological drought under climate change using SPI near-term projection RCP8.5

No	Station	Drought condition			
		Moderate		Severe	Extreme
1	Abayya	2040-2041, 2046-2047, 2056-2057, 2058-2059	2042-2043, 2048-2049, 2057-2058,	2049-2050, 2051-2052, 2054-2055, 2055-2056	2052-2053, 2053-2054, 2059-2060
2	Bilate	2040-2041, 2046-2047, 2055-2056, 20589-2059	2042-2043, 2048-2049, 2056-2057,	2049-2050, 2051-2052, 2054-2055, 2059-2060	2052-2053, 2053-2054
3	Bodity	2040-2041, 2048-2049, 2055-2056, 2058-2059	2042-2043, 2049-2050, 2057-2058,	2049-2050, 2051-2052, 2054-2055, 2059-2060	2052-2053, 2053-2054
4	Humbo	2040-2041, 2047-2048, 2056-2057	2042-2043, 2048-2049,	2049-2050, 2054-2055, 2055-2056, 2057-2058, 2058-2059	2051-2052, 2052-2053, 2053-2054, 2059-2060

5	Wolaita sodo	2042-2043, 2049-2050, 2057-2058, 2058-2059	2048-2049, 2055-2056,	2051-2052, 2059-2060	2054-2055,	2052-2053, 2054	2053-

The analysis of the streamflow drought index (SDI) across the eleven sub-watersheds reveals diverse levels of drought severity over different periods, explained in Table 4.5. In sub-watershed 1, projections indicate extreme drought in 2048-2049, severe droughts in 2054-2055 and 2058-2059, moderate droughts in 2049-2050, 2053-2054, 2055-2056, 2056-2057, and 2059-2060, laterally mild droughts in 2046-2047, 2047-2048, 2050-2051, 2052-2053, and 2057-2058. Similarly, sub-watershed 2 is composed to encounter extreme drought in 2048-2049, severe droughts in 2054-2055 and 2058-2059, moderate droughts in 2050, 2053-2054, 2055-2056, 2056-2057, and 2059-2060, with mild droughts interspersed across similar periods. Sub-watersheds 3 and 4 exhibit similar drought patterns, with both predicted to experience extreme drought in 2048-2049 and severe droughts in 2054-2055, 2055-2056, and 2058-2059. Moderate and mild droughts occur across the corresponding period. Sub-watersheds 5 and 6 showcase considerable drought impacts, with extreme droughts projected in 2048-2049, followed by severe droughts mostly in the 2050s. Moderate and mild droughts persistently affect these areas over the study period. Sub-watersheds 7 through 11 display significant drought severity, with extreme and severe droughts projected across various periods, along with moderate and mild droughts. The assessment under the RCP2.6 scenario indicates that all sub-watersheds will face varying degrees of drought severity, with 2048-2049 the most affected year.

Under the RCP8.5 scenarios for 2030–2060, significant variations in drought intensity are projected across eleven sub-watersheds. Sub-watersheds 1 and 2 are expected to experience extreme drought conditions in 2052-2053, with severe droughts in 2048-2049 and 2051-2052, and multiple moderate and mild droughts particularly in the 2040s and 2050s. Sub-watersheds 3 and 4 show a similar pattern, with extreme droughts in 2052-2053, severe droughts in the same years as sub-watersheds 1 and 2, plus an additional severe drought in 2053-2054, and frequent moderate and mild droughts from 2042 onwards. Sub-watersheds 5 and 6 are likely to face extreme droughts earlier, from 2048-2049 through 2052-2053, and

predominantly severe droughts in the 2050s, with common moderate and mild droughts throughout the period. Sub-watersheds 7 through 11 are projected to endure the severest conditions, with extreme droughts from 2048-2049, 2051-2052, 2052-2053, and 2053-2054, severe droughts in the early 2040s and late 2050s, and frequent moderate and mild droughts in between (Table 4.6).

Table 4.5 Hydrological drought under climate change using SDI near-term projection under RCP2.6

No	Sub	Drought condition			
		Mild	Moderate	Severe	Extreme
1	1	2046-2047, 2047-2048, 2050-2051, 2052-2053, 2057-2058	2049-2050, 2053-2054, 2055-2056, 2056-2057, 2059-2060	2054-2055, 2058-2059,	2048-2049
2	2	2046-2047, 2047-2048, 2050-2051, 2052-2053, 2057-2058	2049-2050, 2053-2054, 2055-2056, 2056-2057, 2059-2060	2054-2055, 2058-2059	2048-2049
3	3	2046-2047, 2047-2048, 2050-2051, 2051-2052, 2057-2058	2049-2050, 2052-2053, 2053-2054, 2056-2057, 2059-2060	2054-2055, 2055-2056, 2058-2059	2048-2049
4	4	2046-2047, 2047-2048, 2050-2051, 2051-2052, 2057-2058	2049-2050, 2052-2053, 2053-2054, 2056-2057, 2059-2060	2054-2055, 2055-2056, 2058-2059	2048-2049
5	5		2046-2047, 2047-2048, 2050-2051, 2051-2052, 2052-2053, 2057-2058	2049-2050, 2053-2054, 2054-2055, 2055-2056, 2056-2057, 2058-2059, 2059-2060	2048-2049
6	6		2046-2047, 2047-2048, 2050-2051, 2051-2052, 2052-2053, 2057-2058	2049-2050, 2053-2054, 2054-2055, 2055-2056, 2056-	2048-2049

			2057, 2058-2059, 2059-2060	
7	7	2046-2047, 2047-2048, 2050-2051, 2051-2052, 2052-2053, 2057-2058	2049-2050, 2053-2054, 2054-2055, 2055-2056, 2056-2057, 2058-2059, 2059-2060	2048-2049
8	8	2046-2047, 2047-2048, 2050-2051, 2051-2052, 2057-2058	2049-2050, 2052-2053, 2053-2054, 2056-2057	2048-2049, 2055-2056, 2058-2059, 2059-2060
9	9	2046-2047, 2047-2048, 2050-2051, 2051-2052, 2057-2058	2049-2050, 2052-2053, 2053-2054, 2056-2057	2048-2049, 2055-2056, 2058-2059, 2059-2060
10	10	2046-2047, 2047-2048, 2050-2051, 2051-2052, 2057-2058	2049-2050, 2052-2053, 2053-2054, 2056-2057	2048-2049, 2055-2056, 2058-2059, 2059-2060
11	11	2046-2047, 2047-2048, 2050-2051, 2051-2052, 2057-2058	2049-2050, 2052-2053, 2053-2054, 2056-2057	2048-2049, 2055-2056, 2058-2059, 2059-2060

Table 4.6 Hydrological drought under climate change using SDI near-term projection under RCP8.5

Sub	Drought condition			
	Mild	Moderate	Severe	Extreme
1	2040-2041, 2045-2046, 2046-2047, 2047-2048, 2050-2051, 2056-2057, 2057-2058	2042-2043, 2049-2050, 2053-2054, 2054-2055, 2055-2056, 2058-2059, 2059-2060	2048-2049, 2051-2052	2052-2053
2	2040-2041, 2045-2046, 2046-2047, 2047-2048, 2050-2051, 2056-2057, 2057-2058	2042-2043, 2049-2050, 2053-2054, 2054-2055, 2055-2056, 2058-2059, 2059-2060	2048-2049, 2051-2052	2052-2053
3	2040-2041, 2045-2046, 2046-2047,	2042-2043, 2049-2050, 2054-2055,	2048-2049, 2051-2052, 2053-2054	2052-2053

	2047-2048, 2050-2051, 2056-2057, 2057-2058	2055-2056, 2058-2059, 2059-2060		
4	2040-2041, 2045-2046, 2046-2047, 2047-2048, 2050-2051, 2056-2057, 2057-2058	2042-2043, 2049-2050, 2054-2055, 2055-2056, 2058-2059, 2059-2060	2048-2049, 2051-2052, 2053-2054	2052-2053
5	2045-2046, 2046-2047, 2047-2048	2040-2041, 2050-2051, 2056-2057, 2057-2058	2042-2043,2049-2050,2053-2054, 2054-2055,2055-2056,2058-2059, 2059-2060	2048-2049, 2051-2052, 2052-2053
6	2045-2046, 2046-2047, 2047-2048	2040-2041, 2050-2051, 2056-2057, 2057-2058	2042-2043,2049-2050,2053-2054, 2054-2055,2055-2056,2058-2059, 2059-2060	2048-2049, 2051-2052, 2052-2053
7	2045-2046, 2046-2047, 2047-2048	2040-2041, 2050-2051, 2056-2057, 2057-2058	2042-2043,2049-2050,2053-2054, 2054-2055,2055-2056,2058-2059, 2059-2060	2048-2049, 2051-2052, 2052-2053
8	2045-2046, 2046-2047, 2047-2048	2040-2041, 2050-2051, 2056-2057, 2057-2058	2042-2043,2049-2050,2053-2054, 2054-2055,2055-2056,2058-2059, 2059-2060	2048-2049, 2051-2052, 2052-2053
9	2045-2046, 2046-2047, 2047-2048	2040-2041, 2050-2051, 2056-2057, 2057-2058	2042-2043,2049-2050,2054-2055,2055-2056,2058-2059, 2059-2060	2048-2049, 2051-2052, 2052-2053, 2053-2054
10	2045-2046, 2046-2047, 2047-2048	2040-2041, 2050-2051, 2056-2057, 2057-2058	2042-2043,2049-2050,2054-2055,2055-2056,2058-2059, 2059-2060	2048-2049, 2051-2052, 2052-2053, 2053-2054
11	2045-2046, 2046-2047, 2047-2048	2040-2041, 2050-2051, 2056-2057, 2057-2058	2042-2043,2049-2050,2054-2055,2055-2056,2058-2059, 2059-2060	2048-2049, 2051-2052, 2052-2053, 2053-2054

4.5.2 Hydrological drought under climate change long-term projection

The hydrological drought analysis using the standardized precipitation index (SPI) for the period 2061-2090 exposes significant variations in drought severity across different stations under two climate scenarios, RCP2.6 and RCP8.5. Under the RCP2.6 scenarios, Humbo station is projected to experience several years of extreme drought, severe drought, and moderate drought. Similarly, Abayya station is expected to face multiple years of extreme drought, severe drought, and moderate drought. Both Bilate and Bodity stations are forecasted to meeting various years of extreme drought, severe drought, and moderate drought. Wolaita Sodo station is predicted to experience years of extreme drought, severe drought, and moderate drought. Overall this scenario suggests a total of many years of moderate drought, severe drought, and extreme drought across the five stations (Table 4.7).

Under the RCP8.5 scenarios, the drought conditions are projected to differ to some extent. Humbo station is expected to experience an increase in the number of years of extreme drought, severe drought, and moderate drought. Abayya station will also face a number of years of extreme drought, severe drought, and moderate drought. Bilate station is similarly projected to have several years of extreme drought, severe drought, and moderate drought. Bodity station's projections include many years of extreme drought, severe drought, and moderate drought. Wolaita Sodo station is expected to experience extreme drought, severe drought, and moderate drought. Overall, this scenario projects several years of moderate drought, severe drought, and extreme drought across the stations (Table 4.8).

Table 4.7 Hydrological drought under climate change using SPI long-term projection under RCP2.6

No	Station	Drought condition		
		Moderate	Severe	Extreme
1	Abayya	2064-2065, 2067-2068	2065-2066, 2066-2067, 2068-2069, 2069-2070, 2070-2071, 2071-2072	2061-2062, 2062-2063, 2063-2064

2	Bilate	2064-2065, 2067-2068, 2070-2071, 2071-2072	2065-2066, 2066-2067, 2068-2069, 2069-2070	2061-2062, 2062-2063, 2063-2064
3	Bodity	2064-2065, 2067-2068, 2070-2071, 2071-2072	2065-2066, 2066-2067, 2068-2069, 2069-2070	2061-2062, 2062-2063, 2063-2064
4	Humbo	2067-2068, 2070-2071	2064-2065, 2065-2066, 2066-2067, 2068-2069, 2069-2070, 2071-2072	2061-2062, 2062-2063, 2063-2064
5	Wolaita sodo	2064-2065, 2067-2068, 2070-2071, 2071-2072	2065-2066, 2066-2067, 2068-2069, 2069-2070	2061-2062, 2062-2063, 2063-2064

Table 4.8 Hydrological drought under climate change using SPI long-term projection under RCP8.5

No	Station	Drought condition		
		Moderate	Severe	Extreme
1	Abayya	2065-2066, 2066-2067, 2067-2068, 2068-2069, 2069-2070, 2070-2071	2068-2069	2061-2062, 2062-2063, 2063-2064, 2064-2065
2	Bilate	2065-2066, 2066-2067, 2067-2068, 2068-2069, 2069-2070	2068-2069	2061-2062, 2062-2063, 2063-2064, 2064-2065
3	Bodity	2065-2066, 2066-2067, 2067-2068, 2069-2070	2063-2064, 2064-2065, 2068-2069	2061-2062, 2062-2063
4	Humbo	2065-2066, 2066-2067, 2067-2068, 2069-2070	2068-2069, 2070-2071	2061-2062, 2062-2063, 2063-2064, 2064-2065
5	Wolaita sodo	2065-2066, 2066-2067, 2068-2069, 2069-2070,	2063-2064, 2064-2065	2061-2062, 2062-2063

The analysis of the streamflow drought index (SDI) for eleven sub-watersheds from 2061 to 2090 under RCP2.6 and RCP8.5 scenarios exposes significant differences in drought severity. Under RCP2.6, all sub-watersheds experience varying levels of drought intensity, with extreme drought mostly affecting the year 2063-2064, severe drought frequently occurring in 2064-2065 and 2069-2070, moderate drought common through several periods including 2065-2066, 2066-2067, and 2068-2069, and mild drought occurring infrequently,

particularly in 2067-2068, 2070-2071, and 2071-2072. In contrast, under RCP8.5, drought conditions are generally more severe, with extreme drought significantly affecting 2064-2065 and 2063-2064, severe drought occurring frequently in 2064-2065, 2065-2066, and 2069-2070, moderate drought common in years 2066-2067, 2067-2068, and 2068-2069, and mild drought being less prevalent, mainly seen in 2070-2071 and 2071-2072. The year 2063-2064 is the most affected under RCP2.6, while 2064-2065 is the most affected year under RCP8.5 (Table 4.9, Table 4.10).

Table 4.9 Hydrological drought under climate change using stream flow drought index long-term projection under RCP2.6

Sub	Drought condition			
	Mild	Moderate	Severe	Extreme
1	2067-2068, 2070-2071, 2071-2072	2065-2066, 2066-2067, 2068-2069	2064-2065, 2069-2070	2063-2064
2	2067-2068, 2070-2071, 2071-2072	2065-2066, 2066-2067, 2068-2069	2064-2065, 2069-2070	2063-2064
3	2067-2068, 2070-2071, 2071-2072	2066-2067, 2068-2069	2064-2065, 2065-2066, 2069-2070	2063-2064
4	2067-2068, 2070-2071, 2071-2072	2066-2067, 2068-2069	2064-2065, 2065-2066, 2069-2070	2063-2064
5	2067-2068	2068-2069, 2070-2071, 2071-2072	2064-2065, 2065-2066, 2066-2067, 2069-2070	2063-2064
6	2067-2068	2068-2069, 2070-2071, 2071-2072	2064-2065, 2065-2066, 2066-2067, 2069-2070	2063-2064
7		2067-2068, 2068-2069, 2070-2071, 2071-2072	2064-2065, 2065-2066, 2066-2067, 2069-2070	2063-2064
8		2067-2068, 2068-2069	2064-2065, 2065-2066, 2066-2067, 2069-2070, 2070-2071, 2071-2072	2063-2064
9		2067-2068, 2068-2069	2064-2065, 2065-2066, 2066-2067, 2069-2070, 2070-2071, 2071-2072	2063-2064

10	2067-2068, 2068-2069	2064-2065, 2066-2067, 2070-2071,	2065-2066, 2069-2070, 2071-2072	2063-2064
11	2067-2068	2064-2065, 2066-2067, 2069-2070, 2071-2072	2065-2066, 2068-2069, 2070-2071,	2063-2064

Table 4.10 Hydrological drought under climate change using stream flow drought index long-term projection under RCP8.5

Sub	Drought condition				
	Mild	Moderate	Severe		Extreme
1	2070-2071, 2071-2072	2066-2067, 2067-2068, 2068-2069	2063-2064, 2069-2070	2065-2066,	2064-2065
2	2070-2071, 2071-2072	2066-2067, 2067-2068, 2068-2069	2063-2064, 2069-2070	2065-2066,	2064-2065
3	2070-2071, 2071-2072	2066-2067, 2067-2068, 2068-2069	2063-2064, 2069-2070	2065-2066,	2064-2065
4	2070-2071, 2071-2072	2066-2067, 2067-2068, 2068-2069	2063-2064, 2069-2070	2065-2066,	2064-2065
5		2068-2069, 2070-2071, 2071-2072	2066-2067, 2069-2070	2067-2068,	2063-2064, 2064-2065, 2065-2066
6		2068-2069, 2070-2071, 2071-2072	2066-2067, 2069-2070	2067-2068,	2063-2064, 2064-2065, 2065-2066
7		2068-2069, 2070-2071, 2071-2072	2066-2067, 2069-2070	2067-2068,	2063-2064, 2064-2065, 2065-2066
8		2068-2069	2066-2067, 2069-2070, 2071-2072	2067-2068 2070-2071,	2063-2064, 2064-2065, 2065-2066
9		2068-2069	2066-2067, 2069-2070, 2071-2072	2067-2068, 2070-2071,	2063-2064, 2064-2065, 2065-2066

10	2068-2069	2066-2067, 2069-2070, 2071-2072	2067-2068, 2070-2071,	2063-2064, 2064-2065, 2065-2066
11	2068-2069	2066-2067, 2069-2070, 2071-2072	2067-2068, 2070-2071,	2063-2064, 2064-2065, 2065-2066

The hydrological drought analysis using the standardized precipitation index (SPI) and streamflow drought index (SDI) for 2030-2090 under RCP2.6 and RCP8.5 scenarios shown significant variations in drought severity across different stations and sub-watersheds. Under RCP2.6, the short-term (2030-2060) projections show a higher frequency of severe droughts, while the long-term (2061-2090) forecasts moderate and severe droughts, particularly around 2063-2064. Conversely, RCP8.5 indicates more extreme droughts in both periods, especially in the early 2050s and mid-2060s, with severe and moderate droughts also dominant. Across both scenarios and timeframes, all stations and sub-watersheds are expected to experience increased drought frequency and severity compared to current conditions, with critical drought years identified as 2048-2049 and 2052-2053 in the short term, and 2063-64, 2064-2065 in the long term. While no scientific study has been conducted specifically on future hydrological drought in the Hamassa watershed, the findings can be supported by a previous study conducted in the Billate watershed in the Rift Valley Basin of Ethiopia by Orke and Li, (2022). Their research indicates that future droughts under climate change are expected to be more severe and continuing compared to the baseline period.

4.6 Drought hotspot area

4.6.1 Drought hotspot area in existing condition

The stream flow drought index result for the selected drought years was used as input in ArcGIS to identify drought-prone areas across the watershed. These drought years were chosen to represent the variation in watershed drought conditions from the start of the analysis period (1994-95), the middle (2003-2004), the most affected year in the watershed (2020-2021), and the end of the analysis period (2021-2022) respectively shown (Figure 4.7).

According to the analysis drought in the watershed area has increased over time from mild to moderate, and moderate to severe drought has affected the watershed severely and extremely in the last three years. Sub-watersheds 8, 9, and 11 are more prone to drought at existing conditions.

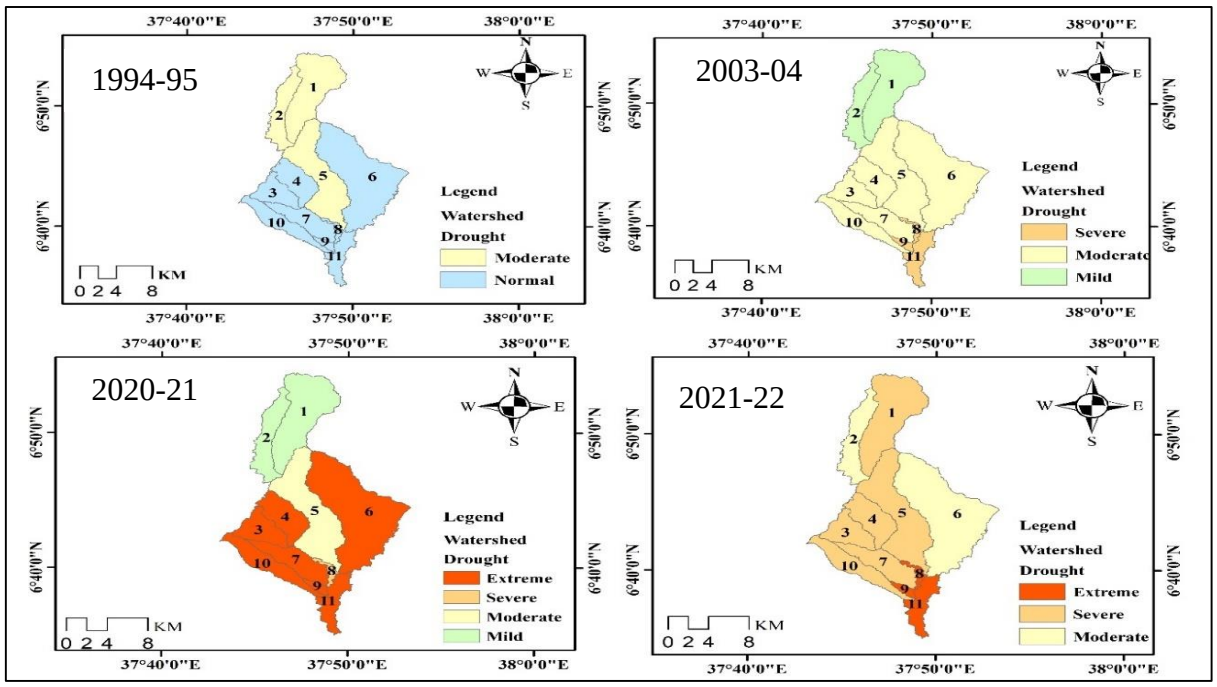

Figure 4.7 Spatial distribution of drought in each sub-watershed at the existing condition

4.6.2 Drought hots pot area under climate change

The stream flow drought index results for the selected drought years were used as input in ArcGIS to identify drought-prone areas across the watershed. These drought years were chosen to represent the variation in watershed drought conditions from the beginning, most affected year, and end of the drought period under both near-term RCP2.6, RCP8.5, and long-term RCP2.6, RCP8.5 scenarios, as shown (Figure 4.8, Figure 4.9, Figure 4.10, Figure 4.11). According to the analysis, drought in the watershed is projected to increase with the expectation that each sub-watershed will be extremely affected in the future (2048-2049, 2052-2053, 2063-2064, 2064-2065). Sub-watersheds 7, 8, 9, 10, and 11 are more prone to

drought under climate change compared to the existing conditions, the drought-prone area is expected to increase in the future.

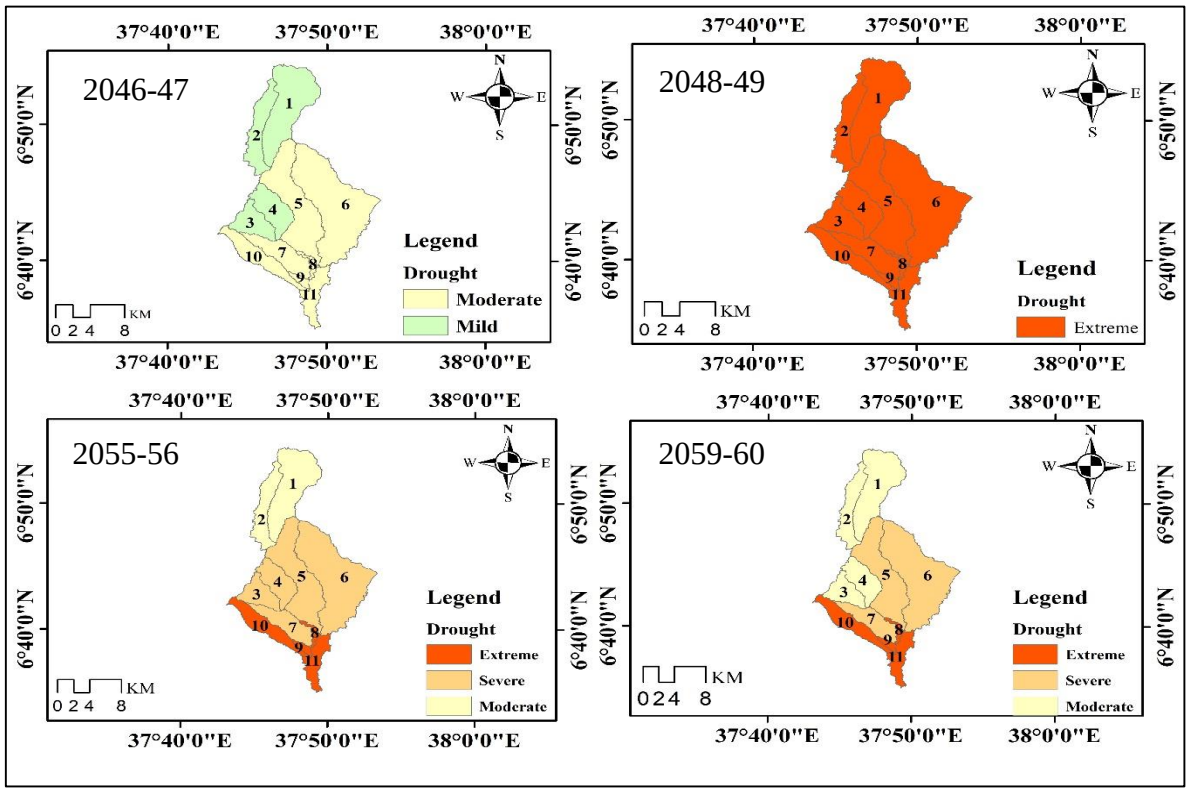

Figure 4.8 Spatial distribution of short-term drought in each sub-watershed under RCP2.6

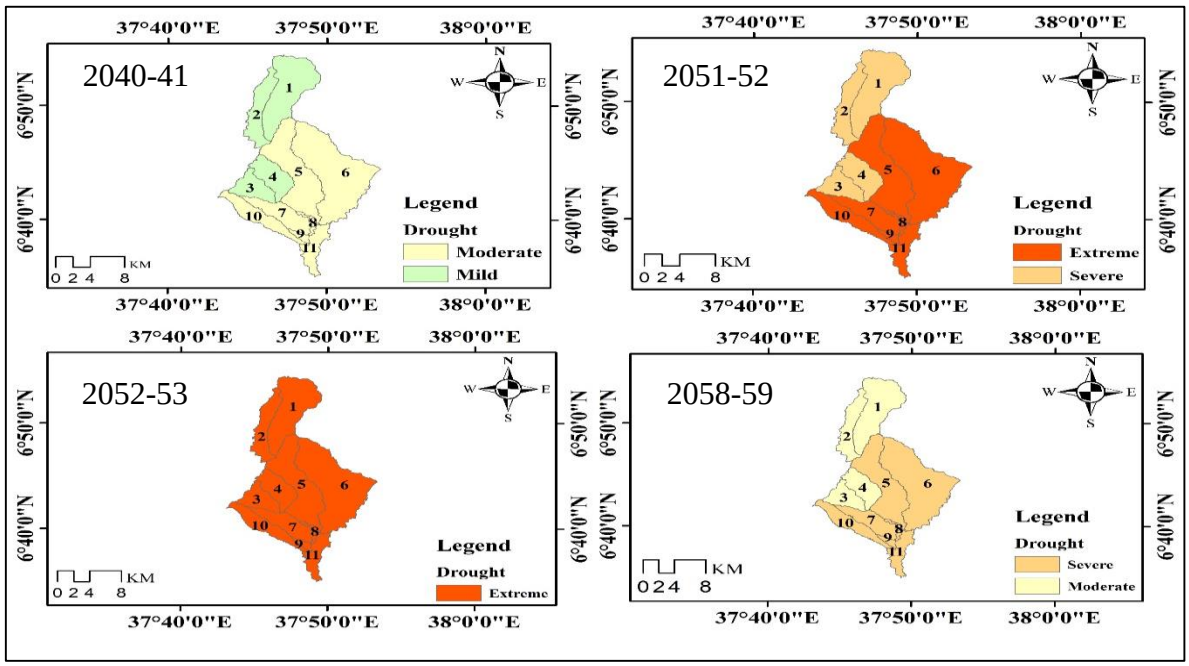

Figure 4.9 Spatial distribution of short-term drought in each sub-watershed under RCP8.5

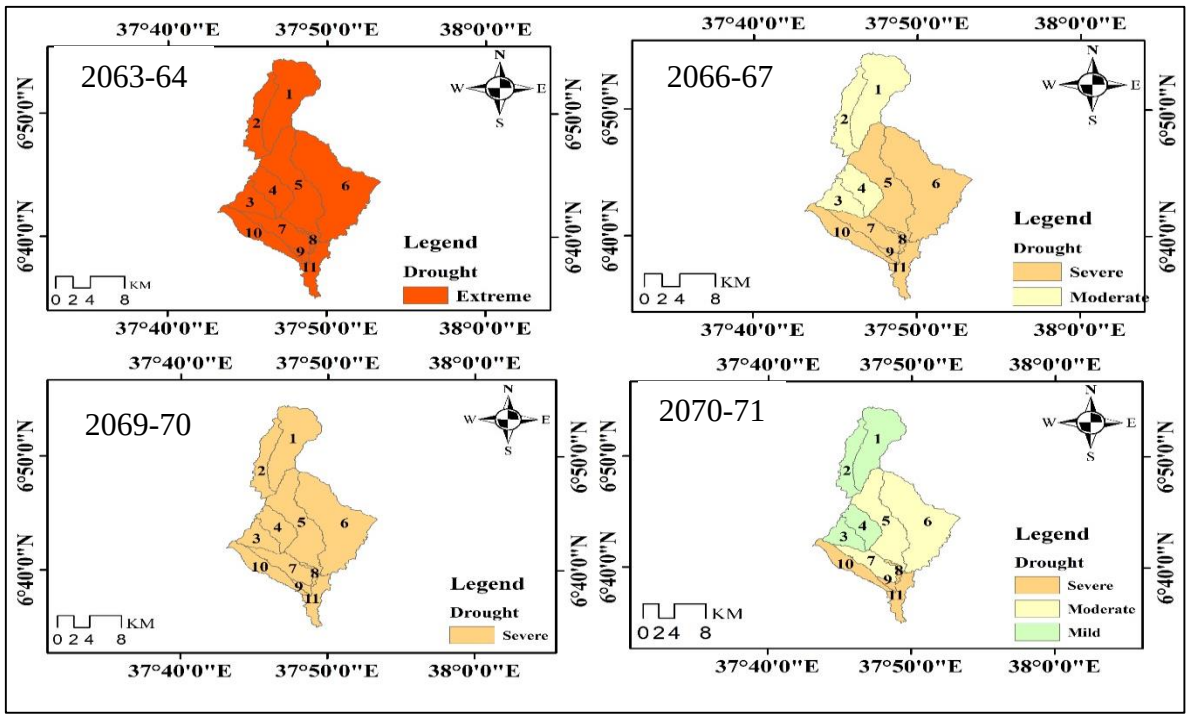

Figure 4.10 Spatial distribution of long-term drought in each sub-watershed under RCP2.6

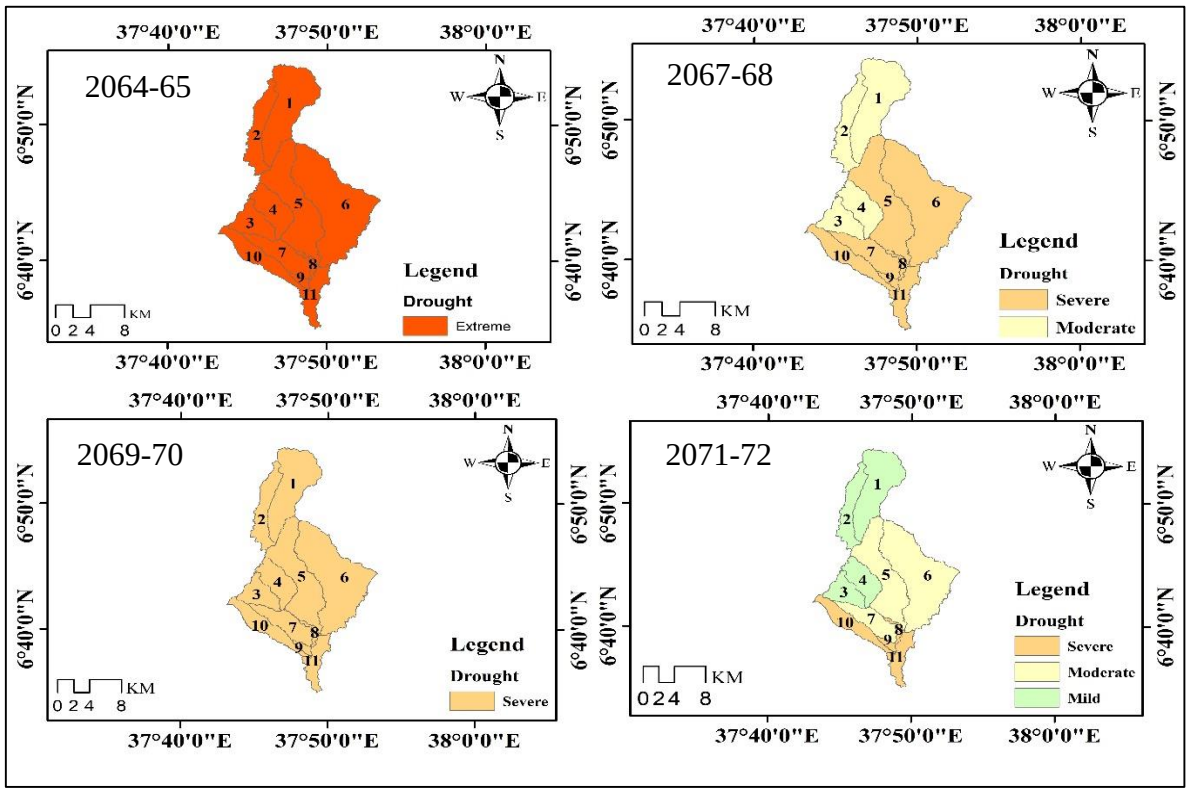

Figure 4.11 Spatial distribution of long-term drought in each sub-watershed under RCP8.5

5 CONCLUSIONS AND RECOMMENDATIONS

5.1 Conclusions

The study analyzed hydrological drought in the Hamassa watershed under existing conditions and climate change using the standard precipitation index (SPI) and stream flow drought index (SDI). Future climate data was extracted and its bias using the CMhyd software package. Among different bias correction methods, power transformation for precipitation and variance scaling for temperature were used. The future climate was analyzed for a near-term (2030 - 2060) and long-term (2061 - 2090) projection under RCP2.6 and RCP8.5 scenarios. The SWAT model was simulated on a monthly base. The calibration and validation of the SWAT model were evaluated from 1994 to 2008 and 2009-2015 respectively. The performance and capability result were Very good R^2 = 0.79, NSE = 0.78, PBIAS = -1.0% for calibration, and R^2 = 0.76, NSE = 0.75, PBIAS = -6.1% for validation.

The SWAT model simulation for the Hamassa watershed provides crucial insights into its hydrological dynamics and seasonal patterns. The analysis reveals that key hydrological components rainfall, surface runoff, stream flow, and total water yield are directly correlated and inversely related to temperature and potential evapotranspiration. Watershed water availability is high during the summer and lower availability in winter. Both RCP2.6 and RCP8.5 scenarios predict increased rainfall, stream flow, surface runoff, and water yield during Kiremt, and decreased values during Bega, alongside higher potential evapotranspiration. Short-term projections (2030-2060) show precipitation peaks in 2030 and lows in 2049 (RCP2.6) and 2053 (RCP8.5). Long-term projections (2061-2090) indicate the highest annual precipitation in 2089 (RCP2.6) and 2084 (RCP8.5), with the lowest in 2062. The inverse relationship between temperature and hydrological components highlights the impact of rising temperatures on reducing water availability, suggesting an increased risk of future hydrological drought.

The SPI was generated using monthly precipitation data collected from five stations to characterize drought under current conditions. Humbo and Abayya stations experienced extreme, severe, and moderate drought conditions, while Billate and Bodity stations experienced severe and moderate drought conditions. The Wolaita sodo station emerged as the wettest station and only had moderate drought levels compared to the others. The SDI was generated based on the simulated stream flow data, the analysis of the stream flow drought index (SDI) for the eleven sub-watersheds showed varying levels of drought intensity across different record periods sub-watersheds 8, 9, and 11, demonstrated high susceptibility to extreme and severe drought events.

The analysis of hydrological drought conditions using the standardized precipitation index (SPI) and streamflow drought index (SDI) under climate change scenarios RCP2.6 and RCP8.5 shows an increase in drought severity and frequency across each stations and sub-watersheds both in the near term (2030-2060) and long term (2060-2090). Under RCP2.6, stations such as Humbo, Abayya, Bilate, Bodity, and Wolaita Sodo are expected to experience a combination of extreme, severe, and moderate droughts, with a notable increase in severe droughts for Humbo and Abayya. The RCP8.5 scenario predicts even more severe conditions, with a higher frequency of extreme and moderate droughts across these stations. The SDI analysis also indicating significant extreme droughts in specific years and extensive severe and moderate droughts throughout the periods. Sub-watersheds 7, 8, 9, 10, and 11 showed high vulnerability to severe and extreme drought. Overall, the study highlights a concerning trend of increasing drought severity and frequency due to climate change, with the RCP8.5 scenario showing the most severe impacts.

5.2 Recommendations

The recommended points are stated as follows:

- ✓ Since the area is exposed to drought, any stakeholders trying to make a drought mitigating structure to resilient the community for both the existing and future drought.
- ✓ Water resource managers could develop strategies to mitigate the negative impacts of climate change on water resources in the Hamassa watershed. One potential approach would be to advocate for the implementation of Ethiopia's Green Legacy afforestation initiative. Expanding forest cover in the watershed through this policy could help offset some of the projected climate change effects on water availability and runoff patterns.
- ✓ Drought is a crucial aspect of water resource planning and management, and gaining a comprehensive understanding of drought patterns is an essential step in addressing drought-related challenges within the realm of water resources. Other researchers have analyzed the projected drought conditions in the Hamassa watershed, considering the potential effects of changes in land use land cover.

6 REFERENCE

Abbaspour, K. C. (2013). Swat-cup 2012. SWAT Calibration and Uncertainty Program—A User Manual, 1–100.

Abbaspour, K. C. (2015). SWAT calibration and uncertainty programs. A User Manual, 103, 17–66.

Abbaspour, K. C., Vaghefi, S. A., & Srinivasan, R. (2017). A guideline for successful calibration and uncertainty analysis for soil and water assessment: a review of papers from the 2016 international SWAT conference. Water, 10(1), 6.

Abbaspour, K. C., Yang, J., Maximov, I., Siber, R., Bogner, K., Mieleitner, J., & Zobrist, J. (2007). Modelling hydrology and water quality in the pre-alpine / alpine Thur watershed using SWAT. 413–430. https://doi.org/10.1016/j.jhydrol.2006.09.014

Abebe, N. A., Ogden, F. L., & Pradhan, N. R. (2010). Sensitivity and uncertainty analysis of the conceptual HBV rainfall–runoff model: Implications for parameter estimation. Journal of Hydrology, 389(3–4), 301–310.

Abera, K., & Gebeyehu, A. (2022). Review of Hydrological Drought Analysis Status in Ethiopia. Drought - Impacts and Management, 7–15. https://doi.org/10.5772/intechopen.102763

Abera Tareke, K., & Gebeyehu Awoke, A. (2022). Hydrological and Meteorological Drought Monitoring and Trend Analysis in Abbay River Basin, Ethiopia. Advances in Meteorology, 2022. https://doi.org/10.1155/2022/2048077

Agutu, N. O., Awange, J. L., Zerihun, A., Ndehedehe, C. E., Kuhn, M., & Fukuda, Y. (2017). Assessing multi-satellite remote sensing, reanalysis, and land surface models' products in characterizing agricultural drought in East Africa. Remote Sensing of Environment, 194, 287–302. https://doi.org/10.1016/j.rse.2017.03.041

Ajmi, R. N., Ati, E. M., & Farooq, H. Z. (2019). IMPACT OF CLIMATE CHANGE ON STREAM FLOW OF TIGRIS WATERSHED , BAGHDAD , IRAQ. 19(2), 4109–4114.

Ali, S., Khorrami, B., Jehanzaib, M., Tariq, A., Ajmal, M., Arshad, A., Shafeeque, M., Dilawar, A., Basit, I., Zhang, L., Sadri, S., Niaz, M. A., Jamil, A., & Khan, S. N. (2023). Spatial Downscaling of GRACE Data Based on XGBoost Model for Improved Understanding of Hydrological Droughts in the Indus Basin Irrigation System (IBIS). Remote Sensing, 15(4), 873. https://doi.org/10.3390/rs15040873

Amrit, K., Pandey, R. P., & Mishra, S. K. (2018). Assessment of meteorological drought

characteristics over Central India. Sustainable Water Resources Management, 4(4), 999–1010. https://doi.org/10.1007/s40899-017-0205-5

Andualem, T. G., Guadie, A., Belay, G., Ahmad, I., & Dar, M. A. (2020). Hydrological modeling of upper ribb watershed, abbay basin, Ethiopia. Global Nest Journal, 22(2), 158–164. https://doi.org/10.30955/gnj.003152

Aragaw, H. M., Mishra, S. K., & Goel, M. K. (2023). Assessing the impact of climate change on the hydrology of Gidabo river sub-basin, Ethiopian Rift Valley Lakes Basin. Sustainable Water Resources Management, 9(3), 1–18. https://doi.org/10.1007/s40899-023-00858-7

Arnold, J. G., Moriasi, D. N., Gassman, P. W., Abbaspour, K. C., White, M. J., Srinivasan, R., Santhi, C., Harmel, R. D., Van Griensven, A., & Van Liew, M. W. (2012). SWAT: Model use, calibration, and validation. Transactions of the ASABE, 55(4), 1491–1508.

Arnold, Kiniry, Srinivasan, Williams, Haney, & Neitsch. (2012). Soil & Water Assessment Tool.

Asadi, A., & Vahdat, F. (2013). The efficiency of meteorological drought indices for drought monitoring and evaluating in Kohgilouye and Boyerahmad Province, Iran. Int. J. Mod. Eng. Res, 3(4), 2407–2411.

Asati, S. R. (2012). Analysis of rainfall data for drought investigation at Agra U . P . International Journal of Life Sciences Biotechnology and Pharma Research, 1(4), 81–86.

Awass, A. A. (2009). Hydrological Drought Analysis-occurrence , severity , risks : the case of Wabi Shebele River Basin. 220.

Ayele, G. T., Teshale, E. Z., Yu, B., Rutherfurd, I. D., & Jeong, J. (2017). EthiopiStreamflow and sediment yield prediction for watershed prioritization in the upper Blue Nile river basin,a. Water (Switzerland), 9(10). https://doi.org/10.3390/w9100782

Bachmair, S., Svensson, C., Hannaford, J., Barker, L. J., & Stahl, K. (2016). A quantitative analysis to objectively appraise drought indicators and model drought impacts. Hydrology and Earth System Sciences, 20(7), 2589–2609. https://doi.org/10.5194/hess-20-2589-2016

Balcha, S. K., Awass, A. A., Hulluka, T. A., Bantider, A., & Ayele, G. T. (2023). Assessment of future climate change impact on water balance components in Central Rift Valley Lakes Basin, Ethiopia. Journal of Water and Climate Change, 14(1), 175–199.

Bayissa, Y. A., Moges, S. A., Xuan, Y., Van Andel, S. J., Maskey, S., Solomatine, D. P.,

Griensven, A. Van, & Tadesse, T. (2015). Influence de la durée des chroniques météorologiques sur la caractérisation des sécheresses météorologiques du bassin supérieur du Nil Bleu (Ethiopie). Hydrological Sciences Journal, 60(11), 1927–1942. https://doi.org/10.1080/02626667.2015.1032291

Beven, K. J. (2011). Rainfall-runoff modelling: the primer. John Wiley & Sons.

Beza, M., Hailu, H., & Teferi, G. (2023). Modeling and Assessing Surface Water Potential Using Combined SWAT Model and Spatial Proximity Regionalization Technique for Ungauged Subwatershed of Jewuha Watershed , Awash Basin , Ethiopia. 2023.

Bhatti, H. A., Rientjes, T., Haile, A. T., Habib, E., & Verhoef, W. (2016). Evaluation of bias correction method for satellite-based rainfall data. Sensors (Switzerland), 16(6), 1–16. https://doi.org/10.3390/s16060884

Bickici Arikan, B., & Kahya, E. (2019). Homogeneity revisited: analysis of updated precipitation series in Turkey. Theoretical and Applied Climatology, 135(1–2), 211–220. https://doi.org/10.1007/s00704-018-2368-x

Blagojevic, B., Plavsic, J., & Mihailovic, V. (2014). Outlier treatment in the flood flow statistical analysis. June. https://doi.org/10.14415/konferencijaGFS2014.081

Blanco-Gómez, P., Jimeno-Sáez, P., Senent-Aparicio, J., & Pérez-Sánchez, J. (2019). Impact of climate change on water balance components and droughts in the Guajoyo River Basin (El Salvador). Water (Switzerland), 11(11). https://doi.org/10.3390/w11112360

Borg, D. S. (2009). An application of drought indices in Malta, case study. European Water, 25(26), 25–38.

Cammalleri, C., Barbosa, P., & Vogt, J. V. (2020). Evaluating simulated daily discharge for operational hydrological drought monitoring in the Global Drought Observatory (GDO). Hydrological Sciences Journal, 65(8), 1316–1325.

Carrão, H., Naumann, G., & Barbosa, P. (2016). Mapping global patterns of drought risk: An empirical framework based on sub-national estimates of hazard, exposure and vulnerability. Global Environmental Change, 39, 108–124. https://doi.org/10.1016/j.gloenvcha.2016.04.012

Chakilu, G. G., Moges, M. A., & Tilahun, S. A. (2015). Evaluating the land use/cover dynamics and its impact on low stream flow of Gumara watershed, upper Blue Nile basin. Ethiopia, 3(November), 2015.

Chow, V. Te, Maidment, D. R., Mays, L. W., & Ven Te Chow, David R. Maidment, L. W. M. (1988). Applied Hydrology Chow 1988.pdf (pp. 1–294).

Collins, W. J., Bellouin, N., Doutriaux-Boucher, M., Gedney, N., Halloran, P., Hinton, T., Hughes, J., Jones, C. D., Joshi, M., Liddicoat, S., Martin, G., O'Connor, F., Rae, J., Senior, C., Sitch, S., Totterdell, I., Wiltshire, A., & Woodward, S. (2011). Development and evaluation of an Earth-System model - HadGEM2. Geoscientific Model Development, 4(4), 1051–1075. https://doi.org/10.5194/gmd-4-1051-2011

Dai, A. (2011). Drought under global warming: A review. Wiley Interdisciplinary Reviews: Climate Change, 2(1), 45–65. https://doi.org/10.1002/wcc.81

Dai, A. (2013). Increasing drought under global warming in observations and models. Nature Climate Change, 3(1), 52–58. https://doi.org/10.1038/nclimate1633

Dalezios, N. R., Dunkel, Z., & Eslamian, S. (2017). Meteorological Drought Indices: Definitions. Handbook of Drought and Water Scarcity, 27–44. https://doi.org/10.1201/9781315404219-3

Dananto, M., Aga, A. O., Yohannes, P., & Shura, L. (2022). Assessing the water-resources potential and soil erosion hotspot areas for sustainable land management in the Gidabo watershed, Rift Valley lake basin of Ethiopia. Sustainability, 14(9), 5262.

Daniel, H. (2023). Performance assessment of bias correction methods using observed and regional climate model data in different watersheds, Ethopia. Water Clim Change 14 (6): 2007–2028.

Daniel, H. (2024). Modeling surface water potential using the SWAT model combined with principal component analysis in the ungauged Gelana watershed, Ethiopia. Journal of Water and Climate Change, 15(2), 703–732. https://doi.org/10.2166/wcc.2023.548

Daniel, H., & Abate, B. (2022a). Effect of climate change on stream fl ow in the Gelana watershed , Rift valley basin ,. 13(5), 2205–2232. https://doi.org/10.2166/wcc.2022.059

Daniel, H., & Abate, B. (2022b). Effect of climate change on streamflow in the Gelana watershed, Rift valley basin, Ethiopia. Journal of Water and Climate Change, 13(5), 2205–2232. https://doi.org/10.2166/wcc.2022.059

Danuso, F. (2002). Climak: a stochastic model for weather data generation. Italian Journal of Agronomy, 6(1), 57–72.

DeFries, R., & Eshleman, K. N. (2004). Land-use change and hydrologic processes: a major focus for the future. Hydrological Processes, 18(11), 2183–2186. https://doi.org/10.1002/hyp.5584

Devia, G. K., Ganasri, B. P., & Dwarakish, G. S. (2015). A Review on Hydrological Models. Aquatic Procedia, 4(Icwrcoe), 1001–1007. https://doi.org/10.1016/j.aqpro.2015.02.126

Dibaba, W. T., Demissie, T. A., & Miegel, K. (2020a). Drivers and implications of land use/land cover dynamics in Finchaa catchment, northwestern Ethiopia. Land, 9(4), 113.

Dibaba, W. T., Demissie, T. A., & Miegel, K. (2020b). Watershed hydrological response to combined land use/land cover and climate change in highland Ethiopia: Finchaa catchment. Water, 12(6), 1801.

Dunne, J. P., Horowitz, L. W., Adcroft, A. J., Ginoux, P., Held, I. M., John, J. G., Krasting, J. P., Malyshev, S., Naik, V., Paulot, F., Shevliakova, E., Stock, C. A., Zadeh, N., Balaji, V., Blanton, C., Dunne, K. A., Dupuis, C., Durachta, J., Dussin, R., … Zhao, M. (2020). The GFDL Earth System Model Version 4.1 (GFDL-ESM 4.1): Overall Coupled Model Description and Simulation Characteristics. Journal of Advances in Modeling Earth Systems, 12(11), 1–56. https://doi.org/10.1029/2019MS002015

Duru, U., Arabi, M., & Wohl, E. E. (2018). Modeling stream flow and sediment yield using the SWAT model: a case study of Ankara River basin, Turkey. Physical Geography, 39(3), 264–289. https://doi.org/10.1080/02723646.2017.1342199

Dutta, D., Kundu, A., Patel, N. R., Saha, S. K., & Siddiqui, A. R. (2015). Assessment of agricultural drought in Rajasthan (India) using remote sensing derived Vegetation Condition Index (VCI) and Standardized Precipitation Index (SPI). Egyptian Journal of Remote Sensing and Space Science, 18(1), 53–63. https://doi.org/10.1016/j.ejrs.2015.03.006

Edalat, M. M., & Stephen, H. (2019). Socio-economic drought assessment in Lake Mead, USA, based on a multivariate standardized water-scarcity index. Hydrological Sciences Journal, 64(5), 555–569. https://doi.org/10.1080/02626667.2019.1593988

Edossa, D. C., Woyessa, Y. E., & Welderufael, W. A. (2014). Analysis of droughts in the central region of South Africa and their association with SST anomalies. International Journal of Atmospheric Sciences, 2014.

Elshorbagy, A. A., Panu, U. S., & Simonovic, S. P. (2000). Group-based estimation of missing hydrological data: I. Approach and general methodology. Hydrological Sciences Journal, 45(6), 849–866. https://doi.org/10.1080/02626660009492388

Fang, G. H., Yang, J., Chen, Y. N., & Zammit, C. (2015). Comparing bias correction methods in downscaling meteorological variables for a hydrologic impact study in an arid area in China. Hydrology and Earth System Sciences, 19(6), 2547–2559. https://doi.org/10.5194/hess-19-2547-2015

Fendeková, M., Gauster, T., Labudová, L., Vrablíková, D., Daná, Z., Fendek, M., & Pekárová, P. (2018). Analysing 21st century meteorological and hydrological drought events in Slovakia. 393–403. https://doi.org/10.2478/johh-2018-0026

Gado, T. A., Mohameden, M. B., And, & Rashwan, I. M. H. (2022). Bias correction of regional climate model simulations for the impact assessment of the climate change in Egypt. Environmental Science and Pollution Research, 29(14), 20200–20220. https://doi.org/10.1007/s11356-021-17189-9

Gassman, P. W., Reyes, M. R., Green, C. H., & Arnold, J. G. (2007). T s w a t : h d , a , f r d. 50(4), 1211–1250.

Gassman, P. W., Sadeghi, A. M., & Srinivasan, R. (2014). Applications of the SWAT model special section: overview and insights. Journal of Environmental Quality, 43(1), 1–8.

Gebisa, B. T., Dibaba, W. T., & Kabeta, A. (2023). Evaluation of historical CMIP6 model simulations and future climate change projections in the Baro River Basin. Journal of Water and Climate Change, 14(8), 2680–2705.

Gebre, S. L., Tadele, K., & Mariam, B. G. (2015). Potential impacts of climate change on the hydrology and water resources availability of Didessa Catchment, Blue Nile River Basin, Ethiopia. J. Geol. Geosci, 4, 193.

Gebrehiwot, S. G., Ilstedt, U., Gärdenas, A. I., & Bishop, K. (2011). Hydrological characterization of watersheds in the Blue Nile Basin, Ethiopia. Hydrology and Earth System Sciences, 15(1), 11–20. https://doi.org/10.5194/hess-15-11-2011

Gebremichael, A., Kebede, A., & Woyessa, Y. E. (2021). Effect of Land Use Land Cover Change on Stream Flow and Sediment Yield in Gibe III Watershed, Omo-Gibe Basin, Ethiopia. Journal of Earth Science & Climatic Change, 12(10), 20.

Gorfu, D., & Ahmed, E. (2012). Crops and agro-ecological zones of Ethiopia. Ethiopian Institute of Agricultural Research.

Gupta, For, A., With, O., By, A., Vijai, H., Sorooshian, S., & Yapo, P. O. (2001). S Tatus of a Utomatic C Alibration for H Ydrologic M Odels : C Omparison With M Ultilevel E Xpert C Alibration. April, 135–143.

Gutiérrez, A. P. A., Engle, N. L., De Nys, E., Molejón, C., & Martins, E. S. (2014). Drought preparedness in Brazil. Weather and Climate Extremes, 3, 95–106.

Guug, S. S., Abdul-Ganiyu, S., & Kasei, R. A. (2020). Application of SWAT hydrological model for assessing water availability at the Sherigu catchment of Ghana and Southern Burkina Faso. HydroResearch, 3, 124–133.

Hasan, H. H., Razali, S. F. M., Muhammad, N. S., & Ahmad, A. (2019). Research trends of hydrological drought: A systematic review. Water (Switzerland), 11(11). https://doi.org/10.3390/w11112252

Heim, R. R. (2002). A review of twentieth-century drought indices used in the United States. In Bulletin of the American Meteorological Society (Vol. 83, Issue 8, pp. 1149–1165). https://doi.org/10.1175/1520-0477(2002)083<1149:AROTDI>2.3.CO;2

Hisdal, H., & Tallaksen, L. M. (2003). Estimation of regional meteorological and hydrological drought characteristics: A case study for Denmark. Journal of Hydrology, 281(3), 230–247. https://doi.org/10.1016/S0022-1694(03)00233-6

Holvoet, K., van Griensven, A., Seuntjens, P., & Vanrolleghem, P. A. (2005). Sensitivity analysis for hydrology and pesticide supply towards the river in SWAT. Physics and Chemistry of the Earth, Parts A/B/C, 30(8–10), 518–526.

Hordofa, A. T., Leta, O. T., Alamirew, T., & Chukalla, A. D. (2022). Spatiotemporal Trend Analysis of Temperature and Rainfall over Ziway Lake Basin, Ethiopia. Hydrology, 9(1). https://doi.org/10.3390/hydrology9010002

Huang, S., Huang, Q., Leng, G., & Liu, S. (2016). A nonparametric multivariate standardized drought index for characterizing socioeconomic drought: A case study in the Heihe River Basin. Journal of Hydrology, 542, 875–883. https://doi.org/10.1016/j.jhydrol.2016.09.059

Husen, D., & Abate, B. (2020). Estimation of Runoff and Sediment Yield Using SWAT Model: The Case of Katar Watershed, Rift Valley Lake Basin of Ethiopia. International Journal of Mechanical Engineering and Applications, 8(6), 125. https://doi.org/10.11648/j.ijmea.20200806.11

Ikhar, R., P., Regulwar, G., D., Kamodkar, & U., R. (2018). Optimal reservoir operation using soil and water assessment tool and genetic algorithm. ISH Journal of Hydraulic Engineering, 24(2), 249–257. https://doi.org/10.1080/09715010.2017.1417754

Jahangir, M. H., & Yarahmadi, Y. (2020). Hydrological drought analyzing and monitoring by using Streamflow Drought Index (SDI) (case study: Lorestan, Iran). Arabian Journal of Geosciences, 13(3). https://doi.org/10.1007/s12517-020-5059-8

Jain, V. K., Pandey, R. P., Jain, M. K., & Byun, H. R. (2015). Comparison of drought indices for appraisal of drought characteristics in the Ken River Basin. Weather and Climate Extremes, 8, 1–11. https://doi.org/10.1016/j.wace.2015.05.002

Jesus, E. T. de, Amorim, J. da S., Junqueira, R., Viola, M. R., & Mello, C. R. de. (2020). Meteorological and hydrological drought from 1987 to 2017 in Doce River Basin, Southeastern Brazil. RBRH, 25, e29.

Juraj M. Cunderlik. (1992). Hydrologic Models for Inverse Climate Change Impact Modeling.

Kamalanandhini, M., Annadurai, R., Dheepak, S., Deepak, P., & Metilda, J. E. (2021). ASSESSMENT OF HYDROLOGICAL DROUGHT CONDITION AND ITS IMPACT ON WATER QUALITY-A CASE STUDY IN PARTS OF CHENGALPATTU DISTRICT , TAMIL NADU , INDIA. 14(1), 51–57.

Kamali, B., Houshmand Kouchi, D., Yang, H., & Abbaspour, K. C. (2017). Multilevel drought hazard assessment under climate change scenarios in semi-arid regions—A case study of the Karkheh river basin in Iran. Water, 9(4), 241.

Kim, J. H., Sung, J. H., Shahid, S., & Chung, E. S. (2022). Future Hydrological Drought Analysis Considering Agricultural Water Withdrawal Under SSP Scenarios. Water Resources Management, 36(9), 2913–2930. https://doi.org/10.1007/s11269-022-03116-1

Kolachian, R., & Saghafian, B. (2021). Hydrological drought class early warning using support vector machines and rough sets. Environmental Earth Sciences, 80(11), 390.

Kwak, J., Kim, S., Jung, J., Singh, V. P., Lee, D. R., & Kim, H. S. (2016). Assessment of Meteorological Drought in Korea under Climate Change. Advances in Meteorology, 2016(Dm). https://doi.org/10.1155/2016/1879024

Kwon, H. J., & Kim, S. J. (2010). Assessment of distributed hydrological drought based on hydrological unit map using SWSI drought index in South Korea. KSCE Journal of Civil Engineering, 14(6), 923–929. https://doi.org/10.1007/s12205-010-0827-8

Lal, R. (2012). Climate change and soil degradation mitigation by sustainable management of soils and other natural resources. Agricultural Research, 1, 199–212.

Liou, Y.-A., & Mulualem, G. M. (2019). Spatio–temporal assessment of drought in Ethiopia and the impact of recent intense droughts. Remote Sensing, 11(15), 1828.

Liu, S., Shi, H., Niu, J., Chen, J., & Kuang, X. (2020). Assessing future socioeconomic drought events under a changing climate over the Pearl River basin in South China. Journal of Hydrology: Regional Studies, 30(May), 100700. https://doi.org/10.1016/j.ejrh.2020.100700

Liu, S., Zhang, J., Wang, N., & Wei, N. (2020). Large-Scale Linkages of Socioeconomic Drought with Climate Variability and Its Evolution Characteristics in Northwest China. Advances in Meteorology, 2020. https://doi.org/10.1155/2020/2814539

Ma, M., Ren, L., Singh, V. P., Yuan, F., Chen, L., Yang, X., & Liu, Y. (2016). Hydrologic model-based Palmer indices for drought characterization in the Yellow River basin, China. Stochastic Environmental Research and Risk Assessment, 30, 1401–1420.

Mami, A., Raimonet, M., Yebdri, D., Sauvage, S., Mami, A., Raimonet, M., Yebdri, D., Sauvage, S., & Zettam, A. (2021). Future climatic and hydrologic changes estimated by bias-adjusted regional climate model outputs of the Cordex-Africa project : case of the Tafna basin (North-Western Africa) To cite this version : HAL Id : hal-03430756. International Journal of Global Warming, 23 (1), pp.58-90.

Mauritsen, T., Bader, J., Becker, T., Behrens, J., Bittner, M., Brokopf, R., Brovkin, V., Claussen, M., Crueger, T., Esch, M., Fast, I., Fiedler, S., Fläschner, D., Gayler, V., Giorgetta, M., Goll, D. S., Haak, H., Hagemann, S., Hedemann, C., … Roeckner, E. (2019). Developments in the MPI-M Earth System Model version 1.2 (MPI-ESM1.2) and Its Response to Increasing CO2. Journal of Advances in Modeling Earth Systems, 11(4), 998–1038. https://doi.org/10.1029/2018MS001400

Mckee, T. B., Doesken, N. J., & Kleist, J. (1993). The relationship of drought frequency and duration to time scales. January, 17–22.

Melesse, A. M., & Kidanewold, B. B. (2022). Assessment of Climate and Catchment Control on Drought Propagation in the Tekeze River Basin, Ethiopia. May. https://doi.org/10.3390/w14101564

Mera, G. A. (2018). Drought and its impacts in Ethiopia. Weather and Climate Extremes, 22(June), 24–35.

Mera, G. A. (2020a). Drought and its impacts in Ethiopia Drought and its impacts in Ethiopia. Weather and Climate Extremes, 22(October 2018), 24–35. https://doi.org/10.1016/j.wace.2018.10.002

Mera, G. A. (2020b). Drought and its impacts in Ethiopia Drought and its impacts in Ethiopia. Weather and Climate Extremes, 22(June), 24–35. https://doi.org/10.1016/j.wace.2018.10.002

Merga, T. F. (2020). Development of Water Allocation and Utilization System for Koka Reservoir under Climate Change and Irrigation Development Scenarios: A Case Study of Upper Awash, Ethiopia. International Journal of Environmental Sciences, 9(4), 109–116.

Mishra, A. K., & Singh, V. P. (2010). A review of drought concepts. Journal of Hydrology, 391(1–2), 202–216. https://doi.org/10.1016/j.jhydrol.2010.07.012

Mishra, S. K., & Singh, V. P. (2013). Soil conservation service curve number (SCS-CN) methodology (Vol. 42). Springer Science & Business Media.

Mittapalli, G. V. S. S., & Gorthi, K. V. (2014). Development of Spatial Analyst toolbar in ArcGIS Development of spatial analyst toolbar in ArcGIS. 1(January 2012), 25–30.

Mohammed, Y., Yimer, F., Tadesse, M., & Tesfaye, K. (2018). Meteorological drought assessment in north east highlands of Ethiopia. International Journal of Climate Change Strategies and Management, 10(1), 142–160. https://doi.org/10.1108/IJCCSM-12-2016-0179

Moshe, A., Beza, M., Daniel, H., & Chala, M. (2024). Integrated watershed management strategies for sustainable resource utilization using the SWAT model: case study of the Kalte River watershed, Rift Valley Basin, Ethiopia. H2Open Journal, 7(2), 163–179. https://doi.org/10.2166/h2oj.2024.107

Muleta, M. K., & Nicklow, J. W. (2005). Sensitivity and uncertainty analysis coupled with automatic calibration for a distributed watershed model. Journal of Hydrology, 306(1–4), 127–145. https://doi.org/10.1016/j.jhydrol.2004.09.005

Najihah, T. S., Ibrahim, M. H., Amalina, N., Zain, M., & Nulit, R. (2020). Activity of the oil palm seedlings exposed to a different rate of potassium fertilizer under water stress condition. 7(January), 46–68. https://doi.org/10.3934/environsci.2020004

Nalbantis, I., & Tsakiris, G. (2009). Assessment of hydrological drought revisited. Water Resources Management, 23(5), 881–897. https://doi.org/10.1007/s11269-008-9305-1

Nash, J. E., & Sutcliffe, J. V. (1970). River Flow Forecasting Through Conceptual Models - Part I - A Discussion of Principles. Journal of Hydrology, 10(1970), 282–290.

Ndomba, P., Mtalo, F., & Killingtveit, A. (2008). SWAT model application in a data scarce tropical complex catchment in Tanzania. Physics and Chemistry of the Earth, 33(8–13), 626–632. https://doi.org/10.1016/j.pce.2008.06.013

Neitsch, S. ., Arnold, J. ., Kiniry, J. ., & Williams, J. . (2011). Soil & Water Assessment Tool Theoretical Documentation Version 2009. Texas Water Resources Institute, 1–647. https://doi.org/10.1016/j.scitotenv.2015.11.063

Neitsch, S. L., Arnold, J. G., Kiniry, J. R., Srinivasan, R., & Williams, J. R. (2002). Soil and Water Assessment Tool User's Manual. TWRI Report TR-192, 412.

NHP. (2018). Hydrologic Modeling, Center of Excellence for Hydrologic Modeling, National Institute of Hydrology, Roorkee, India. 1.

Niemeyer, S. (2008). New drought indices. Options Méditerranéennes, 80(80), 267–274.

Núñez, J., Rivera, D., Oyarzún, R., & Arumí, J. L. (2014). On the use of Standardized Drought Indices under decadal climate variability: Critical assessment and drought policy implications. Journal of Hydrology, 517, 458–470. https://doi.org/10.1016/j.jhydrol.2014.05.038

Orke, Y. A., & Li, M.-H. (2022). Impact of climate change on hydrometeorology and droughts in the Bilate Watershed, Ethiopia. Water, 14(5), 729.

Padhee, S. K. (2013). Agricultural drought assessment under irrigated and rainfed conditions thesis. Thesis Submitted to the Andhra University, Visakhapatnam in Partial Fulfillment of the Requirement for the Award of Master of Technology in Remote Sensing and GIS, 91.

Padrón, R. S., Gudmundsson, L., Decharme, B., Ducharne, A., Lawrence, D. M., Mao, J., Peano, D., Krinner, G., Kim, H., & Seneviratne, S. I. (2020). Observed changes in dry-season water availability attributed to human-induced climate change. Nature Geoscience, 13(7), 477–481.

Palmer, W. C. (1965). Meteorological Drought. In U.S. Weather Bureau, Res. Pap. No. 45 (p. 58).

Pandey, R. P., Dash, B. B., Mishra, S. K., & Singh, R. (2008). Study of indices for drought characterization in KBK districts in Orissa (India). Hydrological Processes: An International Journal, 22(12), 1895–1907.

Pashiardis, S., & Michaelides, S. (2008). Implementation of the standardized precipitation index (SPI) and the reconnaissance drought index (RDI) for regional drought assessment: a case study for Cyprus. European Water, 23(24), 57–65.

PRASANCHUM, H., TUMMA, N., & LOHPAISANKRIT, W. (2022). ESTABLISHING SPATIAL DISTRIBUTIONS OF DROUGHT PHENOMENA ON CULTIVATION SEASONS USING THE SWAT MODEL. Geographia Technica, 17(2).

Raes, D., Willems, P., & Gbaguidi, F. (2006). RAINBOW–A software package for hydrometeorological frequency analysis and testing the homogeneity of historical data sets. Proceedings of the 4th International Workshop on Sustainable Management of Marginal Drylands. Islamabad, Pakistan, 2731, 12.

Rathjens, H., Bieger, K., Srinivasan, R., & Arnold, J. G. (2016). CMhyd User Manual: Documentation for preparing simulated climate change data for hydrologic impact studies.

Refsgaard, J. C. (1997). Parameterisation , calibration and validation of distributed hydrological models. 198, 69–97.

Reshmidevi, T. V, Kumar, D. N., Mehrotra, R., & Sharma, A. (2017). Estimation of the climate change impact on a catchment water balance using an ensemble of GCMs. Journal of Hydrology. https://doi.org/10.1016/j.jhydrol.2017.02.016

Salimi, H., Asadi, E., & Darbandi, S. (2021). Meteorological and hydrological drought monitoring using several drought indices. Applied Water Science, 11, 1–10.

Samavati, A., Babamiri, O., Rezai, Y., & Heidarimozaffar, M. (2023). Investigating the effects of climate change on future hydrological drought in mountainous basins using SWAT model based on CMIP5 model. Stochastic Environmental Research and Risk Assessment, 37(3), 849–875. https://doi.org/10.1007/s00477-022-02319-7

Sardou, F. S., & Bahremand, A. (2014). Hydrological Drought Analysis Using SDI Index in Halilrud Basin of Iran. Environmental Resources Research, 2(1), 1.

Schubert, S. D., Stewart, R. E., Wang, H., Barlow, M., Berbery, E. H., Cai, W., Hoerling, M. P., Kanikicharla, K. K., Koster, R. D., Lyon, B., Mariotti, A., Mechoso, C. R., Müller, O. V., Rodriguez-Fonseca, B., Seager, R., Senevirante, S. I., Zhang, L., & Zhou, T. (2016). Global meteorological drought: A synthesis of current understanding with a focus on sst drivers of precipitation deficits. Journal of Climate, 29(11), 3989–4019. https://doi.org/10.1175/JCLI-D-15-0452.1

Setegn, S. G., Srinivasan, R., & Dargahi, B. (2008). Hydrological modelling in the Lake Tana Basin, Ethiopia using SWAT model. The Open Hydrology Journal, 2(1).

Shadman, F., Sadeghipour, S., Moghavvemi, M., & Saidur, R. (2016). Drought and energy security in key ASEAN countries. Renewable and Sustainable Energy Reviews, 53, 50–58.

Shah, R., Bharadiya, N., & Manekar, V. (2015). Drought Index Computation Using Standardized Precipitation Index (SPI) Method For Surat District, Gujarat. Aquatic Procedia, 4(Icwrcoe), 1243–1249. https://doi.org/10.1016/j.aqpro.2015.02.162

Sheffield, J., Wood, E. F., & Roderick, M. L. (2012). Little change in global drought over the past 60 years. Nature, 491(7424), 435–438. https://doi.org/10.1038/nature11575

Sisay, E., Halefom, A., Khare, D., Singh, L., & Worku, T. (2018). HYDROLOGICAL SIMULATION OF AN UNGAUGED CATCHMENT (KHARUN Hydrological modelling of ungauged urban watershed using SWAT model. Modeling Earth Systems and Environment, 0(0), 0. https://doi.org/10.1007/s40808-017-0328-6

Soriano, E., Mediero, L., & Garijo, C. (2019). Selection of bias correction methods to assess the impact of climate change on flood frequency curves. Water (Switzerland), 11(11). https://doi.org/10.3390/w11112266

Sruthi, S., & Aslam, M. A. M. (2015). Agricultural Drought Analysis Using the NDVI and Land Surface Temperature Data; a Case Study of Raichur District. Aquatic Procedia, 4(Icwrcoe), 1258–1264. https://doi.org/10.1016/j.aqpro.2015.02.164

Sutanto, S. J., & Van Lanen, H. A. J. (2020). Streamflow drought: implication of drought definitions and its application for drought forecasting. Hydrology and Earth System Sciences Discussions, 2020, 1–29.

Svoboda, M., & Fuchs, B. (2017). Handbook of Drought Indicators and Indices* (Issue 1173). https://doi.org/10.1201/9781315265551-12

Swain, S., Surendra Mishra, K., & Pandey, A. (2020). Assessment of meteorological droughts over Hoshangabad district, India. IOP Conference Series: Earth and Environmental Science, 491(1). https://doi.org/10.1088/1755-1315/491/1/012012

Swetalina, N., & Thomas, T. (2016). Evaluation of Hydrological Drought Characteristics for Bearma Basin in Bundelkhand Region of Central India. Procedia Technology, 24, 85–92. https://doi.org/10.1016/j.protcy.2016.05.013

Szalai, S., & Szinell, C. (2000). Comparison of Two Drought Indices for Drought Monitoring in Hungary — A Case Study. 161–166. https://doi.org/10.1007/978-94-015-9472-1_12

Tabari, H., Nikbakht, J., & Hosseinzadeh Talaee, P. (2013). Hydrological Drought Assessment in Northwestern Iran Based on Streamflow Drought Index (SDI). Water Resources Management, 27(1), 137–151. https://doi.org/10.1007/s11269-012-0173-3

Tallaksen, L. M., & Van Lanen, H. A. J. (2004). Hydrological drought: processes and estimation methods for streamflow and groundwater.

Tan, Y., Guzman, S. M., Dong, Z., & Tan, L. (2020). Selection of effective GCM bias correction methods and evaluation of hydrological response under future climate scenarios. Climate, 8(10), 108.

Tareke, K. A., & Awoke, A. G. (2022a). Comparing surface water supply index and streamflow drought index for hydrological drought analysis in Ethiopia. Heliyon, 8(12), e12000. https://doi.org/10.1016/j.heliyon.2022.e12000

Tareke, K. A., & Awoke, A. G. (2022b). Hydrological Drought Analysis using Streamflow Drought Index (SDI) in Ethiopia. Advances in Meteorology, 2022. https://doi.org/10.1155/2022/7067951

Tenagashaw, D. Y., & Andualem, T. G. (2022). Analysis and Characterization of Hydrological Drought Under Future Climate Change Using the SWAT Model in Tana Sub-basin, Ethiopia. Water Conservation Science and Engineering, 7(2), 131–142. https://doi.org/10.1007/s41101-022-00133-4

Terakawa, A. (2003). Hydrological Data Management: Present State and Trends (Issue 48).

Teutschbein, C. and, & Seibert, J. (2012). Bias correction of regional climate model simulations for hydrological climate-change impact studies: Review and evaluation of different methods. Journal of Hydrology, 456–457, 12–29. https://doi.org/10.1016/j.jhydrol.2012.05.052

Tigkas, D., Vangelis, H., Proutsos, N., & Tsakiris, G. (2022). Incorporating aSPI and eRDI in Drought Indices Calculator (DrinC) Software for Agricultural Drought Characterisation and Monitoring. Hydrology, 9(6). https://doi.org/10.3390/hydrology9060100

Tigkas, D., Vangelis, H., & Tsakiris, G. (2015). DrinC: a software for drought analysis based on drought indices. Earth Science Informatics, 8, 697–709.

Trambauer, P., Maskey, S., Winsemius, H., Werner, M., & Uhlenbrook, S. (2013). A review of continental scale hydrological models and their suitability for drought forecasting in (sub-Saharan) Africa. Physics and Chemistry of the Earth, Parts A/B/C, 66, 16–26.

Tripathi, M. P., Panda, R. K., & Raghuwanshi, N. S. (2003). Identification and prioritisation of critical sub-watersheds for soil conservation management using the SWAT model. Biosystems Engineering, 85(3), 365–379. https://doi.org/10.1016/S1537-5110(03)00066-7

Truneh, L. A., Matula, S., & Báťková, K. (2022). Hydroclimate Impact Analyses and Water Management in the Central Rift Valley Basin in Ethiopia. Water, 15(1), 18.

Tsakiris, G., Pangalou, D., & Vangelis, H. (2007). Regional drought assessment based on the Reconnaissance Drought Index (RDI). Water Resources Management, 21(5), 821–833. https://doi.org/10.1007/s11269-006-9105-4

van Griensven, A. van, Meixner, T., Grunwald, S., Bishop, T., Diluzio, M., & Srinivasan, R. (2006). A global sensitivity analysis tool for the parameters of multi-variable catchment models. Journal of Hydrology, 324(1–4), 10–23.

Van Lanen, H. A. J., Laaha, G., Kingston, D. G., Gauster, T., Ionita, M., Vidal, J. P., Vlnas, R., Tallaksen, L. M., Stahl, K., Hannaford, J., Delus, C., Fendekova, M., Mediero, L., Prudhomme, C., Rets, E., Romanowicz, R. J., Gailliez, S., Wong, W. K., Adler, M. J., … Van Loon, A. F. (2016). Hydrology needed to manage droughts: the 2015 European case. Hydrological Processes, 30(17), 3097–3104. https://doi.org/10.1002/hyp.10838

Van Loon, A. F. (2015a). Hydrological drought explained. Wiley Interdisciplinary Reviews: Water, 2(4), 359–392. https://doi.org/10.1002/WAT2.1085

Van Loon, A. F. (2015b). Hydrological drought explained. Wiley Interdisciplinary Reviews: Water, 2(4), 359–392.

Van Loon, A. F., Van Lanen, H. A. J., Seibert, J., & Torfs, P. (2009). Adaptation of the HBV model for the study of drought propagation in European catchments. EGU General Assembly Conference Abstracts, 9589.

Vicente-Serrano, S. M., López-Moreno, J. I., Beguería, S., Lorenzo-Lacruz, J., Azorin-Molina, C., & Morán-Tejeda, E. (2012). Accurate Computation of a Streamflow Drought Index. Journal of Hydrologic Engineering, 17(2), 318–332. https://doi.org/10.1061/(asce)he.1943-5584.0000433

Viste, E., Korecha, D., & Sorteberg, A. (2013a). Recent drought and precipitation tendencies in Ethiopia. Theoretical and Applied Climatology, 112(3–4), 535–551. https://doi.org/10.1007/s00704-012-0746-3

Viste, E., Korecha, D., & Sorteberg, A. (2013b). Recent drought and precipitation tendencies in Ethiopia. Theoretical and Applied Climatology, 112, 535–551.

Voldoire, A., Sanchez-Gomez, E., Salas y Mélia, D., Decharme, B., Cassou, C., Sénési, S., Valcke, S., Beau, I., Alias, A., Chevallier, M., Déqué, M., Deshayes, J., Douville, H., Fernandez, E., Madec, G., Maisonnave, E., Moine, M. P., Planton, S., Saint-Martin, D., … Chauvin, F. (2013). The CNRM-CM5.1 global climate model: Description and basic evaluation. Climate Dynamics, 40(9–10), 2091–2121. https://doi.org/10.1007/s00382-011-1259-y

Wagner, P. D., Kumar, S., Fiener, P., & Schneider, K. (2011). HYDROLOGICAL MODELING WITH SWAT IN A MONSOON-DRIVEN ENVIRONMENT: EXPERIENCE FROM THE WESTERN GHATS, INDIA. American Society of Agricultural and Biological Engineers, 54(5), 1783–1790.

Wang, H., Hu, G., Ma, J., Wei, H., Li, S., Tang, G., & Xiong, L. (2023). Classifying Slope Unit by Combining Terrain Feature Lines Based on Digital Elevation Models. Land, 12(1), 193.

Wilhite, D. A., Glantz, M. H., & And Glantz, M. H. (1985). Glantz,1987.

Wilhite, D. A., & Knutson, C. L. (2006). Drought management planning : Conditions for success. 80, 141–148.

Wilhite, D. A., Sivakumar, M. V. K., & Pulwarty, R. (2014). Managing drought risk in a changing climate : The role of national drought policy. Weather and Climate Extremes, 2013(March 2013), 1–10. https://doi.org/10.1016/j.wace.2014.01.002

Wilhite et al. (1987). The Role of Definitions Understanding : the Drought Phenomenon : The Role of Definitions *. Westview Press, August 2013, 11–27.

Williams, I. P. (1990). Book Review: Asteroids II. Edited by Richard P. Binzel, Tom Gehrels, and Mildred Shapley Matthews. University of Arizona Press, Tucson, 1989. 1200+ pp., $50.00 (clothbound). Icarus, 87(1), 247.

Winchell, M., Srinivasan, R., Luzio, M. DI, & Arnold, J. . (2013). ARCSWAT 2.1 INTERFACE for SWAT2005. Soil and Water.

Winkler, K. (2017). Assessment of agricultural drought over Africa and its relation to El Niño-Southern Oscillation using remote sensing-based time series. January 2017.

WMO. (2012). WMO statement on the status of the global climate in 2012. In World Meteorological Organization (Issue 1108).

Worku, G., Teferi, E., Bantider, A., & Dile, Y. T. (2020). Statistical bias correction of regional climate model simulations for climate change projection in the Jemma sub-basin, upper Blue Nile Basin of Ethiopia. Theoretical and Applied Climatology, 139(3–4), 1569–1588. https://doi.org/10.1007/s00704-019-03053-x

WRA. (2021). Hydrological modeling.

Wu, J., Chen, X., Yu, Z., Yao, H., Li, W., & Zhang, D. (2019). Assessing the impact of human regulations on hydrological drought development and recovery based on a ' simulated-observed ' comparison of the SWAT model. Journal of Hydrology, 577(July), 123990. https://doi.org/10.1016/j.jhydrol.2019.123990

Xu, K., Wu, C., Zhang, C., & Hu, B. X. (2021). Uncertainty assessment of drought characteristics projections in humid subtropical basins in China based on multiple CMIP5 models and different index definitions. Journal of Hydrology, 600, 126502.

Yeboah, K. A., Akpoti, K., Kabo-bah, A. T., Ofosu, E. A., Siabi, E. K., Mortey, E. M., & Okyereh, S. A. (2022). Assessing climate change projections in the Volta Basin using the CORDEX-Africa climate simulations and statistical bias-correction. Environmental Challenges, 6(December 2021). https://doi.org/10.1016/j.envc.2021.100439

Yersaw, B. T., & Chane, M. B. (2024). Regional climate models and bias correction methods for rainfall-runoff modeling in Katar watershed, Ethiopia. Environmental Systems Research, 13(1). https://doi.org/10.1186/s40068-024-00340-z

Yisehak, B., Shiferaw, H., Abrha, H., Gebremedhin, A., Hagos, H., Adhana, K., & Bezabh, T. (2021). Spatio-temporal characteristics of meteorological drought under changing climate in semi-arid region of northern Ethiopia. Environmental Systems Research, 10, 1–10.

Yuan, F., Ma, M., Ren, L., Shen, H., Li, Y., Jiang, S., Yang, X., Zhao, C., & Kong, H. (2016).

Possible future climate change impacts on the hydrological drought events in the weihe river basin, China. Advances in Meteorology, 2016. https://doi.org/10.1155/2016/2905198

Zamani, R., Tabari, H., & Willems, P. (2015). Extreme streamflow drought in the Karkheh river basin (Iran): probabilistic and regional analyses. Natural Hazards, 76, 327–346.

Zeckoski, R. W., Smolen, M. D., Moriasi, D. N., Frankenberger, J. R., & Feyereisen, G. W. (2015). Hydrologic and water quality terminology as applied to modeling. Transactions of the ASABE, 58(6), 1619–1635.

Zhai, Z., Fuchs, A. L., & Lohmann, I. (2010). Cellular analysis of newly identified Hox downstream genes in Drosophila. European Journal of Cell Biology, 89(2–3), 273–278. https://doi.org/10.1016/j.ejcb.2009.11.012

Zhang, Y., Wu, Z., Singh, V. P., Lin, Q., Ning, S., Zhou, Y., Jin, J., Zhou, R., & Ma, Q. (2023). Agricultural drought characteristics in a typical plain region considering irrigation, crop growth, and water demand impacts. Agricultural Water Management, 282, 108266.

Zhao, A., Liu, X., Zhu, X., Pan, Y., & Li, Y. (2015). Spatiotemporal patterns of droughts based on SWAT model for the Weihe River Basin. Prog. Geogr, 34, 1156–1166.

Zhou, J., Chen, X., Xu, C., & Wu, P. (2022). Assessing Socioeconomic Drought Based on a Standardized Supply and Demand Water Index. Water Resources Management, 36(6), 1937–1953. https://doi.org/10.1007/s11269-022-03117-0

7 APPENDIXES

Appendix 7.1 Homogeneity test of Abayya station

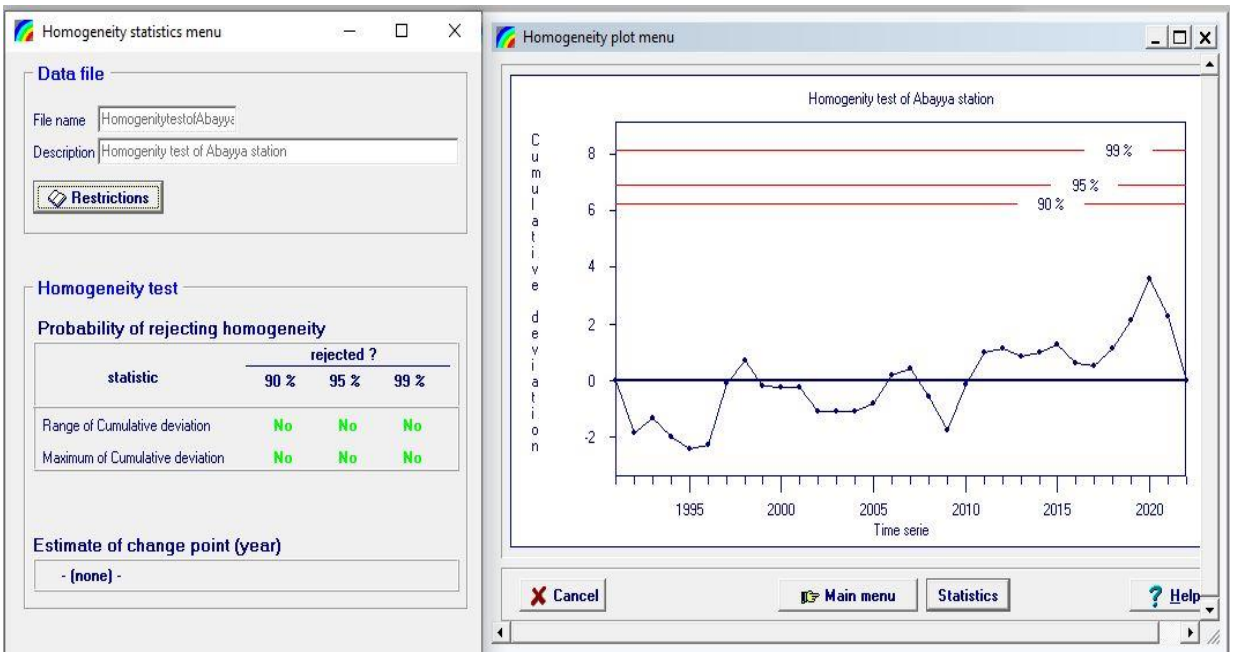

Appendix 7.2 Homogeneity test of Bilate station

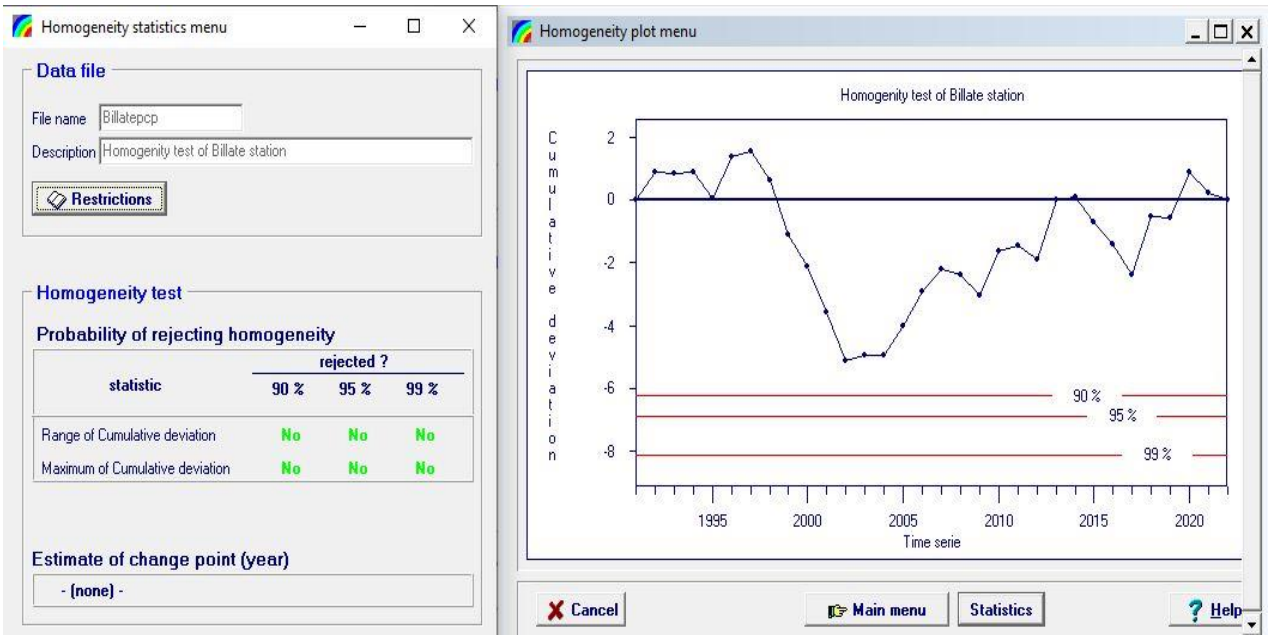

Appendix 7.3 Homogeneity test of Bodity station

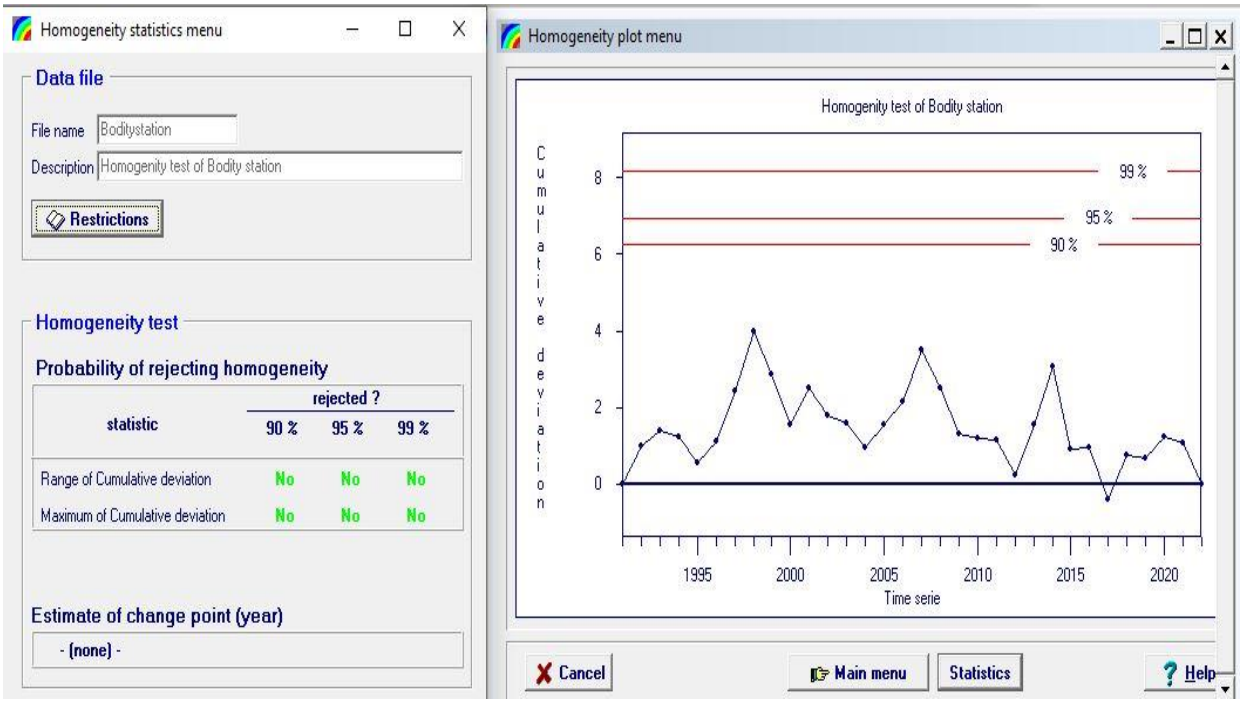

Appendix 7.4 Homogeneity test of Humbo station

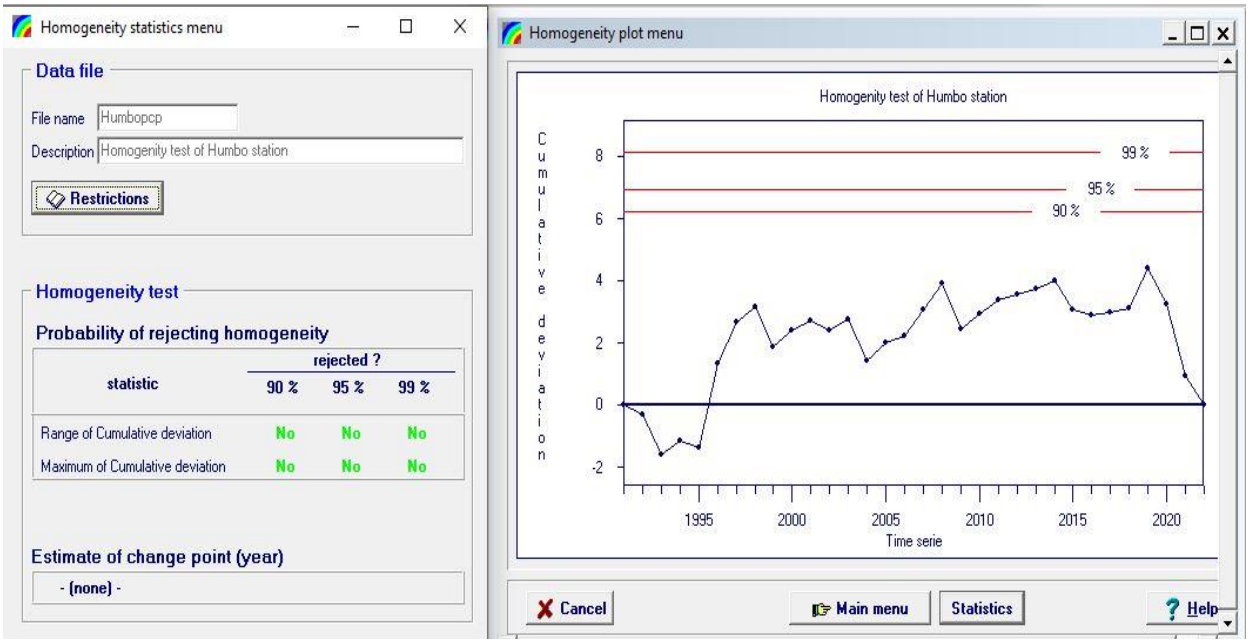

Appendix 7.5 Homogeneity test of Wolaita sodo station

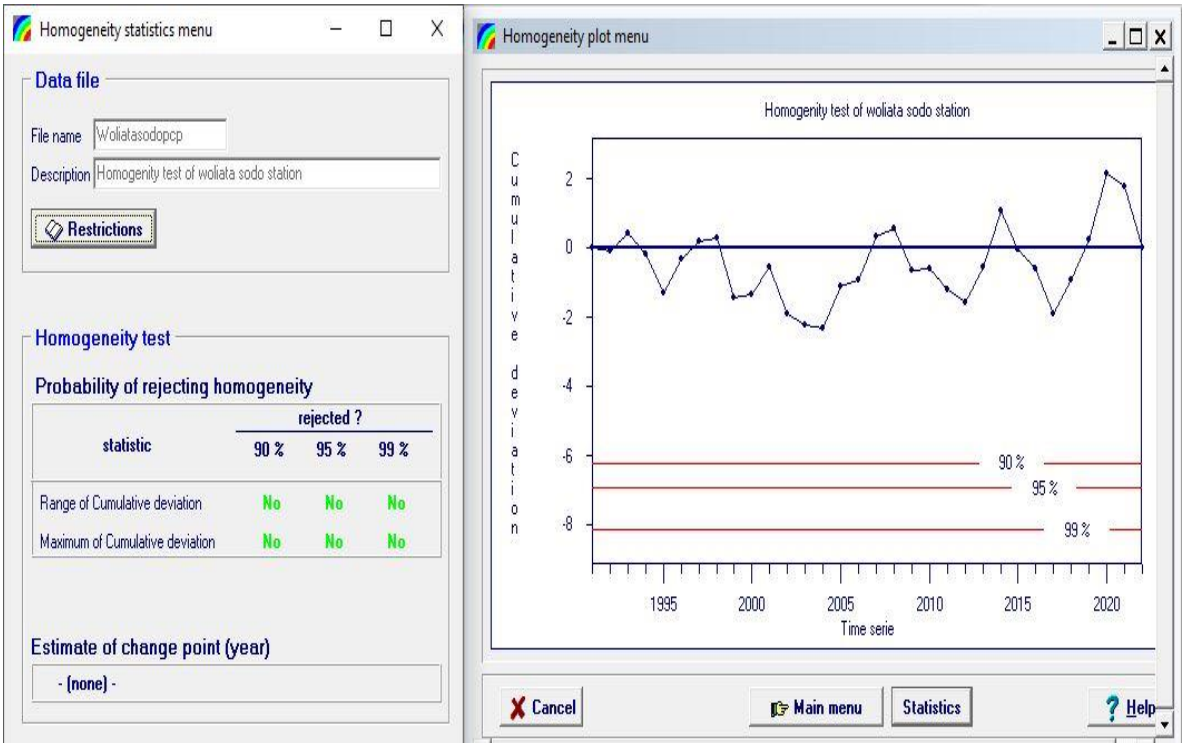

Appendix 7.6 Average monthly rainfall of meteorological station

Month	Abayya	Bilate	Bodity	Humbo	Wolaita Sodo
Jan	20.73	28.83	26.24	27.15	30.36
Feb	24.77	23.79	37.73	19.12	32.89
Mar	52.23	50.75	79.73	65.03	72.62
Apr	126.02	129.48	165.92	129.18	172.84
May	130.09	99.26	163.29	143.60	177.93
Jun	73.02	83.11	128.89	131.62	147.04
Jul	56.82	89.68	158.82	147.95	186.62
Aug	61.85	78.81	158.36	152.56	185.89
Sep	58.66	70.38	124.35	106.66	118.33
Oct	88.28	85.07	86.80	97.68	109.79
Nov	67.60	56.13	60.63	59.78	67.78
Dec	29.86	22.67	28.84	24.49	30.42

Appendix 7.7 Average minimum and maximum temperature of meteorological station

Month	Bilate max	Bilate min	Bodity max	Bodity min	Wolaita Sodo max	Wolaita Sodo min
Jan	31.99	16.00	26.90	12.89	27.47	14.61
Feb	33.09	14.63	27.63	13.83	28.49	15.27
Mar	33.12	16.00	27.47	14.35	28.55	15.31
Apr	30.83	15.50	26.04	14.38	26.68	14.73
May	29.46	16.00	24.72	14.16	25.11	14.77
Jun	27.99	15.50	22.75	13.58	23.39	14.56
Jul	26.88	16.00	21.29	13.07	22.07	14.33
Aug	27.45	16.00	21.78	13.18	22.58	14.53
Sep	28.65	15.50	23.28	13.51	23.94	14.53
Oct	29.73	16.00	24.74	13.33	25.13	14.45
Nov	30.65	15.50	25.67	12.67	26.20	14.70
Dec	31.05	16.00	26.24	12.53	26.71	14.64

Appendix 7.8 Outlier test of stream flow near Wajjiffo gauge station

No	**Year**	**Avg. flow (m^3/s)**	**Log Value Y=Log(Q)**	**No**	**Year**	**Avg. flow (m^3/s)**	**Log Value Y=Log(Q)**
1	1992	5.97	0.78	13	2004	5.35	0.73
2	1993	5.39	0.73	14	2005	12.33	1.09
3	1994	8.52	0.93	15	2006	6.44	0.81
4	1995	6.21	0.79	16	2007	14.26	1.15
5	1996	16.04	1.21	17	2008	8.49	0.93
6	1997	10.98	1.04	18	2009	5.59	0.75
7	1998	12.13	1.08	19	2010	10.09	1.00
8	1999	4.09	0.61	20	2011	9.58	0.98
9	2000	7.17	0.86	21	2012	10.65	1.03
10	2001	13.75	1.14	22	2013	27.42	1.44
11	2002	5.15	0.71	23	2014	21.25	1.33
12	2003	10.73	1.03	24	2015	16.53	1.22
Avg.							0.97
Skew							0.29
St Dev.							0.21
Kn							2.476

Higher outlier	$XH = Xav$ + KNS, 0.97 +2.467*0.21, XH = 1.48 then Q = $10^{2.21}$ =30.16
Lower outlier	$XL = Xav$ – KnS, 0.97 – 2.467*0.21, XL = 0.46 then Q =$10^{1.27}$ =2.88

Appendix 7.9 HRU report

MULTIPLE HRUs land Use/Soil/Slope OPTION		THRESHOLDS : 5 / 10 / 15 [%]	
Number of HRUs: 94			
Number of Sub basins: 11			
		Area [ha]	Area[acres]
Watershed		28640.5000	70772.1075
	Area [ha]	Area[acres]	%Wat.Area
LANDUSE:			
Agricultural Land-Generic --> AGRL	22851.9714	56468.3639	79.79
Residential --> URBN	407.3827	1006.6630	1.42
Range-Brush --> RNGB	3105.5821	7674.0485	10.84
Range-Grasses --> RNGE	2185.7104	5400.9997	7.63
Forest-Mixed --> FRST	89.8534	222.0324	0.31
SOILS:			
Lc67-2b-730	2700.6768	6673.5075	9.43
Nd11-153	2461.4123	6082.2728	8.59
Vc1-2-3a-258	22052.0992	54491.8398	77.00
Lp12-1a-793	1309.2282	3235.1684	4.57
Ne12-2c-155	117.0835	289.3191	0.41
SLOPE:			
15-30	2624.5289	6485.3420	9.16
8-15	9964.5396	24622.8755	34.79
30-9999	760.6483	1879.5999	2.66
3-8	14978.8966	37013.6026	52.30
0-3	311.8867	770.6875	1.09

Appendix 7.10 Weather generator statics for Bilate station

Weather generator statics for Bilate station												
Parameter	Jan	Feb	Mar	Apr	May	Jun	Jul	Aug	Sep	Oct	Nov	Dec
TMPMX	32.0	33.1	33.1	30.8	29.5	28.0	26.9	27.4	28.6	29.7	30.7	31.0
TMPMN	16.9	17.4	17.4	17.0	17.0	16.7	16.7	16.6	16.4	16.1	15.5	16.0
TMPSTDMX	2.3	2.3	2.4	2.9	2.1	2.1	2.2	2.3	2.2	2.2	1.9	2.3
TMPSTDMN	2.1	2.1	1.9	1.6	1.5	1.5	1.5	1.5	1.7	2.0	2.0	2.0
PCPMM	27.0	21.9	46.2	120.8	92.8	78.3	84.6	73.6	63.1	77.9	53.1	20.6
PCPSTD	4.2	3.1	3.9	8.8	7.1	7.0	7.2	6.2	5.3	5.5	6.1	2.9
PCPSKW	9.8	6.9	3.8	3.6	4.1	4.1	4.7	4.5	4.3	3.5	6.3	7.4

PR_W1	0.1	0.1	0.2	0.4	0.3	0.2	0.3	0.3	0.3	0.3	0.1	0.1
PR_W2	0.3	0.3	0.4	0.5	0.4	0.4	0.4	0.4	0.4	0.5	0.5	0.3
PCPD	4.1	3.6	7.7	13.6	11.3	8.3	9.9	9.6	10.1	11.8	6.0	3.2
RAINHHMX	4.2	3.6	4.9	11.1	9.1	9.2	9.8	8.2	6.9	7.0	7.5	3.2
SOLARAV	20.9	21.6	21.5	20.4	19.5	16.3	14.5	16.2	18.0	19.9	21.1	20.7
DEWPT	47.6	46.0	51.6	63.8	69.4	69.6	72.0	70.4	67.7	64.2	53.5	48.6
WNDAV	2.0	2.1	1.8	1.4	1.2	1.3	1.1	1.1	1.1	1.4	2.1	2.2

Appendix 7.11 Weather generator statics for Wolaita sodo station

	Weather generator statics for Wolaita sodo station											
Parameter	Jan	Feb	Mar	Apr	May	Jun	Jul	Aug	Sep	Oct	Nov	Dec
TMPMX	27.5	28.6	28.6	26.7	25.1	23.4	22.1	22.6	23.9	25.1	26.2	26.7
TMPMN	14.6	15.3	15.3	14.7	14.8	14.6	14.3	14.5	14.5	14.4	14.7	14.6
TMPSTDMX	1.8	1.8	1.9	2.0	1.6	1.6	1.8	1.6	1.5	1.6	1.5	1.3
TMPSTDMN	1.8	1.6	2.0	1.5	1.3	1.1	1.1	1.6	1.3	1.6	2.2	1.9
PCPMM	28.0	30.1	67.7	165.4	170.8	140.3	178.4	177.5	111.5	103.3	64.4	28.2
PCPSTD	3.7	3.8	5.8	10.7	10.8	9.9	10.4	10.8	7.6	8.0	7.0	3.9
PCPSKW	6.4	5.6	4.5	3.0	2.9	3.2	2.8	3.1	3.0	4.6	5.0	6.1
PR_W1	0.1	0.1	0.2	0.4	0.4	0.3	0.4	0.4	0.3	0.3	0.1	0.1
PR_W2	0.3	0.3	0.5	0.6	0.5	0.5	0.6	0.6	0.5	0.6	0.5	0.3
PCPD	4.3	4.7	8.9	14.6	14.3	12.3	15.6	15.7	12.6	11.9	6.0	3.7
RAINHHMX	4.2	4.5	6.9	13.7	13.9	12.5	13.6	14.2	9.5	9.9	8.8	4.3
SOLARAV	20.9	21.6	21.5	20.4	19.5	16.3	14.5	16.2	18.0	19.9	21.1	20.7
DEWPT	47.9	44.3	50.6	63.9	73.5	75.9	80.3	77.9	73.2	65.6	53.8	48.6
WNDAV	2.0	2.1	1.8	1.4	1.2	1.3	1.1	1.1	1.1	1.4	2.1	2.2

Appendix 7.12 Description of weather generator (WGEN) parameter

Symbol	**Description**
TMPMX	Average or mean daily maximum air temperature for the month (^{0}C)
TMPMN	Average or mean daily minimum air temperature for the month (^{0}C)
TMPSTDMX	Standard deviation for daily maximum air temperature for the month (^{0}C)
TMPSTDMN	Standard deviation for daily minimum air temperature for the month (^{0}C)
PCPMM	Average or mean total monthly precipitation (mm H_2O)
PCPSTD	Standard deviation for daily precipitation for the month (mm H_2O/day)
PCPSKW	Skew coefficient for daily precipitation in the month

PR_W1	Probability of a wet day following a dry day in the month
PR_W2	Probability of a wet day following a wet day in the month
PCPD	Average number of days of precipitation in a month
RAINHHMX	Maximum half-hour hour rainfall in the entire period of record for the month
SOLARAV	Average daily solar radiation for the month (MJ/m^2 /day)
DEWPT	Average daily dew point temperature in the month (^0C).
WNDAV	Average daily wind speed in the month (m/s)